STEPsCON 2018 – International Scientific Conference on Sustainability and Innovation

7 December 2018, Leverkusen, Germany

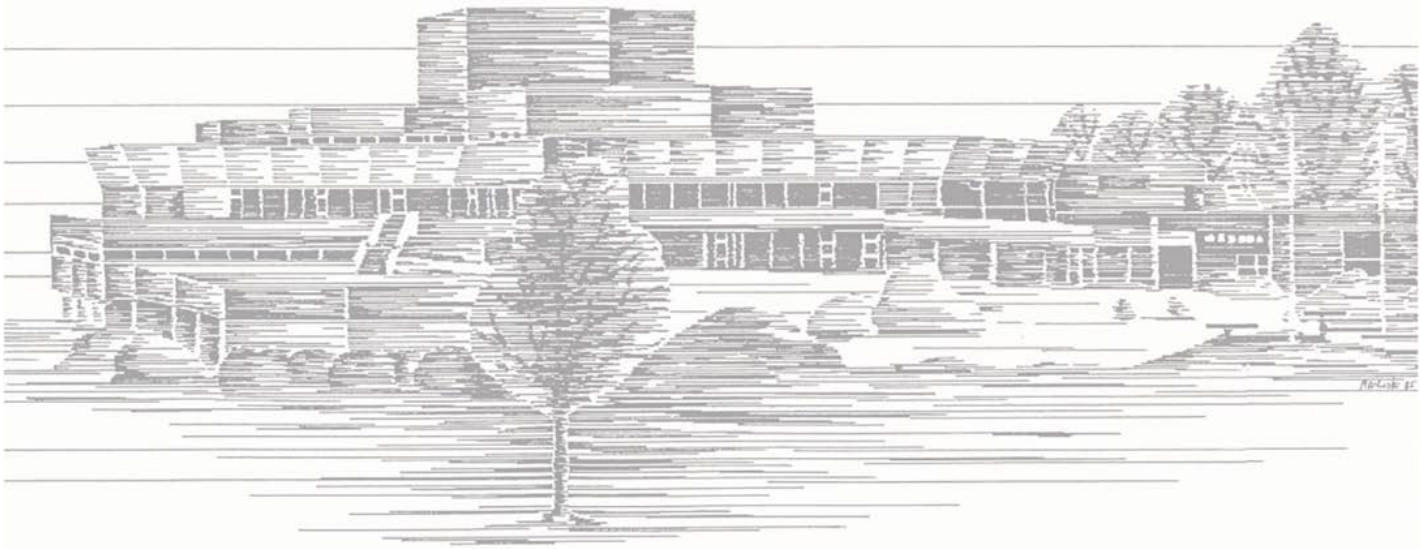

"Arctic Attitude meets German Pragmatism"

Book of Proceedings of STEPsCON 2018

UNIVERSITY OF OULU

LEVERKUSEN OULU 50 Jahre Vuotta 1968 2018 Ystävyyskaupungit Städtepartnerschaft

Technology
Arts Sciences
TH Köln

Preamble

STEPsCON 2018 was jointly organized by the Faculty of Applied Natural Sciences of TH Köln (Germany) and the University of Oulu (Finland) on the occasion of the 50th anniversary of the Leverkusen – Oulu town twinning. The conference focused on sustainability issues and covered the current state of research in four key topics:

1. Sustainable Medicine and Pharmaceuticals
2. Resources and Bioremediation
3. Sustainable Chemistry & Industrial Biotechnology
4. Innovative Materials & Formulations

Book of Proceedings Editor: Prof. Dr. Ulrich Schörken

Conference Organizing Committee:
Prof. Dr. Stéphan Barbe / Prof. Dr. Matthias Hochgürtel / Prof. Dr. Ulrich Schörken
Conference Coordination:
Dr. Claudia Carl / Heike Iven / Emily Kobs / Dr. Irina Polina

Impressum: TH Köln – University of Applied Sciences

Technology
Arts Sciences
TH Köln

Faculty of Applied Natural Sciences
CHEMPARK Leverkusen, Building E28
Kaiser-Wilhelm-Allee, 51368 Leverkusen, Germany
www.th-koeln.de/angewandte-naturwissenschaften/fakultaet-fuer-angewandte-naturwissenschaften_2467.php

Research Institute STEPs
Betzdorfer Str. 2, 50679 Köln, Germany
www.steps.th-koeln.de

Table of contents

New feedstocks for bioethanol production

Josipa Lisičar Vukušić[1, 2], Thomas Millenautzki[1], Abdechafik Mokhlis Saaid[1], Leon Reichert[1], Stéphan Barbe[1]

[1] Technische Hochschule Köln, Faculty of Applied Natural Sciences (Kaiser-Wilhelm-Allee, Gebäude E39, 51373 Leverkusen, Germany)

[2] Leibniz Universität Hannover, Institute of Technical Chemistry (Callinstrasse 5, Gebäude 250, 30167 Hannover, Germany)

***Correspondence:** Stéphan Barbe, Kaiser-Wilhelm-Allee, Gebäude E39, 51373 Leverkusen, Germany

Email: stephan.barbe@th-koeln.de

Abstract

In the last few decades raw material molasses, used in large scale fermentations in the production of bioethanol, citric acid, (baker´s) yeast and yeast extracts, has become more and more expensive. That is why agro-industrial wastes have become an interesting alternative. They are being produced in large volumes every day and represent a serious environmental problem considering its high organic content. The present contribution aims to demonstrate how waste products of wine production can be employed as substrate in bioethanol production. Cultivation of yeast and bioethanol production on molasses and grape pomace extract was studied in flasks in laboratory scale. This work should be regarded as an example of integrated sustainability which demonstrates how the waste from one industrial process is used as feedstock for another.

1. Introduction

Increasing population is the reason of increased energy demand throughout the world. The main source of energy are fossil fuel and non-renewable sources (natural gas, oil and coal), used in the production of transportation fuel, electricity and other goods [1]. 60 % of global utilization of fossil fuels is consumed in transportation sector, which consequently contributes to massive pollution [2]. Consumption of these fuels contributes to the emissions of greenhouse gasses as well as global warming causing climate change, rise in sea level, loss of diversity and urban pollution [3]. This lead to a search for an environmentally friendly, renewable and sustainable source of energy [4, 5], in which priority is given to liquid biofuels [6]. Biofuels are renewable substitutes of fossil fuels [7], defined as transportation fuels derived from biological/agricultural sources, either in liquid form (bioethanol and biodiesel) or in gaseous form (biogas and hydrogen). First generation of biofuels applies raw

materials containing sugars, starch, vegetable oils as well as biodegradable waste from agricultural and forestry industries [8]. However, since this generation competes with food and feed materials, increasing ethical concerns encouraged the search for nonedible feedstock alternatives [9]. That is why the second generation of biofuels, the raw materials such as lignocellulosic material as well as waste oil and animal manure, and the third generation applying marine algae as biofuel feedstock, are gaining more and more interest [8, 9].

Bioethanol is eco-friendly oxygenated fuel, commercially produced from starch/sugar based crops [10], most likely to replace gasoline due to its several advantages. Even though one litre of ethanol provides 66 % of the energy provided by the same amount of gasoline, the higher octane number allows it to act as an antiknock agent. Also the power output is improved with ethanol because of its higher heat of vaporization compared with gasoline [3]. After the oil crisis in the 70´s, Brazil launched the Brazilian National Alcohol Program, aiming at large scale ethanol production and the engine-adaptation to consume the E20 mix (20 % ethanol and 80 % gasoline) or even pure anhydrous ethanol. For decades Brazil was the main producer by utilizing cane molasses, but was surpassed by the production of corn-based ethanol in United States [11]. Global ethanol production is presented in Figure 1. Besides United States and Brazil, covering more than 80 % of the world productions, other large ethanol-producing countries are China, Canada, Thailand, Argentina, India and European Union [12].

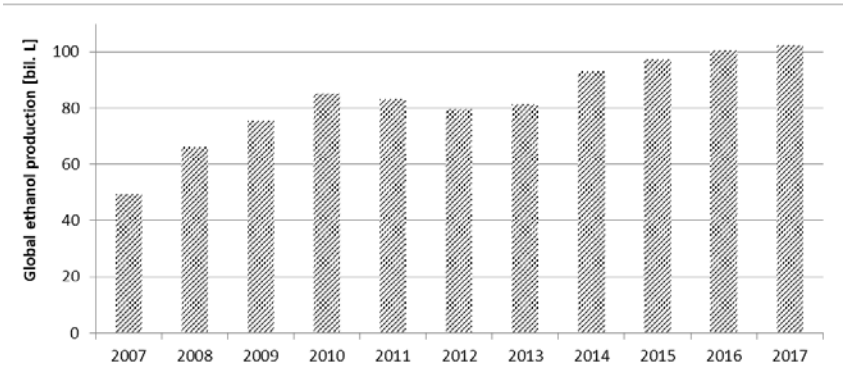

Figure 1. Global ethanol production during the last 10 years in billion litres

Molasses is suitable raw material for ethanol production. However its price has been raising drastically because of the growing demand for this medium. That is why efforts need to be made in order to find alternative raw materials [13]. Ideal raw material for ethanol production would be widely available non-edible feedstock. Although lignocellulosic material appears to be very convenient, the processing steps are energetically and financially costly, which creates a bottleneck in the industrial production [11]. Potential source of raw materials are agro-industrial wastes, which is being produced in large volumes every day and represent a serious environmental problem considering its high organic content [15]. One such potential raw material is grape pomace, which remains after the juice is collected from the pressing of grapes for wine production [14]. When processing grapes, about 75 % is

used in wine making and 25 % of the weight of grapes remains as pomace [16]. Its composition depends on grape variety, method of processing, environmental conditions and the ratio of skin:seeds:stem [12]. Traditionally grape pomace is used as fertilizer or animal feed. However, because of the presence of antinutritive compounds that can negatively affect crop yields and animal weight gain, this utilization present some drawbacks [17]. Corbin et al. [14] demonstrated the potential of employing grape pomace as raw material in ethanol production with the theoretical yield up to 270 L/t. In 2017 770 million litres of wine was produced in Germany (Figure 2) [18].

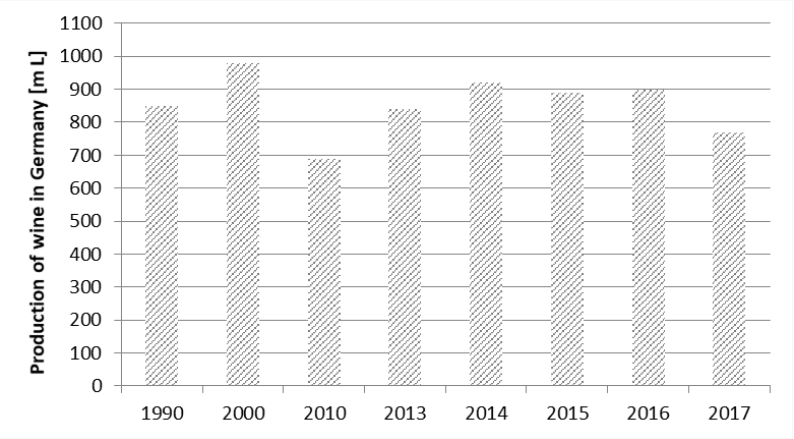

Figure 2. Production of wine in Germany in the last few decades in million litres

The present study aims to access the feasibility of replacing molasses in the production of ethanol by investigating the ethanol production on grape pomace. In this regard, grapes were processed into wine, while waste grape pomace was further processed into grape extract and pellets, therefore creating a concept of zero discharge biorefinery process.

2. Materials and Methods

2.1 Production of wine

84.9 kg of grapes Riesling Mandelberg were washed and pressed by Shark Fruit 1.6 kW (Vares Mnichovice a.s.; Mnichovice, Czech Republic) resulting in 50.4 kg of grape juice and 32.5 kg of grape pomace (grape pomace 1 in Figure 3). Grape juice was supplemented with 10 g of mineral nutrient and inoculated with 10 g of yeast (Alcotec 48 Turbo Yeast Classic). The fermentation was performed at 15 °C and lasted 14 days. Fermentation resulted in 45.2 kg of wine (5.2 kg of CO_2 was evaporated) which was further filtrated (Sheet filter 20x20 FZ 20; Zambelli, Vicenza, Italy; Filter paper MN 540 we, ø 150 mm; Macherey-Nagel GmbH & Co. KG, Düren, Germany) resulting in final product: 32.9 kg of Riesling wine containing alcohol content of 13.3 % vol.

2.2 Production of grape extract and pellets

Grape pomace 1 was mixed with 25 kg of distilled water and boiled for 20 minutes at 90 °C while constantly being stirred. After the extraction the mixture was cooled down to 35 °C and then pressed resulting in 18.8 kg of grape pomace 2 and 28.7 kg of extract. Grape

pomace 2 was dried at 60 °C for 24 hours (Vacuum drying oven Heraeus Instruments; Hanau Germany) and then used as raw material for pellet production (EcoWorxx Pelletmaker PM22E; Raddestorf, Germany). Moisture content was determined at 105 °C until constant weight. Durability was determined according to the standard ISO 17831-1:2015(en) [19]. Net calorific value was determined according to ISO 18125:2017(en) [20]. This extract was concentrated to obtain 4.5 kg concentrated grape extract by evaporation in a scraped surface evaporator (Labor- und Prozesstechnik GmbH; Ilmenau Germany) at a temperature of 87 °C, pressure of 134 mbar and rotation speed of 260 rpm. Centrifugation was performed for 10 minutes at 4,000 rpm (Sorvall RC-5B Plus Superspeed Centrifuge, Thermo Fisher Scientific; Waltham, Massachusetts, USA) resulting in 0.103 kg of tartaric acid and 3.8 kg of concentrated grape extract (Figure 3).

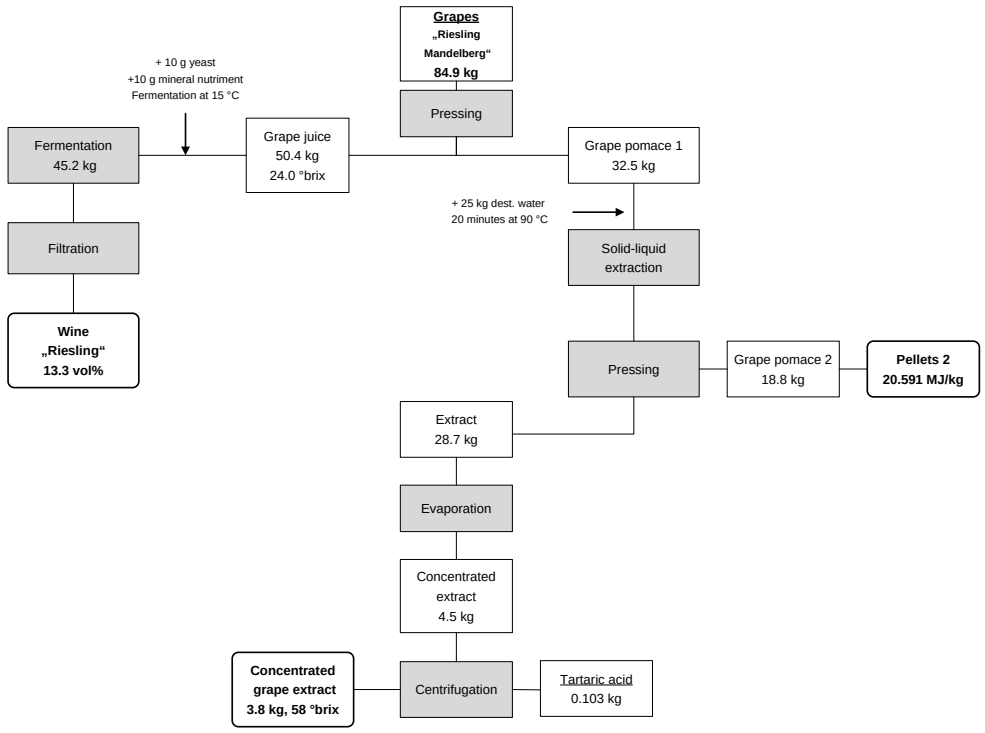

Figure 3. Production of white wine, pellets and concentrated grape extract

2.3 Strain, media and fermentation

Microbial strain used for ethanol production is commercial yeast (Alcotec Turbo Yeast - Classic 48, Hambleton Bard Ltd; Chesterfield, UK).

Molasses mixture, containing beet and cane molasses, and wine extract were adjusted to pH value 3.9 (pH meter PCE-PHD 1, PCE Deutschland GmbH; Meschede, Germany) and 20 °Brix (Refractometer 0-32 %, Greiner Glasinstrumente GmbH; Lemg, Germany) according to Göksungur and Zorlu [21]. Media were sterilized at 121 °C for 20 minutes (Systec DE-150 autoclave, Systec GmbH; Linden, Deutschland).

Erlenmeyer flasks filled with 100 g of the each medium was inoculated with 0.6 g of the commercial yeast and placed on magnetic stirrer (Multiposition magnetic stirrers Variomag

Poly 15; Thermo Fischer Scientific, Waltham, Massachusetts (USA). The flasks were weighed for the determination of ethanol production (Kern PCB 3500, Kern & Sohn GmbH; Balingen, Germany). Fermentation lasted approx. 30 hours. All fermentations were performed in triplicate.

3. Results & Discussion

Grape pellets, with the moisture content of 9.3 %, had the durability index of 92.3 %. Measured net calorific value of 20.6 MJ/kg is very similar to the value obtained with wood pellets [22]. Figure 4 represents the evolution of the ethanol production on molasses mixture and grape extract.

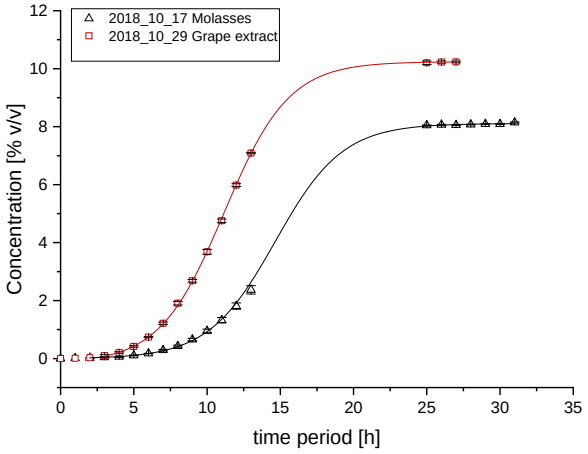

Figure 4. Ethanol production on the molasses medium and grape extract

Adaptation of the yeast on the medium, the lag phase, lasted longer on the molasses medium (approx. 4 hours), than on the grape extract (approx. 3.5 h). After approx. 2 hours from the start of the fermentation, foam formation on the surface of the media occurred because of the CO_2 gas evolution. The grape extract medium discoloured from dark brown colour to orange, while the colour of molasses remained unchanged. After about 30 hours, bubble forming wasn't observed, meaning that the fermentation came to an end, due to the complete utilization of sugars. The fermentations should have been performed at 25 °C. However due to the early start in the morning (approximately at 5:30 am), the room temperature in the laboratory was 15 °C. It took almost 4 hours to reach 25 °C (until 10:00 am). Accordingly, it is possible that this factor could have influenced the duration of the lag phase. Fermentation on molasses medium resulted in the production of 7.88 vol % ethanol, while the fermentation on grape extract has resulted in producing 10.23 vol % ethanol. The fermentation phase of grape extract began earlier than on the molasses medium, therefore the ethanol yield was higher on the grape extract medium. This is demonstrated in the Figure 5; fermentation on grape extract resulted in the release of 7.5 g of CO_2, whilst on molasses medium was up to 5.8 g of CO_2.

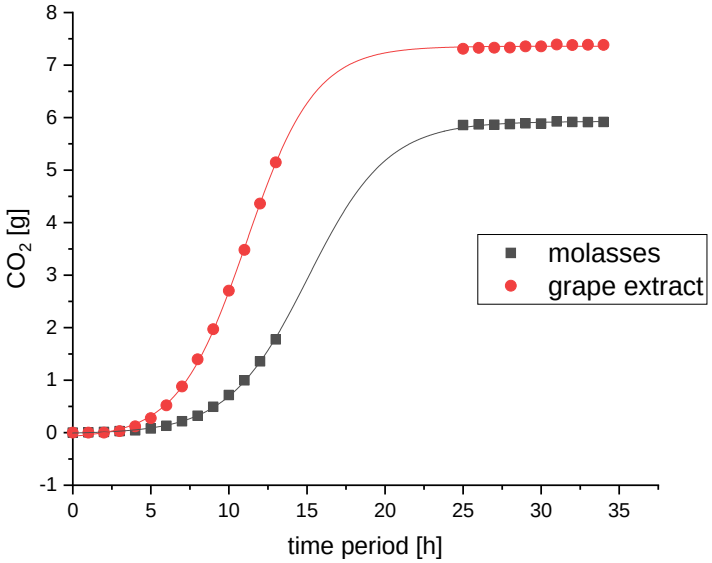

I

Figure 5. CO_2 release during the fermentation on the molasses medium and grape extract

Conclusions

In this study, wine production was reshaped into a biorefinery concept, where not only Riesling wine was produced, but also waste stream of grape pomace was directed into the production of pellets, grape extract and the extraction of tartaric acid. Pellets' measured net calorific value of 20.6 MJ/kg is similar to the value obtained with wood pellets. Produced grape extract was tested as the raw material for ethanol production and compared to the production on the molasses medium. Higher yield of ethanol was achieved on the medium containing grape extract, 10.23 vol %, whereas in the molasses medium 7.88 vol % ethanol was achieved. These results confirm the feasibility of applying grape extract as raw material in the production of ethanol. By this strategy the costs for raw material would be reduced as well as energy could be generated from the pellets.

The authors have declared no conflict of interest.

References

[1] A. Gupta, J.P. Verma, Sustainable bio-ethanol production from agro-residues: A review, Renew. Sust. Energ. Rev. 41 (2015) 550-567. https://doi.org/10.1016/j.rser.2014.08.032.

[2] H.B. Aditiya, T.M.I. Mahila, W.T. Chong, H. Nur, A.H. Sebayang, Second generation bioethanol production: A critical review, Renew. Sust. Energ. Rev. 66 (2016) 631-653. https://doi.org/10.1016/j.rser.2016.07.015.

[3] H. Zabed, J.N. Sahu, A. Suely, A.N. Boyce, G. Faruq, Bioethanol production from renewable sources: Current perspectives and technological progress, Renew. Sust. Energ. Rev. 71 (2017) 475-501. https://doi.org/10.1016/j.rser.2016.12.076.

[4] J. Lisičar Vukušić, A. Kneer, M. Mösche, S. Barbe, Turning industrial aerobic fermentation plants into thermal power stations, Int. J. Energy Res. 43 (2019) 544-551. https://doi.org/10.1002/er.4299.

[5] J. Lisičar, T. Millenautzki, T. Scheper, S. Barbe, New trends in industrial baker's yeast fermentation: Recovery of key biomolecules and low-grade heat conversion, J. Biotechnol. 280S (2018) 17-18. https://doi.org/10.1016/j.jbiotec.2018.06.052.

[6] S.H.M. Azhar, R. Abdulla, S.A. Jambo, H. Marbawi, J.A. Gansau, A.M.M. Faik, K.F. Rodrigues, Yeasts in sustainable bioethanol production: A Review, Biochem. Biophys. Rep. 10 (2017) 52-61. https://doi.org/10.1016/j.bbrep.2017.03.003.

[7] M. Ivančić Šantek, J. Lisičar, L. Mušak, I. Špoljarić Vrana, S. Beluhan, B. Šantek, Lipid production by yeast Trichorporon oleaginosus on the enzymatic hydrolysate of alkaline pretreated corn cobs for biodiesel production, Energy Fuels, 32 (2018) 12501-12513. https://doi.org/10.1021/acs.energyfuels.8b02231.

[8] S.S. Raju, P. Shinoj, P.K. Joshi, Sustainable development of biofuels: Prospects and challenges, Econ. Polit. Wkly. 44 (2009) 65-72. https://doi.org/ 10.2307/25663941.

[9] A. Limayem, S.C. Ricke, Lignocellulosic biomass for bioethanol production: Current perspectives, potential issues and future prospects, Prog. Energy. Combust. Sci. 38 (2012) 449-467. https://doi.org/10.1016/j.pecs.2012.03.002.

[10] M. Guo, W. Song, J. Buhain, Bioenergy and biofuels: History, status and perspectives, Renew. Sust. Energ. Rev. 42 (2015) 712-725. https://doi.org/10.1016/j.rser.2014.10.013

[11] L.C. Basso, T.O. Basso, S.N. Rocha, Ethanol production in Brazil: The industrial process and its impact on yeast fermentation, in: M.A. dos Santos Bernardes (Ed.), Biofuel production-recent development and prospects, InTech, Rijeka (Croatia), 2011, pp. 85-100.

[12] RFA, Industry statistics, Renewable Fuels Association. http://ethanolrfa.org/resources/industry/statistics/#1454099788442-e48b2782-ea5, 2018 (Last accessed 21st November 2018).

[13] J. Lisicar, T. Scheper, S. Barbe, Industrial baker's yeast production: From manufacture to integrated sustainability, J. Biotechnol. 256S (2017) S23-S24. http://dx.doi.org/10.1016/j.jbiotec.2017.06.630.

[14] K.R. Corbin, Y.S.Y. Hsieh, N.S. Betts, C.S. Byrt, M. Henderson, J. Stork, J. DeBolt, S. DeBolt, G.B. Fincher, R.A. Burton, Grape marc as a source of carbohydrates for

bioethanol: Chemical composition, pre-treatment and saccharification, Bioresourc. Technol. 193 (2015) 76-83. http://dx.doi.org/10.1016/j.biortech.2015.06.030.

[15] J. Lisičar, T. Scheper, S. Barbe, Turning industrial baker's yeast manufacture into a powerful zero discharge multipurpose bioprocess, Ind. Biotechnol. 13 (2017) 184-191. https://doi.org/10.1089/ind.2017.0018.

[16] C. Beres, G.N.S. Costa, I. Cabezudo, N.K. da Silva-James, A.C.S. Teles, A.P.G. Cruz, C. Mellinger-Silva, R.V. Tonon, L.M.C. Cabral, S.P. Freitas, Towards integral utilization of grape pomace from winemaking process: A review, Waste Manag. 68 (2017) 581-594. https://doi.org/10.1016/j.wasman.2017.07.017.

[17] J. García-Lomillo, M. L. González-SanJosé, Applications of wine pomace in the food industry: Approaches and functions, Compr. Rev. Food Sci. F. 16 (2017) 3-22. https://doi.org/10.1111/1541-4337.12238.

[18] Deutsches Weininstitut, Deutscher Wein Statistik, https://www.deutscheweine.de/fileadmin/user_upload/Website/Service/Downloads/Statistik_2018-2019.pdf, 2019 (Last accessed 22nd May 2019).

[19] SO 17831-1:2015(en), Solid biofuels — Determination of mechanical durability of pellets and briquettes — Part 1: Pellets, 1st ed. ISO/TC 238 Solid biofuels. https://www.iso.org/standard/60695.html, 2015 (Last accessed 14th May 2018).

[20] ISO 18125:2017(en), Solid biofuels — Determination of calorific value, 1st ed. ISO/TC 238Solid biofuels. https://www.iso.org/standard/61517.html, 2017 (Last accessed 14th May 2018).

[21] Y. Göksungur, N. Zorlu, Production of ethanol from beet molasses by Ca-alginate immobilized yeast cells in a packed-bed bioreactor, Turk. J. Biol. 25 (2001) 265-275.

[22] C. Telmo, J. Lousada, Heating values of wood pellets from different species, Biomass Bioenergy. 35 (2011) 2634-2639. https://doi.org/10.1016/j.biombioe.2011.02.043

Development and optimization of a control algorithm for an industrial combustion plant via flame image analysis

Oleg Antonov[1], Dennis Gersthahn[1], Michael Bongards[1], Christian Wolf[1]

[1] TH Köln - University of Applied Sciences, Metabolon Institute, Am Berkebach 1, 51789 Lindlar

Abstract

Modern industrial biomass combustion plants are regulated by the power and/or combustion control. In this process, the implemented sensors collect the relevant measured data. The aim is to achieve ideal combustion with optimum efficiency and to minimize gas emissions. For this purpose, a group within the research project Metabolon developed new regulatory procedures in order to record the combustion process of a biomass combustion plant using a webcam. The recordings were evaluated automatically and were used for a better monitoring of the process. In addition, the webcam-based method aims, among other things, to provide private homes with a cost-effective variant as an alternative to industrial system solutions.

1. Introduction

The recorded flame images provide information on the quality of combustion by fractionizing the flame into its components such as the flame area and color values. From these parameters, the efficiency, excess air ratio and CO concentration can be determined. Table 1 illustrates the relationship between the flame images in combustion with different levels of excess air and the resulting findings.

Every combustion of biomass requires the largest possible flame surface because a large flame surface usually leads to low excess air. On the other hand, if the excess air ratio is too large, the flame area decreases because the cold air cool down the flame. Furthermore, the large flame surface indicates that there is a high level of efficiency and low pollution levels [1].

Combustion with low excess air There is a large area of flame but with a reddish flame color and many dark areas in the flame. For this reason, it comes to a strong soot formation and a high CO concentration with a medium to high efficiency [1].	
Combustion with to high excess air The flame surface is very small, because the existing air is cooling down the flame. As a result, the efficiency drops below 50%. The CO emission is very high and there is virtually no soot formation [1].	
Combustion with a very good air ratio There is a medium to high efficiency which occurs in a semi-transparent golden yellow flame. Both soot formations and pollutant emissions are low [1].	
Optimal combustion The flame is beautifully bright and has a golden yellow color. Under this condition, there is a medium to high soot formation. However, the CO concentration has a low to medium value at a high efficiency [1].	

Table 1: Representation of the flame images as well as consequences under the influence of different high excess air [1]

2. Measurement

The combustion process is recorded with a camera system and converted into a binary image. The creation of the binary images is done according to the thresholding method of Otsu. Based on this method, a defined threshold indicates the range of the pixel brightness in the image from black (binary value 0) to white (binary value 1). The white pixels represent the flame, whereas the black pixels represent the background of the image. The ratio of the white colored area to the total area indicates the size of the flame. For further procedures, only the flame binary image is crucial. For this reason, the edited binary image is overlaid

upon the original image so that the background disappears and only a portion of the flame remains. In order to obtain color information of the flame from the white flame section, the image is converted into a CIELAB color space and then processed using a method of vector quantization based on k-means clustering. With this algorithm, three different clusters are created which contain the three flame colors (red, yellow and white). Based on these color components, the corresponding temperature of the combustion can be identified [2].

Furthermore, a measurement of the flame under both optimal and noisy combustion conditions must be carried out in order to determine the basic values for the respective states. The combustion is either in the optimal state or there is a disturbance in the form of too much air or lack of air. The noisy combustion state increases soot formation as well as pollutant emissions. By testing different measurement times, it has been proven that one measurement every 20 seconds is best suited. However, in order to counteract the strong fluctuations of the flame and thus of the color values, an average value of the measurements must be determined every minute (Diagrams 1 und 2) [3].

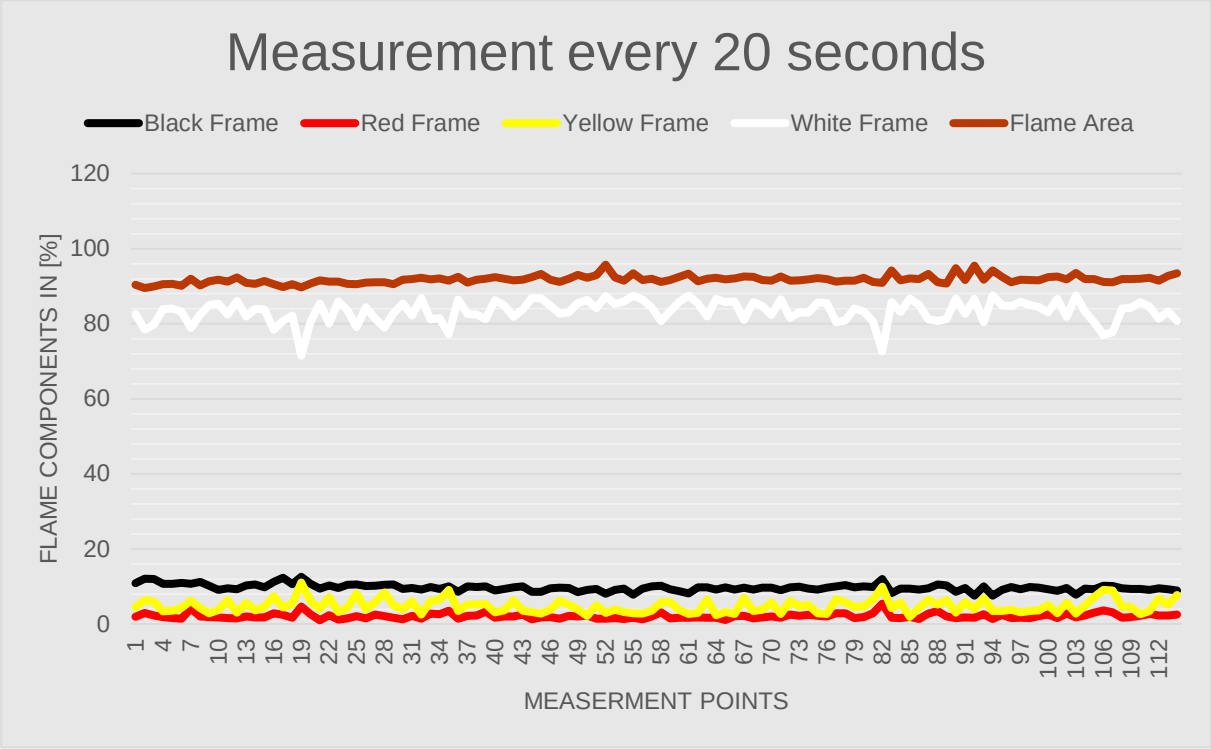

Diagram 1: Recording of the measuring points every 20 seconds

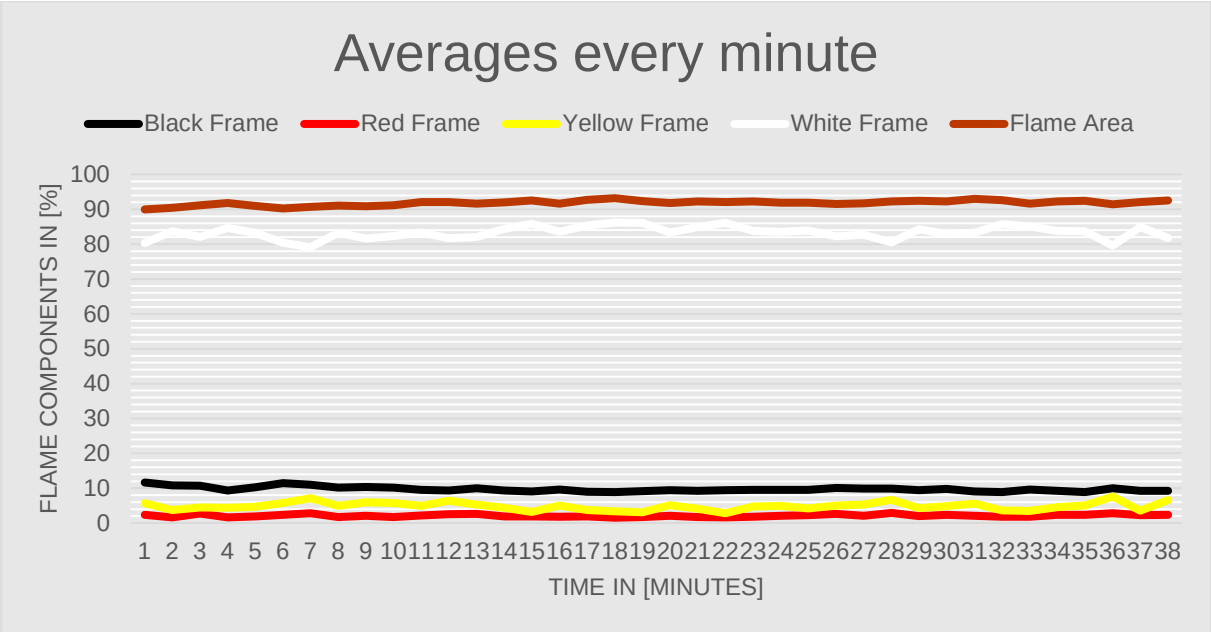

Diagram 2: Formation of the average value

Because of the different compositions and thus different energy densities of the fuel (wood chips), the secondary air supply varies. In order to calculate an optimal secondary air supply, the control is based on the successive approximation in which the optimal secondary air supply is calculated by a stepwise approximation [3].

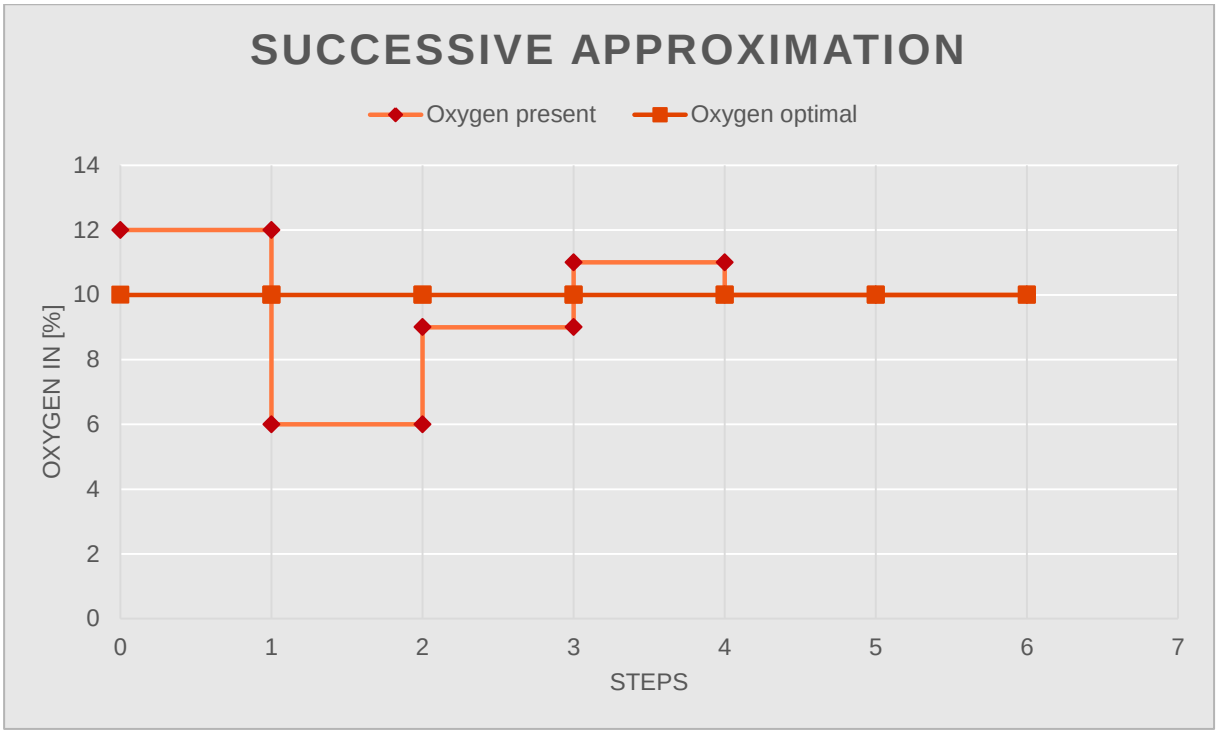

Diagram 3: Successive Approximation

The graphic shows an example of the procedure of a successive approximation when changing to a new type of fuel. The plant was previously operated with a fuel that was optimally burned at a residual oxygen content of 12%. By switching to a new fuel, the

residual oxygen for optimal combustion was also changed. How high this is now must be determined. For a better illustration, the orange curve in the graph represents the new optimum residual oxygen content. Under this course there is a lack of air, which is also recognized by the webcam. Thus, the controller samples the optimum residual oxygen by controlling the secondary air supply in such a way that the residual oxygen content in the exhaust gas is halved with each step.

3. Results & Discussion

The project is not yet completed. For this reason, only the intermediate results already acquired are presented and discussed here.

The measurements were carried out under optimal combustion, settings by the manufacturer, and under the simulation of a lack of air. The following flame pictures including measurements were taken.

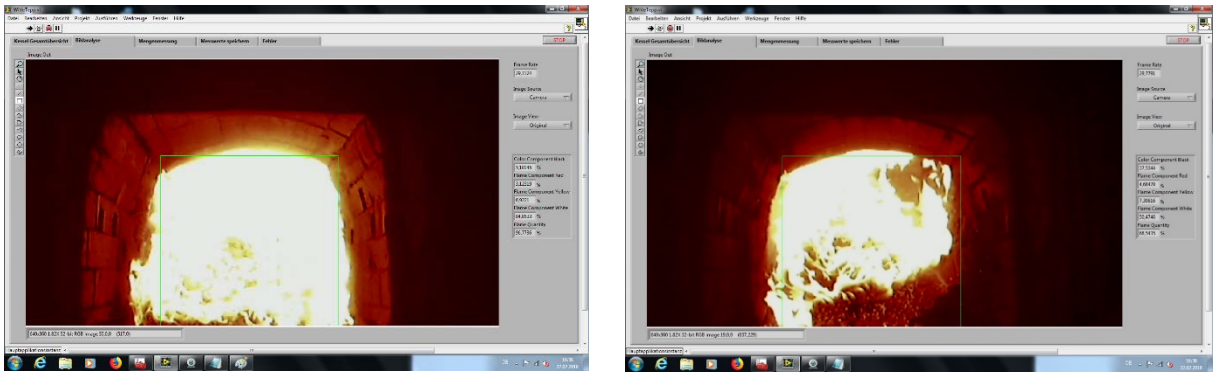

Picture 1: On the left is the flame picture with an optimal combustion. On the right is an image capture with a simulation of a lack of air

The lack of air was simulated by gradually closing the inlet grilles for both the primary and secondary air supplies of the firing system completely, although the secondary air supply is of greater interest to us than the primary one. This is due to the fact that the primary air supply is coupled to the combustion chamber temperature and thus cannot be influenced by the PLC control. Nonetheless, the following measurement results of the flame and the exhaust gas were recorded for both cases.

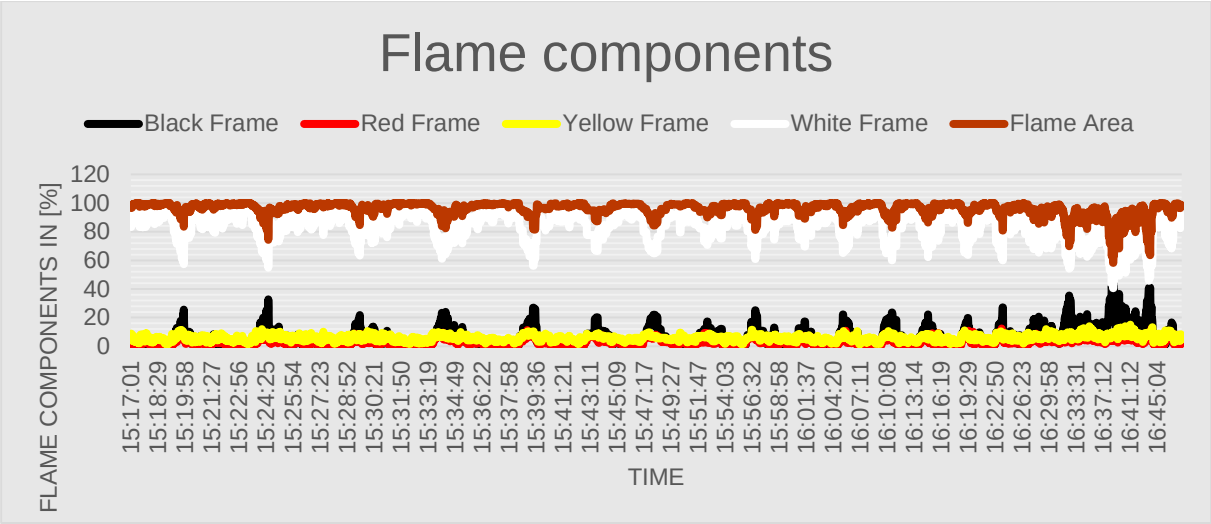

Diagram 4: Recorded Flame components

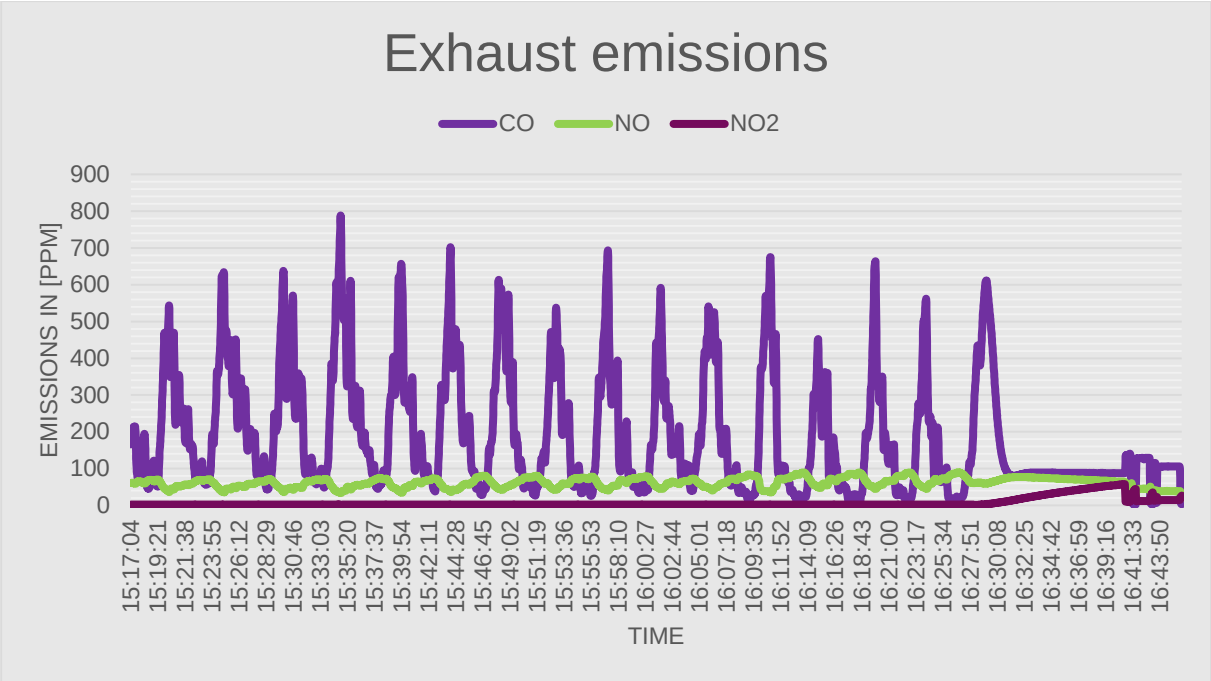

Diagram 5: Recorded exhaust emissions. CO is carbon monoxide, NO is nitrogen oxide and NO2 is nitrogen dioxide

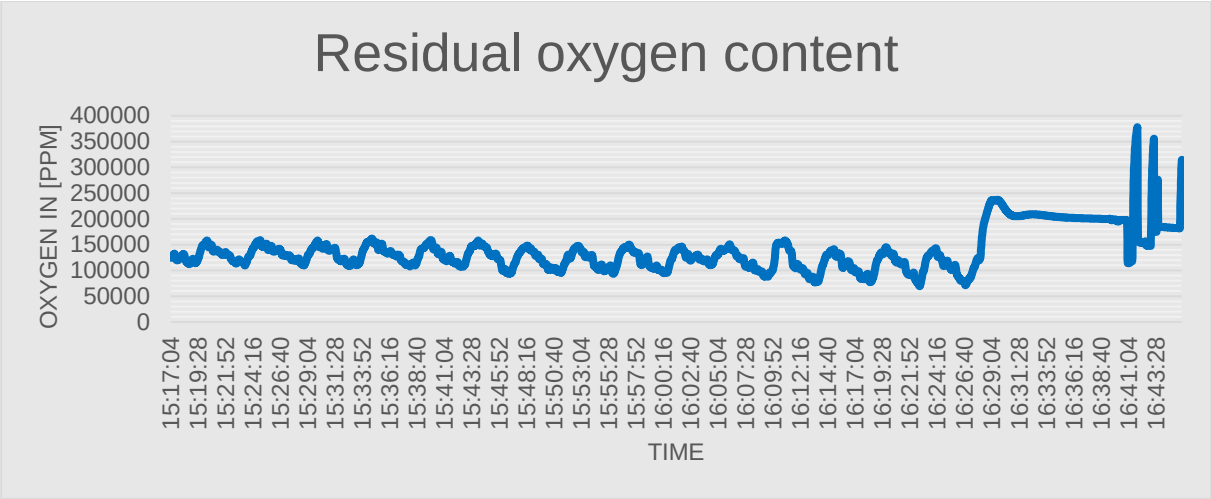

Diagram 6: Recorded residual oxygen content in the exhaust gas

The measured values were recorded every second in order to be able to better detect the reaction to simulated disturbances in a combustion process and to be able to determine the basic values more precisely later. Furthermore, measurements were recorded in the firebox of the furnace. As can be seen from the diagrams 4-6, recording of the measured values started at 15:17:01. The exhaust gas required about 3 seconds to travel from the combustion chamber to the measuring point at which the emissions in the exhaust gas were measured. For this reason, the exhaust emission graphs are offset by 3 seconds compared to the flame component measurement. Starting at 15:28, the intake grille for the secondary air supply was gradually closed to simulate a lack of air in the combustion process. However, it turned out that e.g. the flame surface together with the white part of the flame decreased for a short time and the black part increased, but later on the system tried to counteract the disturbance and the values cancel each other out, so that fluctuations took place. The occurring fluctuations increased from about 15:39 on. This can be seen very clearly in the short intervals.

Closing the intake grilles only increased the fluctuations in the measured values. However, the flame area did not decrease and the emissions did not increase permanently. Actually, it was expected that the flame area would shrink and the color values would also decrease. On the other hand, emissions would have to increase and remain high at all times. Therefore, the intake grilles for the primary air supply were gradually sealed airtight from 16:10 until they were closed at 16:18 to 98%. At 16:30, the influence of air deficiency on the flame could be observed for the first time (see Figure 1). It can also be clearly seen from diagram 4 that e.g. the flame surface and the white content break sharply.

Conclusions

Due to the fact that the air deficiency could only be simulated conditionally, the threshold value for the controller could not be calculated. Consequently, a new process has to be developed to gradually simulate the lack of air. Furthermore, in the new simulation method, additional parameters such as e.g. the timing of the fuel supply or the negative pressure in the furnace are taken into account.

Currently, a new model is being developed to detect the disturbances even better and more accurately. This model focuses on the evaluation of the combustion according to the load factor, color of the flame, the timing of the fuel and the secondary oxygen supply. The evaluation as well as the recording of the measured values is based on the design of experiments (DOE).

Unfortunately, the control could not be tested yet because the PLC control does not allow the control parameters to be taken over Modbus. At the moment, the control parameters can only be transferred manually via the panel. Therefore, a new PLC control is needed to avoid this problem. Alternatively, it should also be checked whether the developed controller can be connected directly to the frequency inverter in order to be able to directly control the secondary air supply in this way.

Acknowledgements

The authors would like to thank the “Bergischer Abfallwirtschaftsverband” (BAV) for the excellent cooperation. A share of the funding for this study is made by the European Commission and the European Regional Development Fund (ERDF) under the slogan “Investing in our future”. The authors have declared no conflict of interest.

References

[1] Faragó Z. (2011): Kaminfeuer Richtig schüren, [online] ww.farago.info/job/ Kaminfeuer/Holzfeuer.htm [27.11.2018].

[2] Rehbach J. (2012): Entwicklung und Erprobung bildanalytischer Methoden zur Optimierung der Verbrennungsprozesse von nachwachsenden Rohstoffen in industriellen Feuerungsanlagen, Cologne University of Applied Sciences Campus Gummersbach, Bachelor-Thesis

[3] Antonov O. (2018): Entwicklung und Optimierung des Regelalgorithmus einer industriellen Feuerungsanlage über die Online-Analyse des Flammbildes, Technical University of Cologne Campus Gummersbach, Bachelor-Thesis.

Pseudozyma antarctica lipase B catalysis in deep eutectic solvents

Beatrice Kleiner, Dominik Ananaba, Sven Schulz, Ulrich Schörken*

Faculty of Applied Natural Sciences; TH Köln – Campus Leverkusen; Chempark Leverkusen E39; Kaiser-Wilhelm-Allee; 51368 Leverkusen; Germany

* Corresponding author: ulrich.schoerken@th-koeln.de

Abstract

Pseudozyma antarctica Lipase B catalyzed esterification and transesterification in deep eutectic solvents (DES) was investigated in reaction systems with alcohols of different polarity. Coconut oil and crude biodiesel were deacidified successfully with non-immobilized CALBL and final acid values of 1.2 for biodiesel and 0.5 for coconut oil were obtained, while no esterification with ethanol was observed without DES. Water depletion of the lipid phase in the presence of water adsorbing DES causes this difference. Analysis of water contents revealed a 10 fold lower water content of the lipid phase in the presence of a second DES phase than in trials without utilization of DES. In contrast reactions of hydrophilic polyols are suppressed in the presence of DES. While the esterification of fructose and the transesterification with glycerol worked well in the polar solvent 2-methyl-2-butanol, almost no fructose esterification and a decreased transesterification with glycerol were observed in the presence of DES. Analysis of logP values of the substrates explains the substrate dependent differences in reactivity. The polar alcohols are probably bound strongly in the hydrogen-bonding network of the DES phase and are thus not available for lipase catalyzed reactions.

Abbreviations: DES: deep eutectic solvents; ChCl:U: urea based DES; ChCl:G: glycerol based DES; ChCl:F: fructose based DES; CALBL: *Pseudozyma antarctica* lipase B, 2M2B: 2-methyl-2-butanol

1. Introduction

Lipase B from *Pseudozyma antarctica* is a versatile enzyme with an exceptional temperature and solvent stability. In reverse hydrolysis and transesterification reactions the synthesis of all kinds of esters is possible; biodiesel and polyesters are examples of accessible products in this respect [1-4]. The immobilized enzyme was used successfully for the synthesis of polyol esters like monoglycerides and sugar esters [5-7], which are commercially available as emulsifiers in food and cosmetical products. Besides reverse hydrolysis and transesterification reaction, non-natural reactions like perhydrolysis and amide bond

formation are catalyzed by the enzyme [8],[9].

The production of cosmetic esters at low temperature with immobilized *P. antarctica* lipase B under continuous water removal with vacuum is done on industrial scale. It was shown that the enzymatic process is advantageous over the chemical one in regard to product quality and number of process steps [10,11]. Additionally, according to an overall LCA assessment, the enzymatic process is more eco-friendly than the chemical one [12]. Besides production of green emollients for the cosmetic industry, vacuum-based synthesis with immobilized *P. antarctica* lipase B is applied for the production of omega-3 fatty acid and conjugated linoleic acid based triglycerides were commercialized [13,14].

Deep eutectic solvents are a new class of green solvents obtained by complexation of quaternary ammonium salts with hydrogen bond donors [15]. DES, being hydrophilic and non-volatile, share some similarity with ionic liquids in this respect. From initial studies by Gorke *et al.* with immobilized *P. antarctica* lipase B [16], several lipase transformations in DES have been performed successfully [17-20]. Enzymatic synthesis of biodiesel was employed in DES with soybean oil as substrate and up to 88 % of ester was obtained within 24 h with commercially available Novozym 435 as biocatalyst [21,22]. A study of different DES revealed that the best biodiesel production was obtained in mixtures with choline acetate [23]. The half-life time of the immobilized lipase could be enhanced considerably in the presence of water and by reducing the amount of denaturing urea in the DES [24]. It was shown that free lipase B from *P. antarctica* is highly active in hydrophilic solvents including DES at low water contents [25]. The synthesis of cosmetic esters proceeded to near completion, because water adsorbing properties of DES shifted the equilibrium towards ester formation. The same effect was originally observed in esterification reactions in the presence of glycerol [26]. Using the water adsorbing effect of DES, biodiesel in high yields and a low content of residual fatty acids could be synthesized successfully with free *P. antarctica* lipase by our group [27].

The aim of this work was the evaluation of lipase B from *Pseudozyma antarctica* in DES for the synthesis of polyol esters and for esterification with short chain alcohols. Esterification with short chain alcohols was evaluated in deacidification reactions with biodiesel and coconut oil. Preesterification of crude acidic coconut oil may be used as preparatory step for fatty alcohol production via subsequent alkaline transesterification and hydrogenation. Deacidification of biodiesel could be interesting for enzymatic processes starting from acid rich raw materials like deodorizer distillates and tall oil fatty acids. Transesterification of olive oil with glycerol to yield partial glycerides and the synthesis of fructose esters were chosen as example compounds for hydrophilic polyol transformations.

2. Materials and methods

2.1 Materials

All chemicals were of synthesis grade. BSTFA + 1% TMCS and reference standards for GC

calibration were from Sigma Aldrich (Steinheim, Germany). Liquid and immobilized lipase B preparations from *Pseudozyma antarctica* (Lipozyme CALBL and Novozym 435) are products from Novozymes A/S and Accurel MP 1000 is a macroporous polypropylene from Membrana. Refined rapeseed oil, olive oil and coconut oil were obtained from a local supermarket. All other chemicals were brought from Carl Roth GmbH (Karlsruhe, Germany) or VWR International (Darmstadt, Germany).

2,2 Preparation of DES, immobilized lipase and lipid substrates

Choline chloride and urea (ChCl:U) or choline chloride and glycerol (ChCl:G) in a molar composition of 1:2 were weighed directly into bottles, sealed immediately and mixed by vigorous shaking. Liquid DES were obtained within a few hours by incubation on an orbital shaker (Infors HT) at 250 rpm and 60°C. ChCl:F was produced in the same way by mixing choline chloride and fructose in a molar composition of 1:3.

Lipozyme CALBL was immobilized onto Accurel MP 1000 by adsorption as described in [28]. 10 g of Accurel MP 1000 were soaked for 30 min in ethanol. Ethanol was removed and 40 ml of water and 20 ml of Lipozyme CALBL were added and incubated on a rotary shaker overnight at room temperature. The immobilized enzyme was filtered, dried on a sheet of paper and stored at 8 °C.

Biodiesel was produced chemically from refined rapeseed oil. 500 g of oil and 100 g of dried ethanol were heated in stirred reactor to 80 °C and the reaction was started by addition of 8 g sodium ethylate in ethanol (21 wt%). The mixture was stirred under reflux at 95 °C for 2 hours and the glycerol phase was separated after cooling. The lipid phase was acidified with diluted phosphoric acid to a pH of < 5 and the hydrophilic phase was separated. The lipid phase was washed twice with 200 ml of water and then dried with a rotary evaporator. Acid value of the biodiesel was adjusted by adding oleic acid.

20 g of coconut oil were mixed with 3 ml of water and 100 µl of Lipozyme CALBL and incubated for 24 h on a rotary shaker at 45 °C. The water phase was separated and the lipid phase was heated to 80 °C for 1 h to deactivate the enzyme. After analyzing the acid value the partially hydrolyzed coconut oil was mixed with refined coconut oil to adjust the acid value.

2,3 Biocatalytic reactions

In a typical deacidification experiment 20 g of lipid (acidified biodiesel or acidified coconut oil) were mixed with 20 g of DES (CHCl:U or CHCl:G), 1 g ethanol and 1 g of water and the reaction was started by addition of 100 µl of Lipozyme CALBL. The mixtures were incubated in sealed bottles at 30 °C and 250 rpm on an Infors Multitron rotary shaker. Variations in composition are outlined in the results section in detail. Comparative examples were done with 0.1 g of Novozym 435, 2 g of ethanol and no water addition. Samples were taken at different time intervals for further analysis.

For fructose ester syntheses 4.2 g of lauric acid, 4 g of fructose and 20 g ChCl:F were mixed

in sealed flasks, 0.5 ml liquid Lipozyme CALBL and 0.5 ml water or 0.5 g immobilized CALB L without additional water were added and the mixtures were incubated at 250 rpm on an Infors Multitron rotary shaker. In comparative trials 30 g of 2-methyl-2-butanol and 1 g immobilized CALBL were used. Reactions with immobilized enzymes were run at 60 °C while reactions with liquid CALBL were incubated at 50 °C. In trials with water removal 30 g of oleic acid and 20 g fructose were mixed in a stirred reactor with 150 g 2-methyl-2-butanol and 5 g immobilized CALBL was added. A column packed with 20 g molecular sieve 3A and a cooler was mounted on top of the reactor. The temperature was set to 65 °C and vacuum was applied until a reflux was observed.

10 g of olive oil, 5 g of glycerol and 0.5 g of water were mixed with 10 g of 2-methyl-2-butanol in sealed bottles for monoglyceride synthesis by glycerolysis. After addition of 0.2 g of Novozym 435 the mixtures were incubated at 45 °C and 250 rpm on an Infors Multitron rotary shaker. 10 g of 2-methyl-2-butanol and 20 g of ChCl:U were used in experiments with a mixed solvent system. Samples were withdrawn from the reaction mixtures for further analysis at different time intervals.

2.4 Analytical methods and calculations

In routine analysis 10 µL of the lipid phase were dissolved in 940 µl of heptane in a GC-vial and 50 µl silylation agent (BSTFA + 1% TMCS) were added. The samples were sealed and incubated in an oven at 80°C for one hour. Analysis was done with a Shimadzu GC 2010 Plus using a MTX Biodiesel TG column (RESTEK, length 14m, ∅ 0.53 mm, film thickness 0.16 µm) connected to a FID detector with helium as carrier gas and a temperature gradient from 75°C to 410 °C. A split ratio of 5 with an injection volume of 1.5 µl was applied.

Calculation of fatty acid content from acid values was done with molecular masses of 282 g/mol for oleic acid, 200 g/mol for lauric acid and 211 g/mol for mixed coconut fatty acids. An acid value of 10 corresponds to 5 % oleic acid, 3.6 % lauric acid or 3.8 % mixed coconut fatty acids. Analysis of lipids was done according to the DGF standard method C-V 2 “Acid value and free fatty acid content (Acidity)” [29] with 0.2 – 2 g of lipid sample dissolved in ethanol. Acid values of samples containing organic solvents were normalized to the lipid content in the organic phase. The acid value was determined by titration with 0.1 M KOH solution against phenolphthalein using a Metrohm Dosimat E535 and calculated with the following equation:

$$\mathrm{AV} = \frac{\mathrm{ml\ KOH\ consumed} \cdot [\mathrm{KOH}] \cdot \mathrm{M_{KOH}}}{\mathrm{g\ sample}}$$

The water amount of the lipid phase was determined according to the method of Fischer with an automatic titrator (Metrohm 870 KF Titrinoplus). LogP values were calculated with the program MedChem Designer from Simulations Plus Inc. using the company’s internal calculation model (S+logP) or the logP values according to Moriguchi (MlogP). LogP values of DES could not be given precisely, as DES are multi-component mixtures.

3. Results and discussion

3.1 Deacidification of biodiesel and coconut oil

Acid values of biodiesel and coconut oil were adjusted to 11.5 and 10.9 respectively, which correspond to fatty acid contents of 5.8 % for biodiesel and 4.1 % for acidified coconut oil. Comparative deacidification trials were done in the presence of DES and without DES (Fig. 1). An acid value reduction was observed in the presence of DES in all experiments, while acid values increased in solvent free experiments.

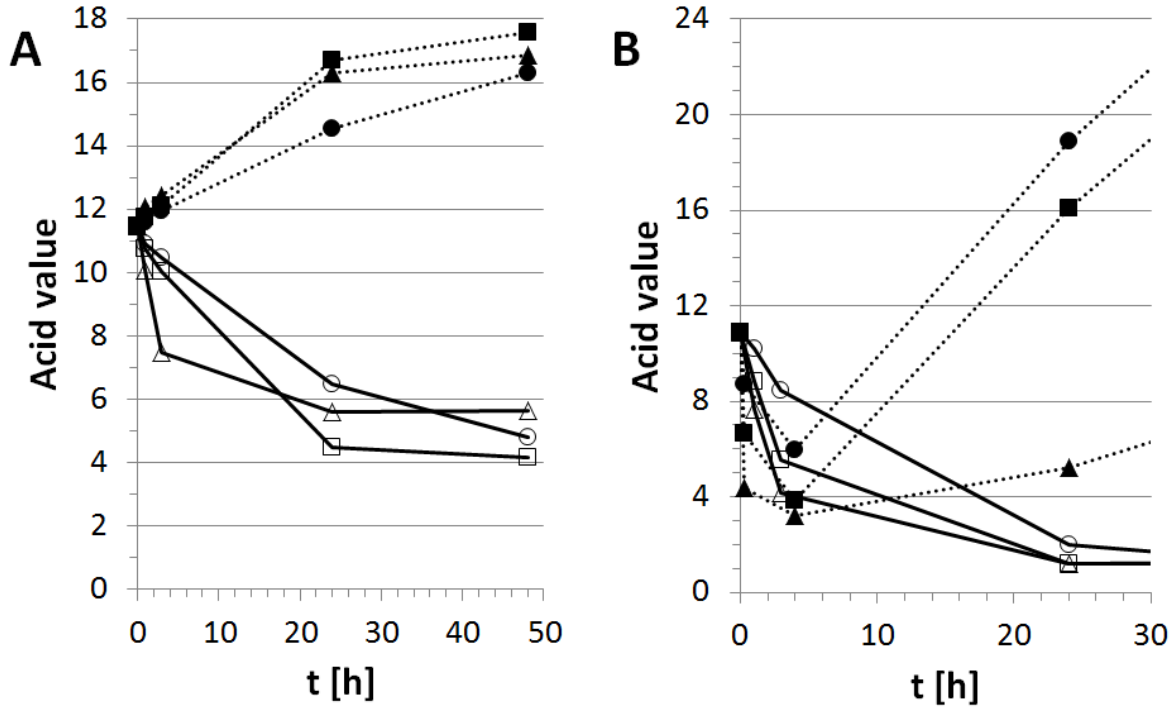

Fig. 1: Time dependent deacidification of biodiesel (**A**) and coconut oil (**B**) in dependence of enzyme concentration and presence of DES; open symbols, straight lines = with DES; closed symbols, dotted lines = without DES; **A)** ●,○ = 20 µl CALB L; ■, □ = 100 µl CALB L; ▲,△ = 1000 µl CALB L, **B)** ●,○ = 20 µl CALB L; ■, □ = 50 µl CALB L; ▲,△ = 100 µl CALB L.

The acid value of biodiesel under standard reaction conditions with 1000 µl of ethanol and 1000 µl of water was decreased to 4 (Fig. 1A), which corresponds to a residual acid content of 2 %. A clear dependence of reaction velocity was observed at different enzyme concentrations. The highest velocities were obtained with 1000 µl of liquid CALBL; however, a final acid value of > 5 remains in the mixture, probably caused by the water content of the liquid enzyme preparation. To elucidate the influence of water in more detail, experiments with different ethanol to water ratios were performed (Table 1). Low water conditions lead to lower acid values; however negatively influenced the enzyme activity. Increasing the concentration of ethanol lead to enzyme deactivation; thus low concentrations of water and low concentrations of short chain alcohol have to be selected for optimum reactivity. Best results with an acid value of 1.2 were obtained with 300 µl of water, though lower concentrations of water may result in lower acid values after prolonged reaction times.

Dosage of ethanol at low water concentration could be a means to further reduce the acid content to meet a value of 0.5 corresponding to 0.25 % fatty acid, which is the maximum allowed concentration according to the EN 14214 European Biodiesel norm [30].

Trials with acidified coconut oil revealed some differences to biodiesel deacidification. While the influence of enzyme concentration on reaction velocity and the decrease of acid values in the presence of DES are comparable, overall reaction velocities and equilibrium compositions differ significantly (Fig. 1B). Deacidification of coconut oil is faster than esterification in biodiesel at the same enzyme concentration. In the presence of DES final acid values of slightly higher than 1 corresponding to acid contents of 0.4 were reached under standard reaction conditions and the final acid values were less dependent on enzyme concentration. Complex behavior, with deacidification at the beginning and a steep rise in acid value at longer reaction times, was observed in trials without DES. GC analyses revealed, that enzymatic transesterification took place simultaneously. With the formation of partial glycerides the mixture becomes more hydrophilic and obtains some emulsifying properties. Better solubility of water in the partial glycerides containing coconut oil may be the reason for the increase in hydrolysis observed after 24 h of reaction time. Additionally ethanol concentration is decreased by transesterification leading to a higher surplus of water and thus a change in the hydrolysis / esterification equilibrium of the system. In trials with DES a slight increase in acid values is only observed at reaction times exceeding 120 h. A less pronounced effect of ethanol to water ratio was observed with coconut oil in comparison to experiments with biodiesel (Table 1). Lowest acid values 0f 0.5 – 0.6, corresponding to 0.2 % of free fatty acids, were obtained with 0 – 100 µl of water added to the reaction mixture.

Table 1: Acid values after deacidification of biodiesel (left) and coconut oil (right) in dependence of ethanol / water composition (* = equilibrium was not reached after 120 h)

Substrate	Composition [µl] ethanol/water	Acid value	Substrate	Composition [µl] ethanol/water	Acid value
Biodiesel	1000 / 0	6.7*	Coconut oil	1000 / 0	0.5
Biodiesel	1000 / 100	4.1*	Coconut oil	1000 / 100	0.6
Biodiesel	1000 / 300	1.2	Coconut oil	1000 / 300	1.0
Biodiesel	1000 / 500	2.6	Coconut oil	1000 / 500	0.8
Biodiesel	1000 / 1000	4.1	Coconut oil	1000 / 1000	1.2

3.2 Polyol esters by synthesis and glycerolysis

The synthesis of fructose esters starting from fructose and lauric acid was compared in reaction systems with DES and 2-methyl-2-butanol (2M2B) as solvents. In 2M2B lauric acid

and fructose are solubilized and form a system composed of one liquid phase plus residual non-dissolved fructose as solid second phase. The reaction proceeded smoothly towards ester formation in the presence of immobilized CALBL with a significant improvement in esterification velocity and shift of reaction equilibrium towards esterification in the presence of water absorbing molecular sieves (Fig. 2A). CALBL esterifies preferably the primary hydroxyl groups of fructose and thus mono- and diesters are formed as outlined in Fig. 2B on the basis of the cyclic fructofuranose structure. Almost equimolar amounts of fructose mono- and dilaurate were detected by GC analysis accordingly. In DES a different phase behavior was observed. Fructose is dissolved completely in the DES phase and a liquid two-phase system consisting of a hydrophobic lauric acid and a hydrophilic sugar – DES phase is generated. The two-phase system was not suited well for the synthesis of fructose esters neither with immobilized nor with non-immobilized lipase. Less than 20 % lauric acid was esterified in all cases, though fructose was completely dissolved in the reaction system.

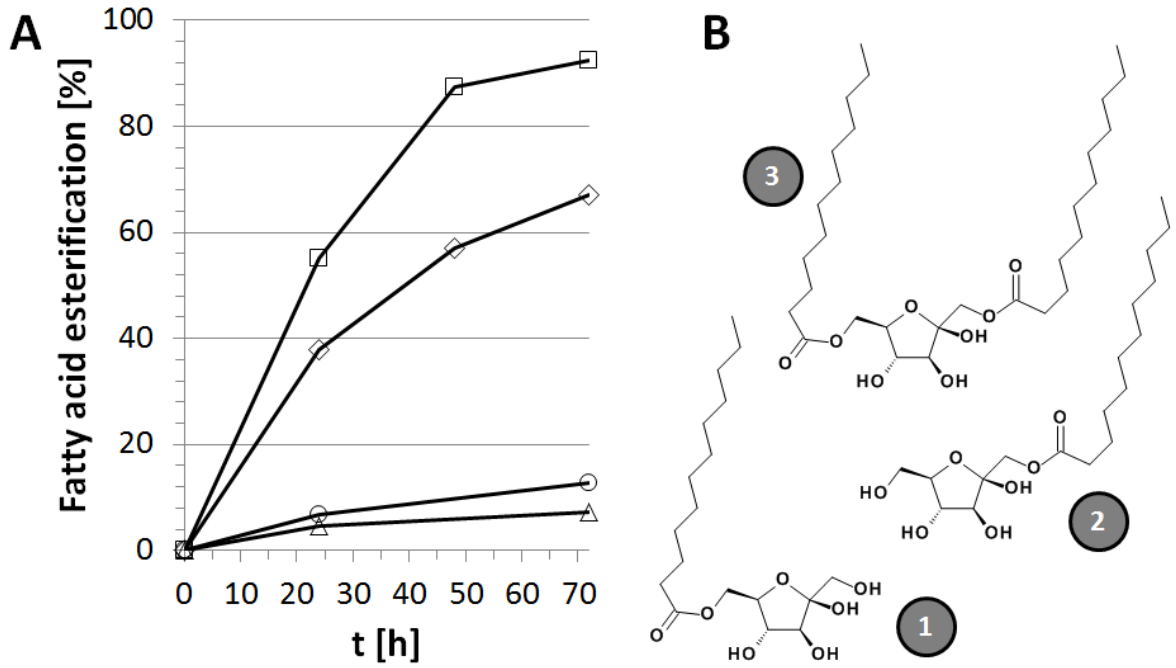

Fig. 2: A) Time dependent esterification in fructose ester synthesis: △ = free Lipozyme CALB L dissolved in DES ○ = immobilized Lipozyme CALB L in DES, ◇ = immobilized Lipozyme CALB L in 2-methyl-2-butanol without water removal, □ = immobilized Lipozyme CALB L in 2-methyl-2-butanol with molecular sieve based water removal; **B**) Fructose monolaurate (1, 2) and fructose dilaurate (3) obtained by enzymatic esterification of the primary hydroxyl groups of fructofuranose.

The immobilized CALBL catalyzed transesterification of olive oil with a surplus of glycerol was evaluated in the presence of 2M2B and in a mixed 2M2B / DES solvent system. In 2M2B a single-phase system composed of polar solvent, hydrophobic olive oil and hydrophilic glycerol is formed. Triglycerides were transesterified to > 98 % and an equilibrium mixture with 60 % monoglycerides and 10 % diglycerides was yielded (Fig. 3A). The addition of 2 % of water resulted in the formation of around 25 % of fatty acids through hydrolysis, thus water

is competing with glycerol in the single phase system. By addition of DES a two-phase system formed, because 2M2B and DES are only partially miscible and phase behavior as well as equilibrium yields changed significantly. Transesterification only proceeded to 90 % of triglyceride consumption and a partial glyceride mixture with 35 % of diglycerides and 20 % of monoglycerides was obtained (Fig. 3B). Transfer of glycerol into the hydrophilic DES phase and thus depletion of glycerol concentration in the 2M2B phase may explain the different equilibrium composition obtained. The formation of fatty acid as byproduct is even stronger than in the pure 2M2B system, though water is adsorbed strongly by the DES phase [25].

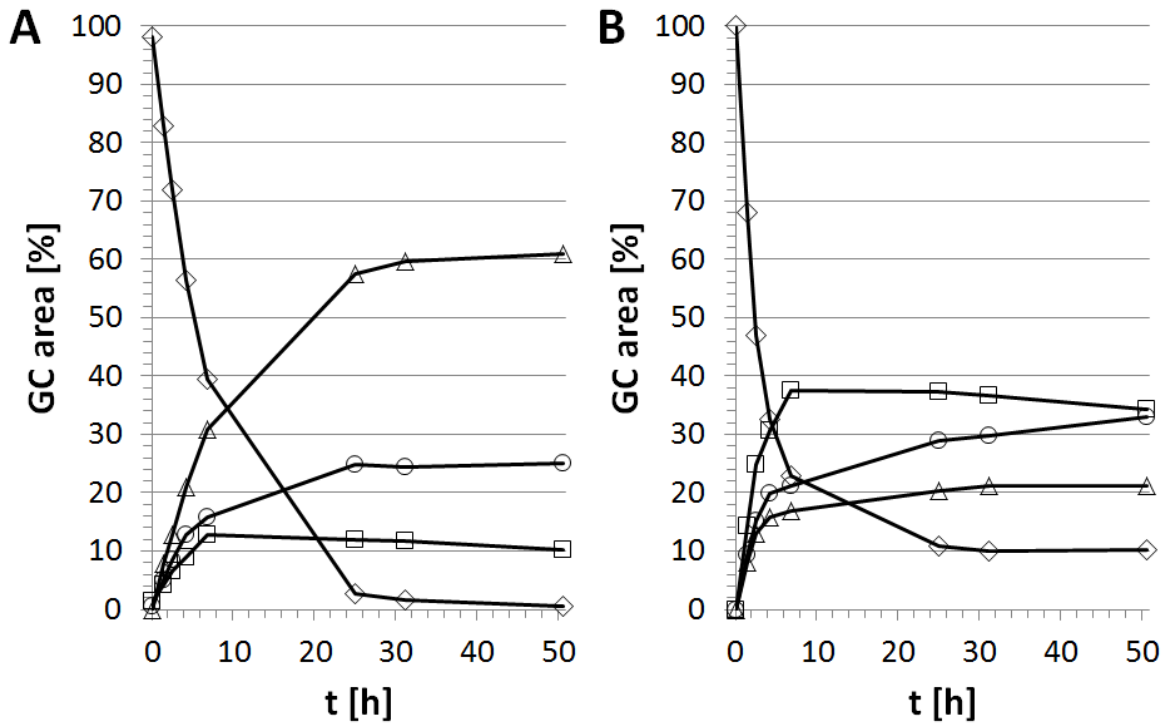

Fig. 3: Time dependent glycerolysis of olive oil in 2-methyl-2-butanol (**A**) and a mixed 2-methyl-2-butanol / DES solvent system (**B**); ○ = fatty acids, ◇ = triglycerides, □ = diglycerides, △ = monoglycerides.

3.3 Comparative analysis of lipase B catalysis in DES

Addition of hydrophilic DES solvents to hydrophobic lipid substrates results in the formation of two-phase systems, which can shift the equilibrium towards ester synthesis and prevent the formation of fatty acid byproducts in transesterification reactions through water adsorption [27][25],[27]. This effect was employed successfully for the deacidification of crude biodiesel and coconut oil with ethanol as polar alcohol (Fig. 4). Analysis of water contents in biodiesel deacidification support the water adsorbing effect with 0.4 mg/ml of water in the presence of DES and 4 mg/ml in the lipid phase without DES. Similar water concentrations of 0.3 mg/ml in the lipid phase with DES and 3.4 mg/ml without DES were obtained with immobilized CALBL.

Trials with the hydrophilic polyols fructose and glycerol revealed that the solubility of the polyols is high in DES; however, the water adsorbing effect of DES does not positively influence esterification yield and does not suppress fatty acid formation in transesterification reactions. Hence, DES induced equilibrium shifts are substrate dependent and the positive effects found for alcohols ranging from long chain fatty alcohols to polar methanol cannot be transferred to all lipase substrates.

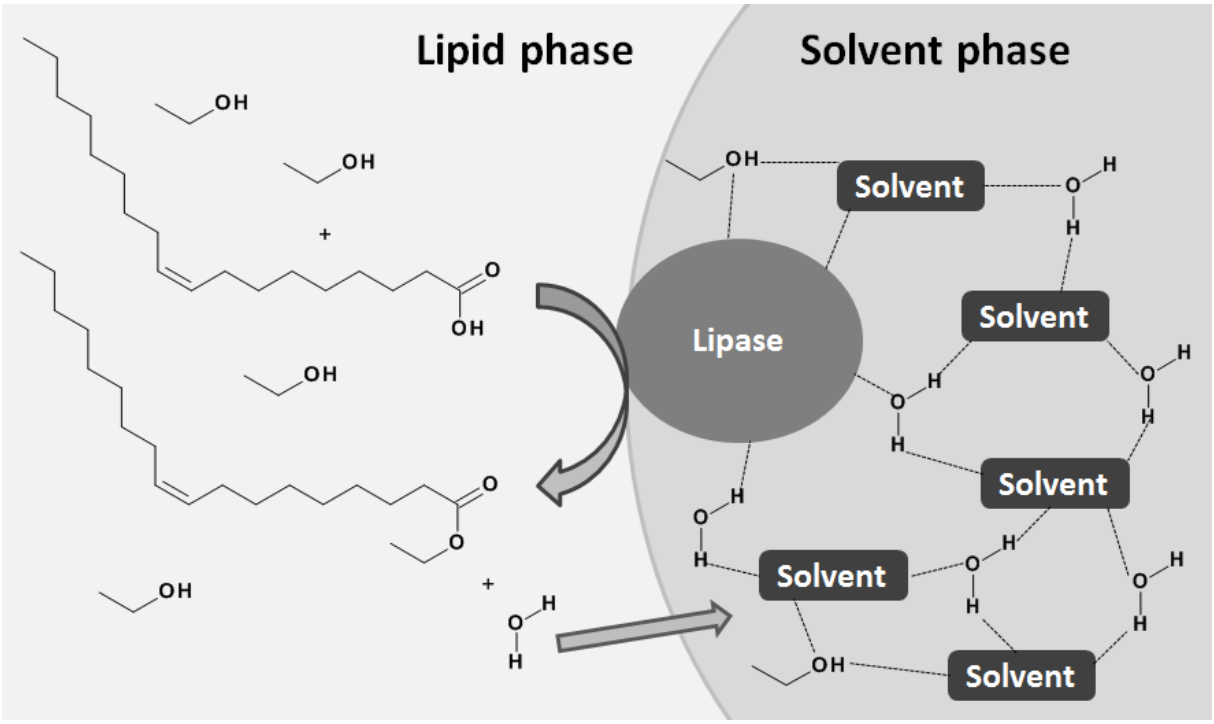

Fig. 4: Scheme of esterification of oleic acid with ethanol as model for biodiesel deacidification. Water is more strongly adsorbed to the hydrophilic phase than the polar alcohol ethanol and the equilibrium is shifted towards ethyl oleate synthesis.

Table 2: LogP values for solvents and substrates used for ester synthesis and transesterification

Substance	logP (S+logP)	logP (MlogP)	Substance	logP (S+logP)	logP (MlogP)
Lauric acid	4.9	2.8	Glycerol	- 1.9	- 1.4
Oleic acid	7.2	4.3	Fructose	- 2.5	- 2.5
Decanol	4.1	2.9	ChCl:U	< - 2	< - 2
Ethanol	- 0.3	- 0.2	ChCl:G	< - 2	< - 2
Methanol	- 0.7	- 0.8	ChCl:F	< - 2	< - 2
Water	- 1.1	- 2.1	2-methyl-2-butanol	0.9	1.2

Analysis of logP values of substrates and solvents (Table 2) can explain the varying effects of DES in dependence of alcohol substrates. While the polar alcohols methanol and ethanol are more hydrophobic than water, logP values of glycerol and fructose are comparable to or even lower than that of water. Therefore partitioning of substrates and water into the lipid and DES phases will be different; for substrates less polar than water a relative increase in substrate to water ratio in the lipid phase is expected, while for substrates similar in logP no significant changes of substrate to water ratio in the lipid phase are predicted. An increase of substrate to water ratio in the lipid phase favors esterification, which was observed for all substrates less polar than water. In contrast no shift towards esterification is expected for hydrophilic polyols and additionally hydrophilic substrate concentration will be low in the lipid phase in the presence of DES, which results in a decreased ester synthesis in comparison to the 2M2B solvent system, which dissolves significant amounts of hydrophilic polyols. The solubility effect is not counterbalanced by the better overall solubility of fructose or glycerol in DES.

Conclusions

DES are suitable solvents for lipase catalyzed esterification and transesterification reactions, which influence esterification yield and fatty acid byproduct formation in dependence of substrate polarity. While no positive effects were observed for hydrophilic polyols with logP values similar to water, an increase in esterification yield was obtained for all polar and non-polar alcohols with logP values higher than water. Thus we could show that the two-phase reaction system is well suited for esterification and transesterification reactions with substrates more hydrophobic than water.

References

[1] Y. Shimada, Y. Watanabe, T. Samukawa, A. Sugihara, H. Noda, H. Fukuda, Y. Tominaga, Conversion of vegetable oil to biodiesel using immobilized *Candida antarctica* lipase, J. Am. Oil Chem. Soc.76, (1999) 789–793.

[2] T. Tan, J. Lu, K. Nie, L. Deng, F. Wang, Biodiesel production with immobilized lipase: a review, Biotechnol Adv. 28 (2010) 628–634.

[3] B. Chen, J. Hu, E.M. Miller, W. Xie, M. Cai, R.A. Gross, *Candida antarctica* Lipase B Chemically Immobilized on Epoxy-Activated Micro- and Nanobeads: Catalysts for Polyester Synthesis, Biomacromolecules 9(2008) 463–471.

[4] C. Ortiz, M.L. Ferreira, O. Barbosa, J.C.S. dos Santos, R.C. Rodrigues, Á. Berenguer-Murcia, L.E. Briand, R. Fernandez-Lafuente, Novozym 435: the “perfect” lipase immobilized biocatalyst?, Catal. Sci. Technol., 9 (2019) 2380–2420.

[5] U.T. Bornscheuer, Lipase-catalyzed syntheses of monoacylglycerols, Enz. Microb. Technol.17 (1995) 578-586.

[6] R.T. Otto, H. Scheib, U.T. Bornscheuer, J. Pleiss, C. Syldatk, R.D. Schmid, Substrate specificity of lipase B from *Candida antarctica* in the synthesis of arylaliphatic glycolipids, J. Mol. Catal. B: Enz. 8 (2000) 201–211.

[7] T. Kobayashi, Lipase-catalyzed syntheses of sugar esters in non-aqueous media, Biotechnol. Lett. 33 (2011) 1911–1919.

[8] C. Carboni-Oerlemans, P. Dominguez de Maria, B. Tuin, G. Bargeman, A. van der Meer, R. van Gemert, Hydrolase-catalysed synthesis of peroxycarboxylic acids: Biocatalytic promiscuity for practical applications, J. Biotechnol. 126 (2006) 140–151.

[9] V. Gotor-Fernández, E. Busto, V. Gotor, *Candida antarctica* Lipase B: An Ideal Biocatalyst for the Preparation of Nitrogenated Organic Compounds, Adv. Synth. & Catal.348 (2006) 797–812.

[10] G. Hills, Industrial use of lipases to produce fatty acid esters. Eur. J. Lipid Sci. Technol. 105 (2003) 601–607.

[11] M.B. Ansorge-Schumacher, O. Thum, Immobilized lipases in the cosmetics industry. Chem. Soc. Rev. 42 (2013) 6475-6490.

[12] O. Thum, K.M. Oxenbøll, Biocatalysis – A Sustainable Method for the Production of Emollient Esters, SOFW Journal 134 (2008) 44-47..

[13] U. Schörken, P. Kempers, Lipid biotechnology: Industrially relevant production processes, Eur. J. Lipid Sci. Technol. 111 (2009) 627-645.

[14] S. Busch, P. Horlacher, S. Both, A. Westfechtel, U. Schörken, Green synthesis routes towards triglycerides of conjugated linoleic acid, Eur. J. Lipid Sci. Technol. 113 (2011) 92-99.

[15] A.P. Abbott, G. Capper, D.L. Davies, R.K. Rasheed, V. Tambyrajah, Novel solvent properties of choline chloride/urea mixtures. Chem. Commun.. 1, (2003) 70–71.

[16] J.T. Gorke, F. Srienc, R.J. Kazlauskas, Deep Eutectic Solvents for *Candida Antarctica*, ACS Symposium Serie, 1038 (2010) 169-180.

[17] E. Durand, J. Lecomte, B. Baréa, G.E. Piombo, E. Dubreucq, P. Villeneuve, Evaluation of deep eutectic solvents as new media for *Candida antarctica* B lipase catalyzed reactions, Process Biochem. 47 (2012) 2081–2089.

[18] E. Durand, J. Lecomte, P. Villeneuve, Deep eutectic solvents: Synthesis, application, and focus on lipase-catalyzed reactions, Eur. J. Lipid Sci. Technol. 115 (2013) 379-385.

[19] P. Xu, G. Zheng, M.Zong,N. Li, W. Lou, Recent progress on deep eutectic solvents in biocatalysis. Bioresour.. Bioprocess. 4 (2017) 34.

[20] M. Pätzold, S. Siebenhaller, S. Kara, A. Liese, C. Syldatk, D. Holtmann, Deep Eutectic Solvents as Efficient Solvents in Biocatalysis. Trends Biotechnol. (2019) 10.1016/j.tibtech.2019.03.007.

[21] H. Zhao, G.A. Baker, S. Holmes, New eutectic ionic liquids for lipase activation and enzymatic preparation of biodiesel, Org. Biomol. Chem. 9 (2011). 1908–1916.

[22] H. Zhao, C. Zhang, T.D. Crittle, “holine-based deep eutectic solvents for enzymatic preparation of biodiesel from soybean oil, J. Mol. Catal. B: Enz. 85–86 (2013) 243–247.

[23] Z.L. Huang, B.P. Wu, Q. Wen, T.X. Yang, Z. Yang, Deep eutectic solvents can be viable enzyme activators and stabilizers, J. Chem. Technol. Biotechnol. 89 (2014) 1975–1981.

[24] E. Durand, J. Lecomte, B. Baréa, P. Villeneuve, Towards a better understanding of how to improve lipase catalyzed reactions using deep eutectic solvents based on choline chloride, Eur. J. Lipid Sci. Technol. 116 (2014) 16–23.

[25] B. Kleiner, U. Schörken, Native lipase dissolved in hydrophilic green solvents: A versatile 2-phase reaction system for high yield ester synthesis, Eur. J. Lipid Sci. Technol. 117 (2014) 167–177.

[26] Y. Watanabe, T. Nagao, Y. Nishida, Y. Takagi, Y. Shimada, Enzymatic production of fatty acid methyl esters by hydrolysis of acid oil followed by esterification, J. Am. Oil Chem. Soc. 84 (2007) 1015–1021.

[27] B. Kleiner, P. Fleischer, U. Schörken, Biocatalytic synthesis of biodiesel utilizing deep eutectic solvents: A two-step-one-pot approach with free lipases suitable for acidic and used oil processing, Process Biochem., 51 (2016) 1808-1816.

[28] M. Persson, I. Mladenoska, E. Wehtje, P. Adlercreutz, Preparation of lipases for use in organic solvents, Enz. Microb. Technol. 31 (2002) 833-841.

[29] Deutsche Einheitsmethoden zur Untersuchung von Fetten, Fettprodukten, Tensiden und verwandten Stoffen (DGF standard methods), 2nd Edition. Wissenschaftliche Verlagsgesellschaft Stuttgart; (2015) ISBN 978-3-8047-3024-3.

[30] EN 14214:2012: Liquid petroleum products - Fatty acid methyl esters (FAME) for use in diesel engines and heating applications - Requirements and test met

Process development and process monitoring of landfill leachate treatment in combination with complementary long-term addition of process water from fermenter

Nitesh Babu Annepogu, Christoph Steiner, Astrid Rehorek

TH Cologne Computer Science and Engineering: metabolon Institute

Abstract

Before transporting the landfill leachate to municipal wastewater treatment plant it has to be treated in a landfill leachate treatment plant, as it comprises high concentrations of ammonium. The elimination of ammonium load in the leachate is usually done by the combined processes of nitrification and denitrification with a specially adapted biocenosis in the activated sludge (AS). For each of the steps, specialized bacteria such as *Nitrosomonas*, *Nitrobacter* and *Paracoccus* are used to transfer the ammonia to gaseous nitrogen. The aim of this investigation was to find suitable process parameters for a complementary treatment of fermentation water from a biogas plant together with landfill leachate. The processed water of the biogas plant consists of a higher concentration of ammonium and carbon sources or easily degradable volatile fatty acids. It can save the usage of external carbon source (acetic acid) and additionally it could also compensate the missing volumes of leachate in times of low rain and low leachate flows. To maintain the high workload for the existing leachate treatment pilot plant (LTPP), a combined treatment of landfill leachate and process water is also of economic and of ecological interest. The long-term adaption process of the biocenosis needs to be done step-by-step. Innovative process monitoring is needed to prevent biocenosis collapse. In our study, we present our set-up, a closer look at the ongoing experiment and the long-term changes in the biocenosis.

1. Introduction

Since earlier days, landfills are most common methods of organized waste disposals and remained so in many regions of the world [1]. In Germany in Rheinische-Bergisch, Oberbergischer Kreis in Lindlar Remshagen, there is such a landfill, the so-called Leppe landfill. The Bergischer Abfallwirtschaftsverband (BAV) operates this landfill since 1982. The landfill site produces approximately 400 m^3 leachate water per day [2]. This leachate water has to be treated before transporting it to the municipal wastewater treatment plant in Bickenbach, as it contains a high amount of nitrogen compounds. A classical wastewater treatment plant alone cannot clean it, because those are mainly designed for the reduction of mainly carbon containing organic compounds.

In most cases, the main source of the landfill leachate water is rainfall, Ground-water inflow, surface water runoff, and biological decomposition also lead to the production of landfill leachate water [3]. The composition of the leachate can vary depending on the landfill age [4]. During the years, the landfill leachate changes itself due to the different decomposition in the plant (Table 1).

Table 1: Landfill leachate classification vs. age [5]

	Young	Medium	Old
Age (year)	<1	1-5	>5.0
pH	<6.5	6.5-7.5	>7.5
COD (g L^{-1})	>15	3.0-15	<3.0
BOD_5/COD	0.5-1	0.1-0.5	<0.1
TOC/COD	<0.3	0.3-0.5	>0.5
NH_3-N (mg L^{-1})	<400	400	>400
Heavy metals (mg L^{-1})	>2.0	<2.0	<2.0
Organic compound	80% VFA	5-30% VFA+ HA+FA	HA+FA

1.1 Activated sludge process

The activated sludge process is the most extensively used biological process for municipal and industrial wastewater treatments [6]. It is a process of utilizing microorganisms to convert organic matter into carbon dioxide, water, and inorganic compounds [7]. There are a lot of different bacteria and protozoa in activated sludge, the sum of all organisms and their life together in this ecological system is called “biocoenosis”. This biocoenosis describes the interaction of all organisms in the system. It is subjected to a continuous change in the amount and the composition of the bacteria as an adaption to varying substrates in their feed. Different process parameters can lead to a different composition. As an example, also the temperature dependency of bacteria could be mentioned. For different temperatures, different bacteria can survive and/or have their thermal optimum [8].

1.2 Nitrification and denitrification

Nitrification is the first essential step in the removal of the ammonium from landfill leachate water. The process in an aerated reactor with activated sludge in which ammonia is oxidized to nitrite (with ammonia-oxidizing bacteria and archaea) and nitrite to nitrate (nitrite oxidizing bacteria and archaea) is called nitrification. A simplistic chemical equation for the whole process is outlined in Table 2.

Equation 1: Nitrification [9]

Ammonia oxidation	$NH_4^+ + 1{,}5\ O_2 \rightarrow NO_2^- + H_2O + 2H^+$
Nitrite oxidation	$NO_2^- + 0{,}5\ O_2 \rightarrow NO_3^-$
Nitrification	$NH_4^+ + 2\ O_2 \rightarrow NO_3^- + H_2O + 2H^+$

Denitrification is the second step in the nitrogen elimination process. It is a microbial process of reducing NO_3 to Nitrogen gas (N_2) by facultative heterotrophic bacteria [6]. The denitrification process takes several steps with different enzymes. No oxygen but an external carbon source is needed. It can be expressed as a redox reaction.

Equation 2: Denitrification [9]

Denitrification $2\ NO_3^- + 10\ e^- + 12\ H^+ \rightarrow N_2 + 6\ H_2O$

With	NH_4^+	=	Ammonia	*with*	O_2	=	Molecular oxygen
	NO_2^-	=	Nitrite-Ion		H^+	=	Hydrogen proton
	NO_3^-	=	Nitrate-Ion		e^-	=	Electron
					H_2O	=	Water

1.3 Pilot plant for landfill leachate treatment

The pilot plant (semi-technical scale) used for landfill leachate treatment is a scale-down of the industrial plant from BAV and a scale-up of the lab scale leachate water treatment plant.

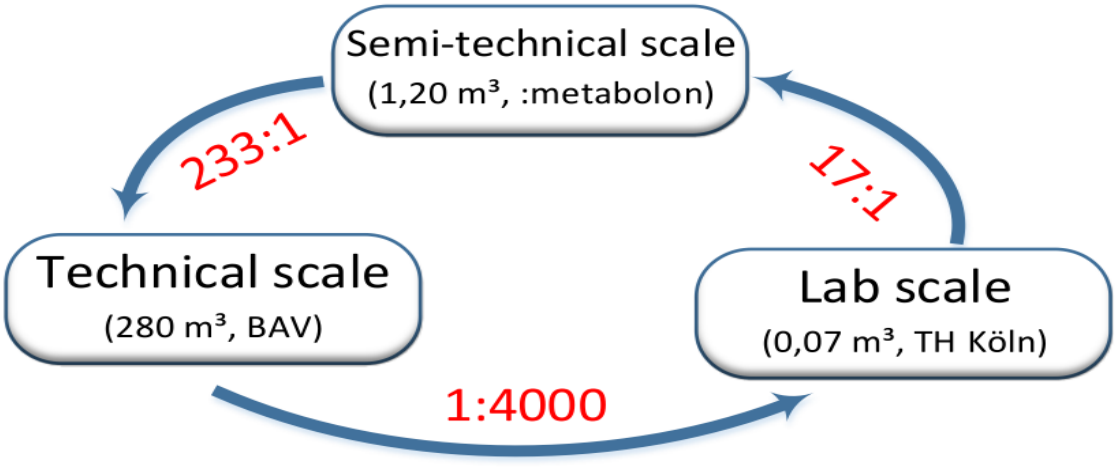

Figure 1: Different volumes of the plants and volumetric scale up factors [10]

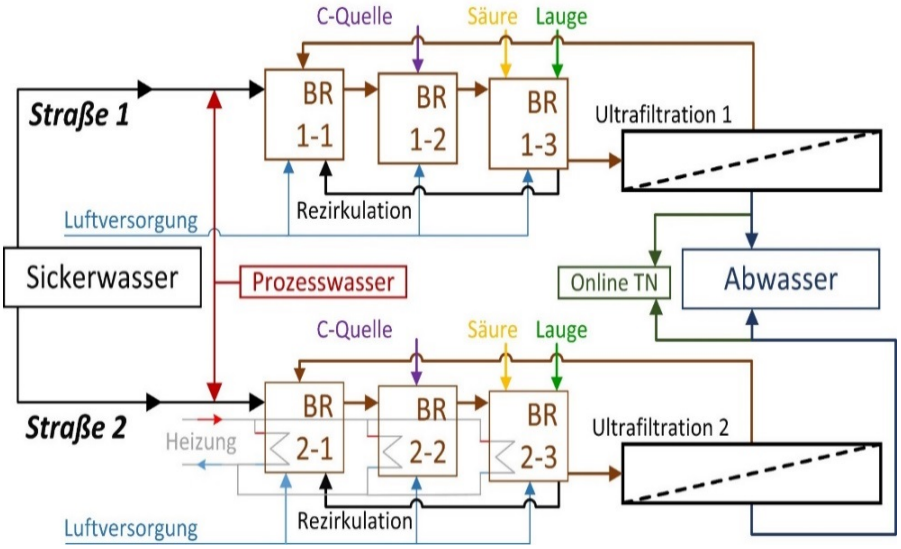

Figure 2: Schematic representation of Pilot plant [11].

As shown in Figure 2 the pilot plant for landfill leachate treatment was designed in two lanes (street 1 & street 2). A direct and valid scientific comparison between two different process strategies is possible. In the pilot plant data management software, automation with LabVIEW and enhanced analytical tools are used, as shown in following picture (Figure 3).

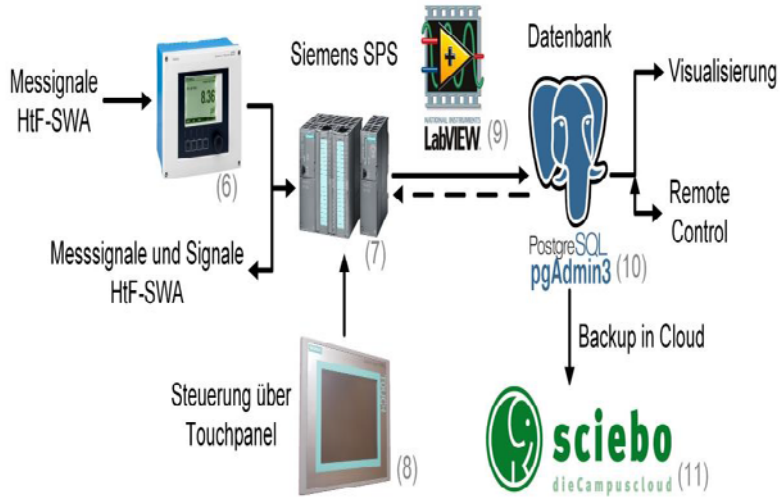

Figure 3: Simplified and general presentation of the data flow of the Pilot plant [11]

1.4 Process water from biogas plant

Generally, the water generated during the processes such as softening, demineralization biogas and others. operations are known as process water. According to the German law, purification of this contaminated water has to be done before transporting it to municipal wastewater treatment plant. In the area of wastewater purification, process water is defined as wastewater from sludge thickening and sludge dewatering on sewage treatment plants with anaerobic sludge stabilization [12]. In this study, the process water was obtained from the research site: metabolon i.e. from fermentation and composting plant (AVEA). The combined fermentation and composting plant went into operation in 1997 and utilized

approx. 660,000 tons of bio-waste by the end of 2017. This resulted in a production of electricity. The completion of additional tunnel composting has increased the processing capacity from 45,000 tons to 75,000 tons since the end of 2018 [11].The anaerobic digestion is carried out according to so called Valorga method under mesophilic conditions (temperature about 40 ° C). The organic material is fermented with a residence time of about 28 days.

After some required separations, the obtained bio waste is transferred to a mixing unit. Subsequently, the stream is diluted with water and pumped into the fermentation tank. The cylindrical fermentation tank is divided by a middle wall with an inlet and outlet on opposite sides. The wall rotates around its own axis and pushes the biomass around in a circle until it overflows into a collecting container. The cylinder also consists of a plate with nozzles for blowing air from the bottom. As the biomass rots, it slowly moves upwards by the rotating wall but remains in the reactor for a certain period and the gas is expelled. The gas is collected at the top and the overflowing biomass is dewatered and processed. The gas is burned for energy. As shown in figure 4, the process water obtained after belt filtration was used in this study.

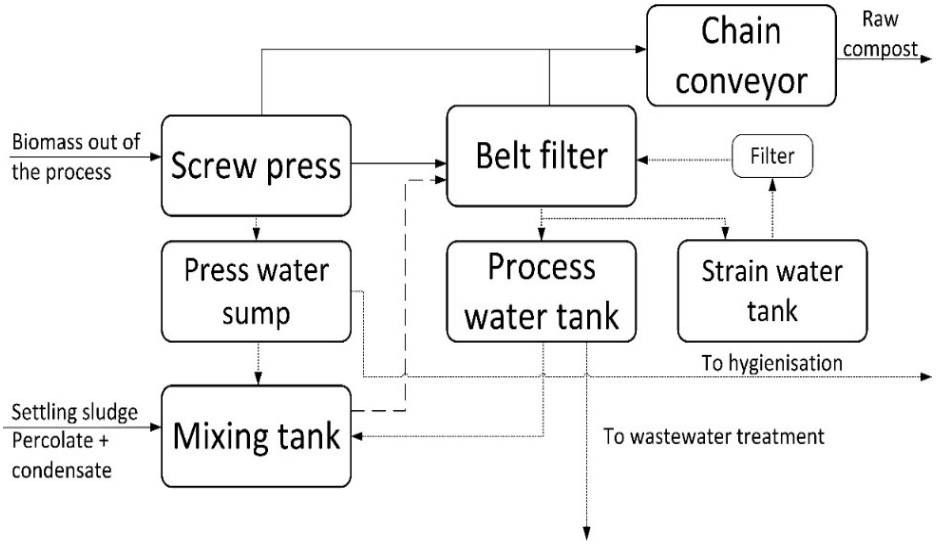

Figure 4: Process water tank was the sample collection point in biogas plant.

1.5 Objectives:

- Optimizing the leachate treatment pilot plant with two identical streets for the experiment of long-term adaptation of micro biocenosis with fermentation wastewater (process water).
- Monitoring the nitrogen metabolism in both streets during the entire experiment.
- Investigating the morphology of the activated sludge by light microscope.
- Examining the particle size of the activated sludge floc.

In this investigation street one (S1) was used to treat process water (PW) and leachate whereas, S2 (control) was used only for leachate treatment. The PW share was increased periodically in S1 from 1.01 % (v/v) to 48,78 % (v/v) (Phase 1) and then ammonium load was increased by increasing the inflow rate (stress test) (Phase 2). The NH_4-N load of 500 mg/L (approx) was maintained in both streets during phase 1. In phase 2 (stress test) NH_4-N load was gradually increased to examine the stress phase of biological process in pilot plant.

2. Material and Methods

During the leachate water treatment, several factors can influence the efficiency of the activated sludge process and can show a huge influence on the results. Certain parameters of the pilot plant, like pH, redox potential, dissolved oxygen are continuously monitored and maintained in the range for efficient treatment. Some of the necessary materials are mentioned in the following tables.

Table 2: Chemicals and equipment for pilot-scale tests

Chemical / unit	Manufacturer	Purity / Specs	item number
Acetic acid	Brenntag	60%, technically	-
Microbalance	Core	ACJ 320-4M	WB12AC0129
Microscope	Zeiss	Axio Lab A1	3136005267
Microscope (camera)	Zeiss	Axio cam 105 color	10000007517
Muffle furnace	Nabertherm	LT 9/11 / C450	352447
Particle analyser	Ankersmid	Eyetech	09501101
Phosphoric acid	Brenntag	75% strength,technically	-
Photometer laboratory	Hach & Lange	DR 6000	1524699
Photometer	Hach & Lange	DR 2800	1264930
Buffer solution	Merck	pH 7.00	1.99057.0500
Buffer solution	Merck	pH 4.00	1.09445.0500
Ultrapure water plant	Werner	Nanopure®	383337-113
Sulphuric acid	Merck	98%	1.12080.2510
Syringe Filters	MN	Chromafil CA_45 / 25	729027
Drying cabinet	Memmert	UN 55	B212.0472
RE water system	Werner	AQUADEM ®	20 SDF
Libra technical	PCE	TS-150	T150325024

centre			
Webcam	Vimtag	VT 361	1JFEGBP1JCA
Centrifuge laboratory	Hermle	Z 326 K	66130235
Centrifuge	Hettich	EBA 20, 6,000 rpm	008547
Landfill leachate		From technical scale plant	
Activated sludge		From technical scale plant	
Process water		Avea (fermentation and composting plant)	

Table 3: Analysis directly associated with the pilot plant

Device name	Parameter	Manufacture	Installation
Cerabar M PMC51	Level [%]	Endress + Hauser	BR 1-3, BR 2-3
Cerabar T. PMP 131	Pressure sensor [bar]	Endress + Hauser	UF S1 + S2
CondumaxCLS21D	Conductivity [µS / cm]	Endress + Hauser	Inlet S1 + S2 Sequence S1 + S2
Dipsy's CPA-4-0A	Redox potential [mV]	Endress + Hauser	BR 1-1, BR 2-1
ISEmax CAS 40D	NH_4+ , NO_3 , K^+ , Cl^- [mg / L]; pH	Endress + Hauser	BR 1-2, 1-3 BR 2-2, 2-3
Liquicap T FMI21	Level [%]	Endress + Hauser	B-2000
Liquipoint FTW32	Measuring leakage via conductivity	Endress + Hauser	10 m³ tanks
Orbsint CPS11D	pH	Endress + Hauser	Inlet S1 + S2 Sequence S1 + S2
OxyMax COS61D	dO2 [mg / L]	Endress + Hauser	BR 1-1, 1-3 BR 2-1, 2-3
Promag 50H	Flow rate [L / min]	Endress + Hauser	Recirculation S1 + S2 Inlet S1 + S2
TMR 31	Temperature [° C]	Endress + Hauser	BR 1-1, 1-2, 1-3 BR 2-1, 2-2, 2-3
Turbimax CUS52D	Turbidity [FTU]	Endress + Hauser	Sequence S1 + S2
QuickTOCN ®	TOC, DOC	LAR	Offline
Multi meter	Various	WTW	handheld instrument

FDO925	DO_2 measurement	WTW	handheld instrument
SenTix® 940-3	pH measurement	WTW	handheld instrument

Table 4: Devices of the pilot plant

Device name	Parameter	Manufacture	Installation
Ecoline	ISM1079	Ismatec	Pump PW
Frequency converter for stirrers	-	Lenze ACTech	Tank PW
Gala 1000 PVT200	0-12.33 mL / h	Prominent	C source S1 + S2 Acid + alkali S1 + S2
MA II 5-230	Max: 95 L / min	Lutz	Logistics DSW / VAB
Movitec VSF6 / 5B	104.33 L / min	KSB	ultrafiltration S1 + S2
OXYFLEX-MT300 coarse-bubble	0.07 m² gassing area	Subratec	Membrane aerators of all reactors
Rapid R3	1,568 L / min	Verderflex	Logistics DSW
Stirrer	-	SIMIX	Tank VAB
SK 1282AFSH-63L / 4 GMF 0.18 / 78	Rotary-speed stirrer 100 ± 1 * 1	RVT	Agitator of all reactors Motor of all reactors
Smart S10	0-1.7 L / min	Verderflex	Inlet S1 + S2 recirculation S1 + S2
PLC * 2	S7-300	Siemens	HtF -SWA
PLC * 2	S7-300	Siemens	UF
Tank VAB	250 liters	-	Tank VAB
Touch panel	KTP 1000	Siemens	HtF -SWA
Touch panel	TP 700	Siemens	UF
Transport tanks (IBC)	1000 liters	Various	Logistics DSW
Ultrafiltration membranes	0.51 m^2	Memos	Ultrafiltration S1 + S2

2.1 Photometric tests

For the analysis of NH_4-N, NO_2-N, NO_3-N, and COD during biological treatment processes a photometric test is performed by a photometer with Hach-Lange cuvette test (see Table 5). 10 ml sample was collected in centrifuge tubes from the reactors twice a week and

centrifuged for 5 min at 60000 Us^{-1}. The supernatant obtained after centrifugation were collected in plastic tubes for immediate analysis. If the concentration of the compounds (NH_4-N, NO_2-N, NO_3-N) is higher than the measurement range of the cuvettes (see Table 5), the samples were further diluted (1:2 or 1:5) with deionized water and then measured. Only 2-5 ml of the sample was utilized for the measurements. The remaining sample was stored in a freezer at -20 °C for further use and other analytics.

Table 5: Cuvettes used during the experiments from the company Hach

Measured variable (Ion)	**Abbreviation**	**Method**	**Article No**	**Measuring range**
Ammonium nitrogen (NH_4 -N)	NH_4-N	ISO 7150-1, DIN 38406 E5-1, UNI 11669: 2017	LCK 304 LCK 303	0.015-2.0 mg / L 2.0-47.0 mg / L
Nitrate Nitrogen (NO_3 -N)	NO_3 -N	ISO 7890-1-2-1986, DIN 38405 D9-2	LCK 340	5.0-35.0 mg / L
Nitrite-Nitrogen (NO_2-N)	NO_2-N	EN ISO 26777, DIN 38405 D10	LCK 342	0.6-6.0 mg / L
Total Phosphorus Phosphorus (PO_4-P)	PO_4 -P	ISO 6878-1-1986, DIN 38405 D11-4	LCK 348	0.5-5.0 mg / L
Chemical oxygen demand (COD)	CSB	ISO 15705	LCI 400	0.0-1000.0 mg / L

2.2 Dynamic Image Analysis by EyeTech

To have a better knowledge on activated sludge flocs in the pilot scale plant, the morphology of activated sludge flocs were examined by a dynamic image analyzer (EyeTech) from the company Ankersmid (The Netherlands). With this instrument, even floc size distribution can be evaluated. The floc size distribution gives required information to estimate the particle occurrence frequency in different size ranges. The sludge samples (3 mL) to be analyzed were diluted in 500 mL tap water and measured with ACM 104L fiber measurement cell by pumping the sample continuously through the cell during measurements. The activated sludge sample is collected from all six reactors in S-1 (PW Street) and S-2 (Control Street). The sludge samples were collected with a micropipette. To avoid shear stress to the sludge particles during sample collection, a small portion of the micropipette tip was removed using cutter. The video measurement mode was used in this work; there is a possibility for a user to set up a precise dynamic image analysis so that a method can be developed for measurements.

In this study, the following method was used for all measurements.

- Stirrer speed: Normal
- Dilution:1.5 ml sample in 500 ml tap water
- Illumination: Exposure: 2, Intensity: 8
- Image control: Gain:127, Contrast:255, Brightness:153
- Threshold Range: 0 – 100
- Remove Unfocused: Used, Focus Level = 8
- Pre-processing commands: contrast enhancement, high path medium, histogram equalization
- Morphological commands: remove touching frame objects, fill holes

2.3 Morphological investigation of activated sludge by light microscope

From the first reactors of each street of the pilot plant 50 mL of activated sludge were collected. With the help of a pipette few drops of sludge was placed on a glass slide and a cover slip was placed on the drops; it was ensured that there were no bubbles trapped. The slide was then placed under the Zeiss light microscope (see table 2) for examination. A camera (Axio cam 105 color) from Zeiss was used to capture the images of microorganisms in activated sludge. Throughout the study 40x magnification was used to visualize the microorganisms.

3. Results and discussion:

The results of the NH_4-N concentration in pilot plant over the entire test duration of 532 days are shown in following graph.

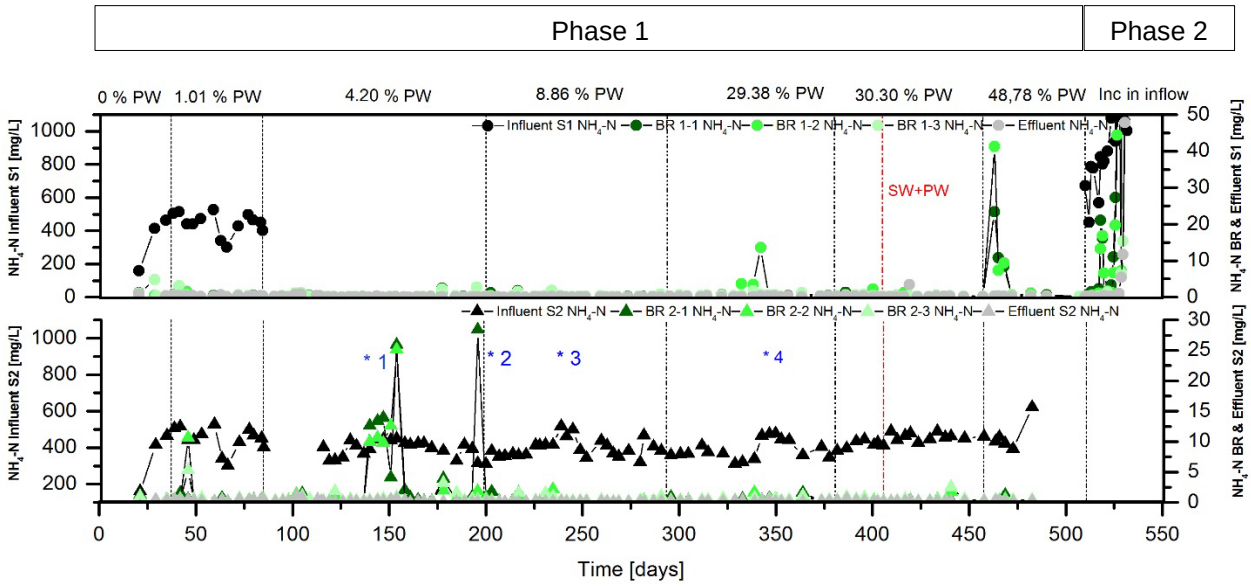

Figure 5: Overview of NH_4-N concentrations over the entire experiment.

The disturbances shown in Figure 5 are explained as follows:

- * 1: Power failure: Failure of various parts of the system during automatic restart.
- * 2: Recirculation pump malfunction: recirculation was stopped.
- * 3: Malfunction of the pump of the PW: Increased volume flow in the Pilot plant.
- * 4: Failure of the compressor for air in the PW Street.

Apart from these system disruptions, a stable operation of the pilot plant was achieved.

As shown in the Figure 5, the complete experiment was divided into two phases. During phase-1 NH_4-N, concentration was approximately 500 mg/L in both street, In PW street the volume of leachate was reduced and PW was used instead to maintain the same ammonium load in both streets. Periodically the volume of leachates were decreased and volume of PW was increased. As shown in Figure 5, PW concentration was increased from 1.01 % (v/v) to 48.78 % (v/v). Later on, the NH_4-N load was increased in street one by increasing the volume of inflow. From day 32 to 407, required volume of PW and leachate were pumped with two different pumps. Later in order to avoid the malfunctioning of PW pump, from day 408 both leachate and PW were mixed in 250 Liters tanks and then pumped accordingly. Except in few cases of disturbances as shown above, NH_4-N degradation was almost comparable in both streets. There was no NH_4-N accumulation in the bioreactors. The micro biocenosis of the activated sludge was successfully adapted by successively increasing the proportion of PW at a constant nitrogen load. The plant could be operated stably up to a share of 48.78 % PW in the total volume flow for 25 days. After a necessary change of the streets by conversion measures and restarting of the plant, the performance of the micro biocenosis was tested in a stress phase. The volume flow was increased gradually with a constant proportion of PW. In the last step of the increase, the inflow of the plant was three times to that of the regular experiment. Furthermore, it was found during the stress test that the Pilot plant functioned stably up to 1.6 times increase in feed stream.

On the other hand, the results obtained from the EyeTech (Figure 6) showed the particles with higher average ferret diameter (AFD) in S1 and comparatively lower AFD particles in S2. The results shown above are the average of 23 measurements of each bioreactor respectively. The bigger particle size in S1 might be due to the large sized waste particles in PW as well as due to green waste. AFD of the sludge particles in S1 were in between 20-520 µm (approximately) whereas, the particles in S2 were in between 20-350µm (approximately). The presence of particles with higher AFD did not showed any negative influence on the nitrogen metabolism.

The microscopic images shown above in the Figure 7 were taken during a period of 8 months. These results showed more filamentous bacteria in S2 than S1. The presence of PW might be toxic to the filamentous bacteria. It is recommended to do further research in these criteria to find out the precise reasons behind the influence of PW on the filamentous bacteria present in the activated sludge of the technical scale plant.

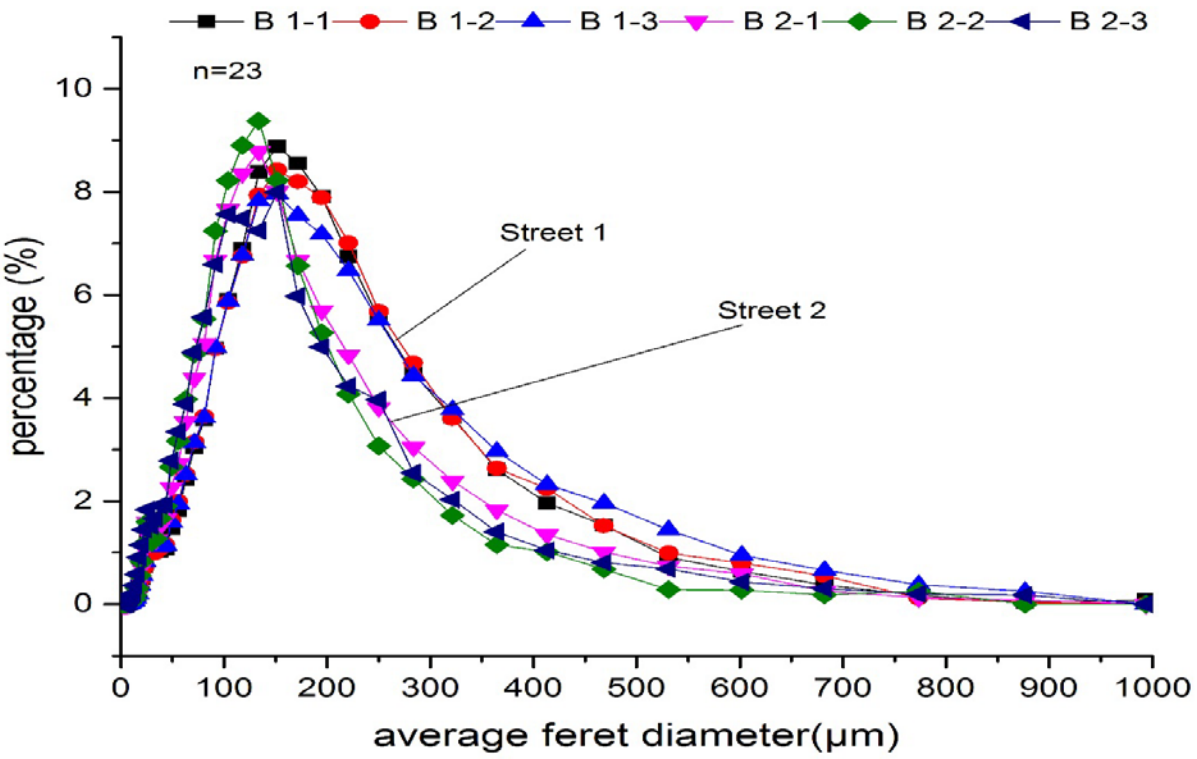

Figure 6: Particle size of the activated sludge flocs in S1 & S2 of pilot plant.

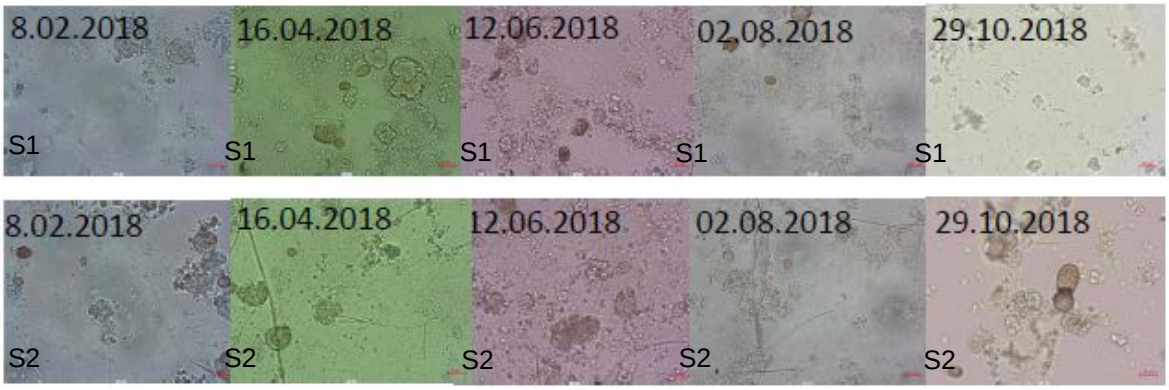

Figure 7: Microscopic images of the activated sludge in the nitrification reactors.

Conclusions

The micro biocenosis of the activated sludge was successfully adapted by successively increasing the proportion of PW at a constant nitrogen load. There were no differences in the process stability of the street with PW compared to the control street. The plant could be operated stably up to a share of 48.78% PW in the total volume flow for 25 days. After a necessary change of the Street and restarting the pilot plant, the performance of the micro biocenosis was tested in stress phase. The volume flow was increased progressively with a constant proportion of PW. In the last step of the increase, the inflow of the plant was three times to that of the regular experiment. Furthermore, it was found during the stress test that the pilot plant functioned stable. The stable plant performance can be confirmed by measurements of the relevant groups of organisms by CenoTox measurements [13].

Although the method still needs to be optimized in terms of aeration time, the analytical process used to assess process stability is helpful. The detailed results regarding this experiment can be found in [13]. The results of EyeTech showed higher AFD particles in S1 but they did not have a negative influence on the ammonia degradation. The above results showed that the combined treatment of PW from fermentation reactor of biogas plant with leachate is possible by suitable adaptation of the biocenosis.

References

[1] Eggen, Moeder, and Arukwe, Municipal landfill leachates: a significant source for new and emerging pollutants., *The Science of the total environment*, no. 21, pp. 5147–5157, Oct. 2010.

[2] Lucht, A., and Rehorek, A., Prozesscharakterisierung im Belebtschlammverfahren einer Labor - Sickerwasseranlage zur Optimierung der Stickstoffeliminierung für eine betriebliche Großanlage Masterthesis, 2015.

[3] Abbas et al., Review on Land fi ll Leachate Treatments, no. 4, pp. 672–684, 2009.

[4] ATV, ATV. pp. 82–87, 1988.

[5] Alvarez-Vazquez, Jefferson, and Judd, Membrane bioreactors vs conventional biological treatment of landfill leachate: A brief review, *Journal of Chemical Technology and Biotechnology*, no. 10, pp. 1043–1049, 2004.

[6] Annepogu, N., The effect of contaminated carbon source on activated sludge process in mini - scale leachate water treatment plant for optimization of an industrial - scale plant Master Thesis, no. January, 2017.

[7] Grady, Daigger, and Lim, Biological wastewater treatment, *Hazardous Waste*, no. 19, p. 1076, 1999.

[8] Gujer, Siedlungs- wasserwirtschaft.

[9] Fuchs, Eitinger, and Schlegel, *Allgemeine Mikrobiologie*. Thieme, 2007.

[10] Steiner, C., Denecke,M., and Rehorek, A., Research in pilot plant scale: Closing the scale up gap in leachate water treatment, in *Wasser*, 2016.

[11] Steiner, C., Rehorek, A., Prozessoptimierung in der Deponiesickerwasserreinigung – Forschung im halbtechnischen Maßstab und Einfluss von Prozessparametern auf die Proteinzusammensetzung in Belebtschlamm.

[12] T. Osthoff, „Weitergehende Abwasserreinigung“, 12-Dez-2016. .

[13] Steiner, C., Rehorek, A., Denecke, Entwicklung in der Deponienachsorge – Forschungs-Sickerwasseranlage im halbtechnischen Maßstab, in Recy&Depotech, 2016, p. 350-356.

Tools for reactor evaluation in bioprocesses

Petri Tervasmäki[1*], Dmitry Gradov[2], Marko Latva-Kokko[3], Tuomas Koiranen[2], Juha Tanskanen[1]

[1] Chemical Process Engineering, University of Oulu, P.O. Box 4000, FI-90014 Oulu, Finland,

[2] School of Engineering Science, Lappeenranta University of Technology, P.O. Box 20, FI-53851 Lappeenranta, Finland

[3] Outotec (Finland) Oy, Outotec Research Center, P.O. Box 69, FI-23101 Pori, Finland

***Corresponding author, Email: petri.tervasmaki@oulu.fi**

Abstract

Aerobic microbial cultivations are industrially important group of processes and pose challenges for the reactor design. In particular, estimation of industrial scale conditions is difficult from laboratory and pilot scale data. Due to complex interaction of gas/liquid phase hydrodynamics, mass transfer parameters and microbial metabolism, both improvement of modelling tools and reactor design are desired. We present an approach to estimate growth conditions in industrial scale reactor by combining black-box metabolic models with CFD-model.

The reactor type used here is Outotec OKTOP9000®, which is used in the industrial hydrometallurgical processes at 900 m^3 scale. It is adopted to a laboratory setting and compared to stirred tank reactor (STR) in gas dispersion, mass transfer and yeast cultivation experiments. In addition, a kinetic model for the yeast growth is developed based on literature sources and validated by the laboratory scale batch cultivations. This kinetic model is used along with CFD-model that is developed to describe the flow and mass transfer conditions in the industrial scale reactor.

The laboratory scale experiments show the feasibility of OKTOP9000® reactor when compared to STR, particularly with improved gas handling capacity. The modelling approach shows qualitatively similar behavior in the large scale simulations when compared to laboratory scale cultivations.

1. Introduction

Aerobic microbial cultivations pose challenges for the design of industrial reactors. One limitation for the process performance is often the interfacial mass transfer rate of oxygen from gas to liquid phase. Furthermore, due to high oxygen demand of the process, air is introduced into the reactors with relatively high flow rate thus affecting the hydrodynamics of the reactor. There are complex interactions between the hydrodynamics, mass transfer parameters and microbial growth. Since the scale of the process affects in a different way for

each phenomena, it is difficult to generalize experimental results obtained in the laboratory scale and use them as a basis for industrial scale designs. [1], [2] Simple scale-up rules are often used to estimate the conditions in the large scale based on the results obtained in the laboratory. The most common scale-independent parameters to describe reactor operation include volumetric power input of agitation (P/V in W/m^3) and superficial gas velocity (v_s in m/s), and dimensionless groups such as Froude number and gas flow number. The common measured/estimated parameters are volumetric mass transfer coefficient k_La and gas volume fraction.

However, even the scale-independent and dimensionless correlations include experimental parameters that are only valid for a narrow range of scales. Thus, the correlations are generally not reliable from 100 liter to 100 m^3 reactor, for example [3]. Furthermore, although superficial gas velocity is a feasible scale-independent parameter to describe the hydrodynamic regime of gas flow, constant v_s results in decreasing volumetric gas input measured in volume gas per volume liquid per minute (VVM). The latter would be a desired approach for scaling up the gas flow in the stoichiometric point of view but would result in too high gas flow when the hydrodynamics are also considered. In fact, in scaling up industrial processes, the value of VVM is usually decreased while v_s is increased so that stirred tank reactors are operated in the loading regime with insufficient gas recirculation at the lowest impeller [4].

Here we present results from studies of new reactor type for industrial scale aerobic microbial processes with modelling approach to estimate the growth conditions in the large scale. The original research has been published in [5]–[7], and the main results are presented here. The reactor used in the studies is Outotec OKTOP9000® reactor with draft tube and a single agitator placed below the draft tube. The impeller creates downward flow inside the draft tube while dispersing inflowing gas, introduced under the impeller, radially. It has been developed for direct leaching of zinc concentrate and designed to have good gas dispersion and mass transfer capacity and bulk liquid circulation at low power input. Laboratory scale experiments for gas dispersion and mass transfer rate are carried out with stirred tank reactor (STR) as a reference. A growth model for oxygen sensitive yeast is developed in the laboratory scale and combined with CFD-model to simulate growth conditions in the industrial scale. The industrial scale reactor and adaptation to CFD-model are presented in Figure 1.

Figure 2. Industrial scale OKTOP®9000 reactor (left) and CAD geometry for large-scale reactor and impeller (right). Adapted with permission from Outotec Oyj

2. Materials and Methods

2.1 Reactor types and mixing / mass transfer experiments

Experiments were carried out in laboratory scale Biostat C (Sartorius, Germany) reactor with a total volume of 15 liters and a diameter of 190 mm. The OKTOP9000® reactor was constructed in the same vessel from stainless steel parts except the impeller, which was 3D-printed from alumina reinforced plastic. Regular stirred tank reactor (STR) with three Rushton turbines was used as a reference, and the reactor geometries are shown in Figure 2. The electrical impedance tomography (EIT) measurements were carried out in plastic (PMMA) vessels with similar geometry as the Biostat C. The 32 electrodes in the EIT-vessel were distributed in four layers (at 4.5, 12.9, 25.5 and 33.9 cm heights) with eight electrodes each. Current injection was made by a modified opposite injection pattern with 0.7 A amplitude at 10 kHz frequency. The EIT-measurements give directly the estimated three-dimensional conductivity distribution, from which the distribution of local gas volume fraction can be estimated by Maxwell model with an assumption that the conductivity of the dispersed phase (air) is zero. Overall gas-liquid mass transfer coefficient (k_La) was estimated

by gas in / gas out experiments using air and nitrogen, respectively. The value for k_La was estimated from the saturation phase using probe response time of 15 s, plug flow model for gas, and ideally mixed assumption for the liquid phase. More detailed procedures are described in [5].

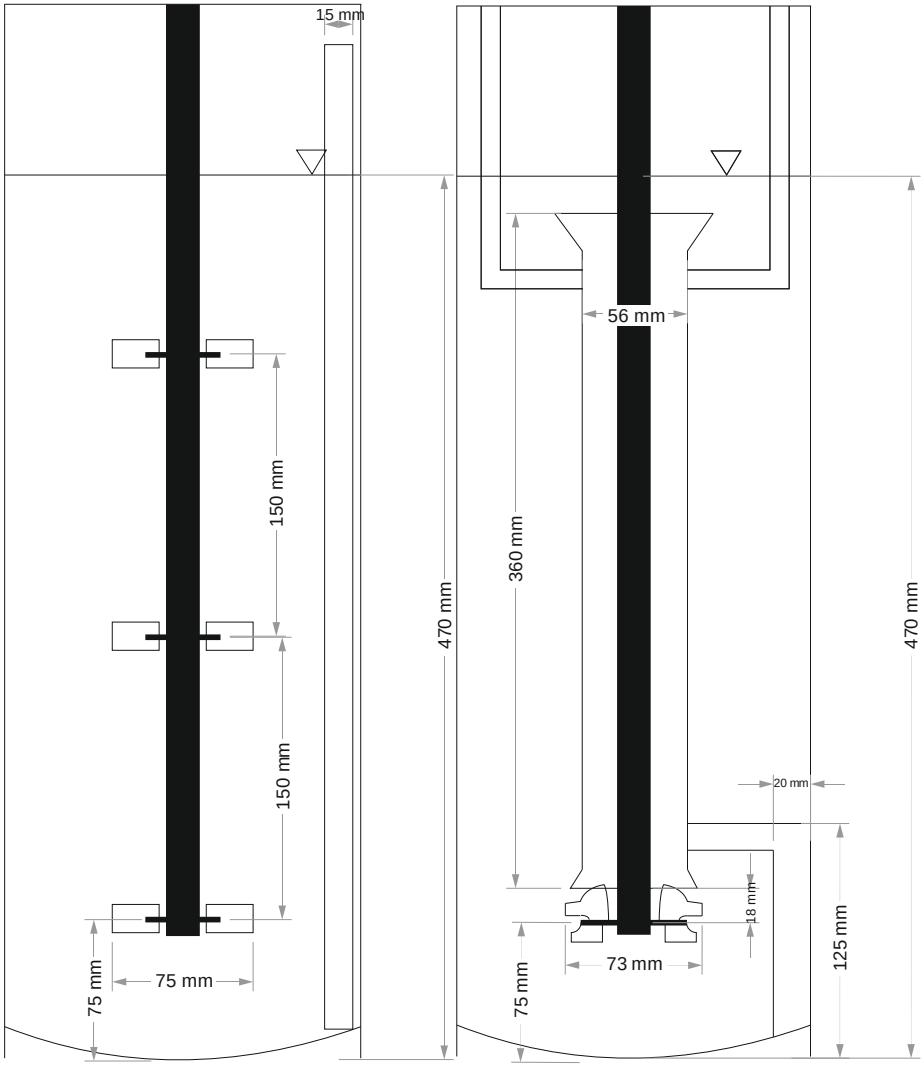

Figure 3. Stirred tank and OKTOP9000® reactor geometries in laboratory scale. Reprinted with permission from Elsevier [5]

2.2 Yeast cultivations

Yeast cultivations were carried out with *Pichia pastoris* X33 yeast strain and basal salt medium (BSM) with PTM_1-trace salt supplement in the reactors described in the previous chapter. Glucose concentration was 80 g/l. Aqueous ammonium hydroxide (25 %) was used to maintain pH between 5.0 – 5.5, pH was measured with EasyFerm Plus pH-electrode (Hamilton, Switzerland) and dissolved oxygen with Oxyferm (at 10 cm from vessel bottom) and Visiferm (at 10 cm from surface) DO-probes (Hamilton, Switzerland). Gas flow rate was maintained at 18 l/min, which results in superficial gas velocity v_s = 0.011 m/s. Agitation rate was 450 rpm (STR) or 650 rpm (OKTOP9000®) which yielded in mixing power of about 500 W/m^3 for each reactor.

2.3 Kinetic model

The full description of the model can be found in [6], and a short summary is presented here. The three metabolic routes are schematically presented in Figure 3 and in equations (1)-(3). The aim is to describe respirative metabolism on glucose (blue, equation (1)), fermentative metabolism on glucose if oxygen supply is limited/unavailable (red, equation (2)), and respirative metabolism on ethanol (purple, equation (3)). The growth kinetics are described with Monod-type equations for the substrate uptake rate (glucose equations (1)-(2) or ethanol equation (3)) with additional terms for oxygen.

$$q_{\mathrm{g}}^{\mathrm{ox}} = \frac{\mu_{\mathrm{max}}^{\mathrm{ox}}}{Y_{\mathrm{xg}}^{\mathrm{ox}}} \frac{c_{\mathrm{g}}}{c_{\mathrm{g}} + K_{\mathrm{g}}} \frac{c_{\mathrm{o}}}{c_{\mathrm{o}} + K_{\mathrm{o}}} \quad (1)$$

$$q_{\mathrm{g}}^{\mathrm{ferm}} = \frac{\mu_{\mathrm{max}}^{\mathrm{ferm}}}{Y_{\mathrm{xg}}^{\mathrm{ferm}}} \frac{c_{\mathrm{g}}}{c_{\mathrm{g}} + K_{\mathrm{g}}} \left(1 - \frac{c_{\mathrm{o}}}{c_{\mathrm{o}} + K_{\mathrm{o}}}\right) \quad (2)$$

$$q_{\mathrm{e}}^{\mathrm{ox}} = \frac{\mu_{\mathrm{max}}^{\mathrm{e}}}{Y_{\mathrm{xe}}^{\mathrm{ox}}} \frac{c_{\mathrm{e}}}{c_{\mathrm{e}} + K_{\mathrm{e}}} \frac{K_{\mathrm{i}}}{c_{\mathrm{g}} + K_{\mathrm{i}}} \frac{c_{\mathrm{o}}}{c_{\mathrm{o}} + K_{\mathrm{o}}} \quad (3)$$

Where q_i is specific rate of component *i* ($g_i\ g_x^{-1}\ h^{-1}$) and x, g, e and o denote cells, glucose, ethanol and oxygen, respectively. K_i is the saturation concentration of Monod-type kinetics, c_i is the concentration of component *i*, and μ_{max} and *Y are parameters for maximum growth rate and yield coefficient.*

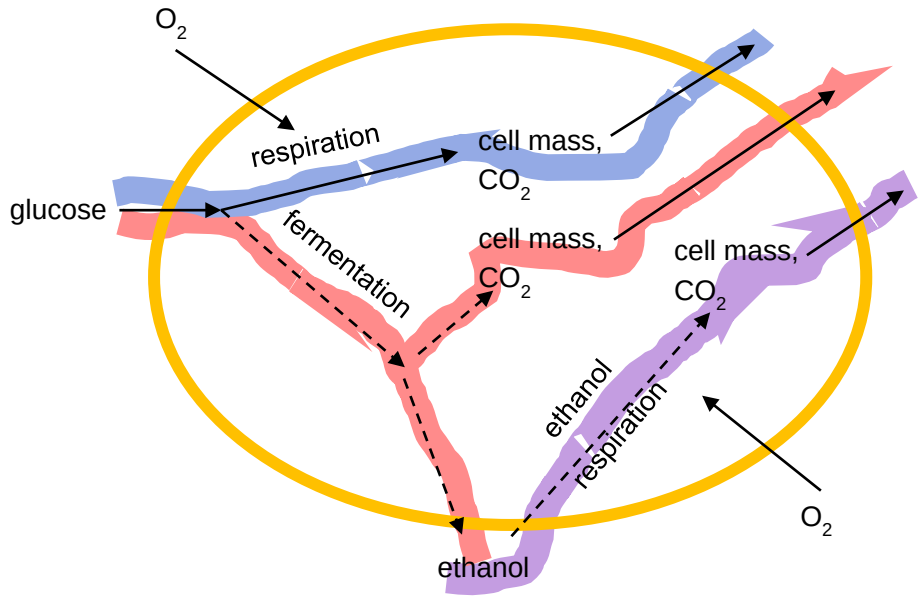

Figure 4. A schematic presentation of the main metabolic routes inculed in the model

2.3 CFD model

CFD-model of industrial scale OKTOP9000® reactor (T = 7.6 m, V = 800 m^3) was developed in ANSYS Fluent 18 with user defined functions to accommodate the yeast growth model. Eulerian-Eulerian multiphase approach was used to simulate gas-liquid flow, and Reynolds-averaged Naviers Stoke's (RANS) with realizable k-ε model was used to model turbulence. More information on the assumptions regarding phase interaction, boundary conditions, the estimation of mass transfer conditions based on the converged CFD-model, and inclusion of the yeast growth kinetics can be found in the original publication [7]. A schematic presentation of the numerical approach is in Figure 4.

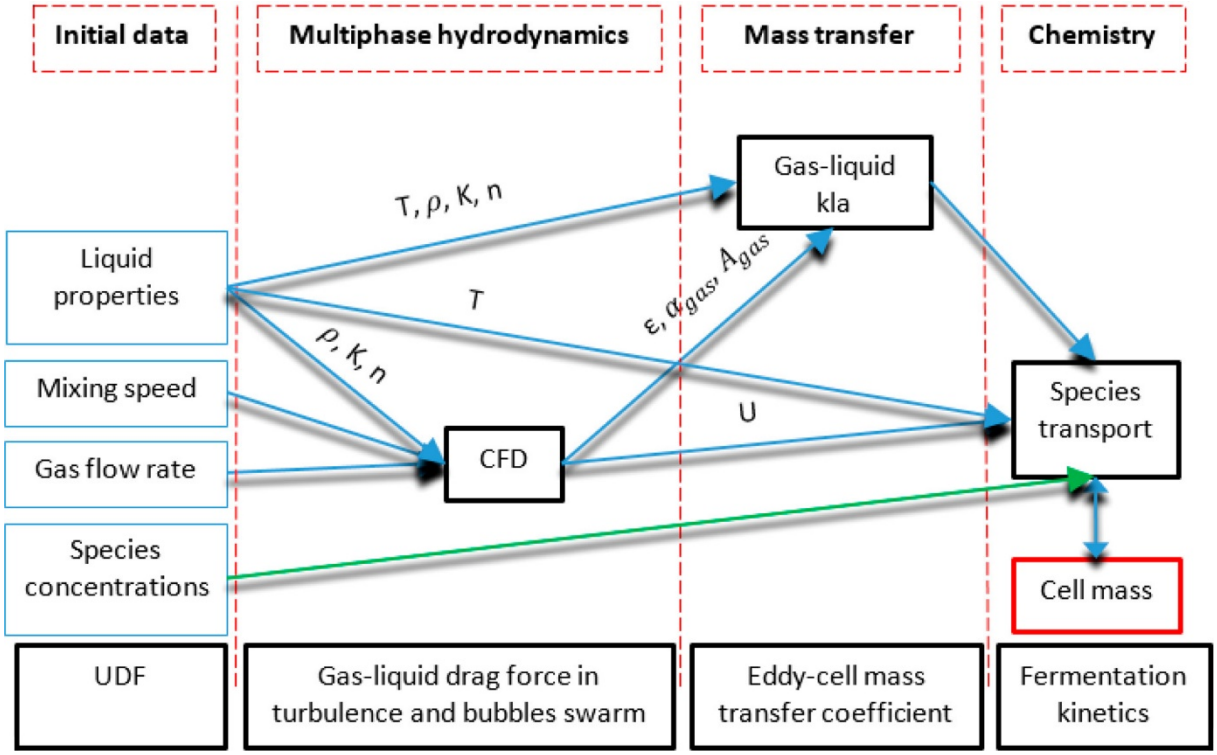

Figure 5. Numerical approach for the combined CFD, mass transfer and yeast growth model simulations. Reprinted from [7] under CC-BY license.

3. Results & Discussion

3.1 Yeast model

The model parameters were estimated based on literature data from chemostat cultivations with varying glucose feed concentration, dilution rate and oxygen content in the inlet gas [8]–[11]. In addition, the reactor setup was different in the experiments and a relative value for k_La was estimated based on the reported geometry and operational conditions. The simulated values for steady-state concentrations of cell mass, ethanol, and dissolved oxygen (DO) are shown in Figure 5. The effect of oxygen content on the concentrations at constant inlet glucose concentrations and dilution rate is shown in (a) and a parity plot for all

experiments in (b). The calibrated model can fit the literature data quite well although there are some deviation especially for the ethanol concentration. For validation, the model was used to predict the time course of batch cultivation with initial glucose concentration of 40 g/l. The agitation and aeration were maintained constant and, thus, a constant value for k_La was assumed. The results are shown in Figure 6 for glucose, ethanol and cell mass (a) and dissolved oxygen (b) concentrations.

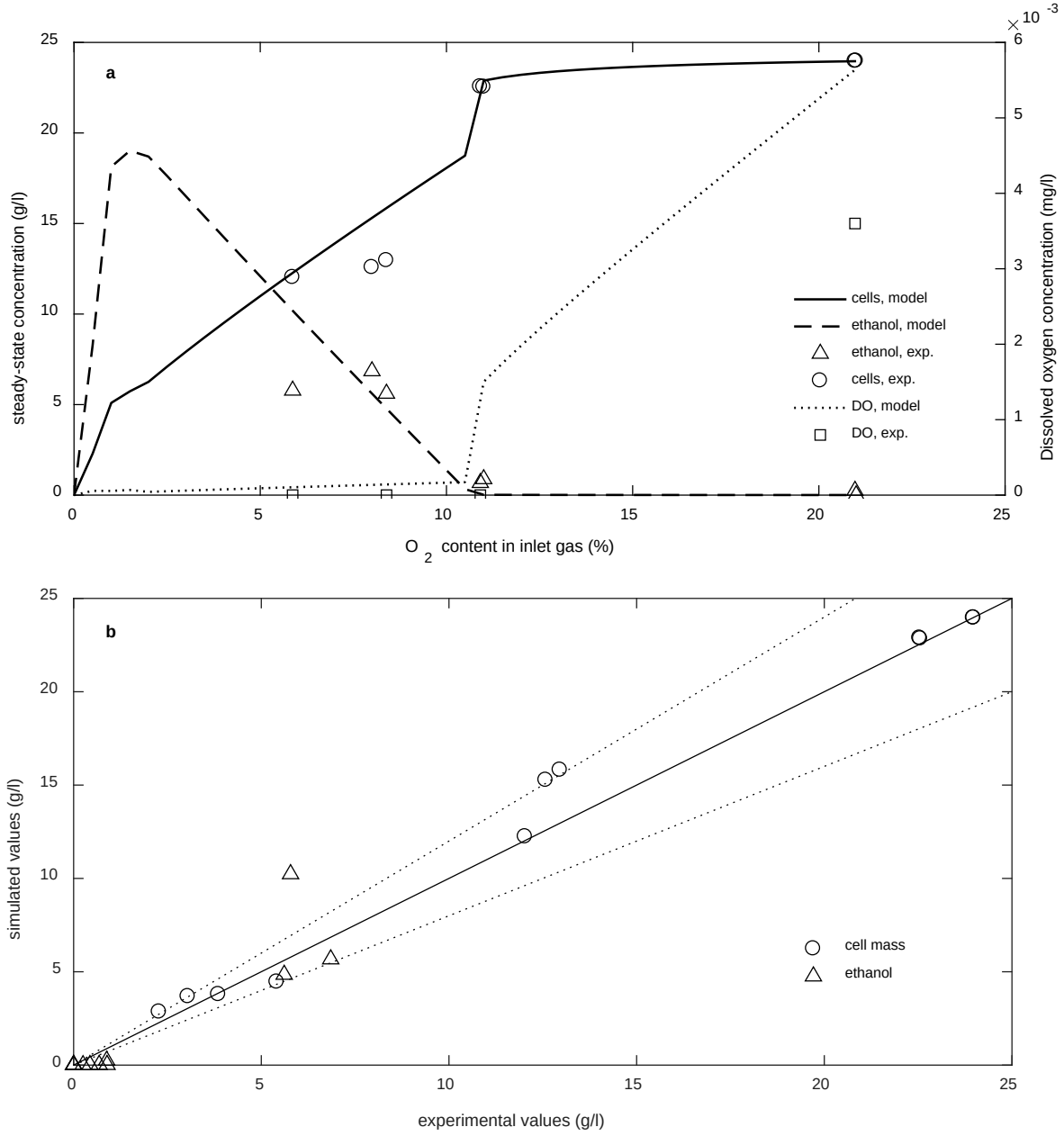

Figure 6. a) Steady-state concentration of cell mass, ethanol and DO (experimental and simulated) gas for $c_{g,in}$ = 50 g/l and D = 0.1 h-1 as reported in [10], [11]. b) Simulated and experimental values for steady-state concentration of cell mass and ethanol in all chemostat cultivation conditions in the literature, dotted lines show +/- 20% margin. Reprinted from [6] with permission from Elsevier.

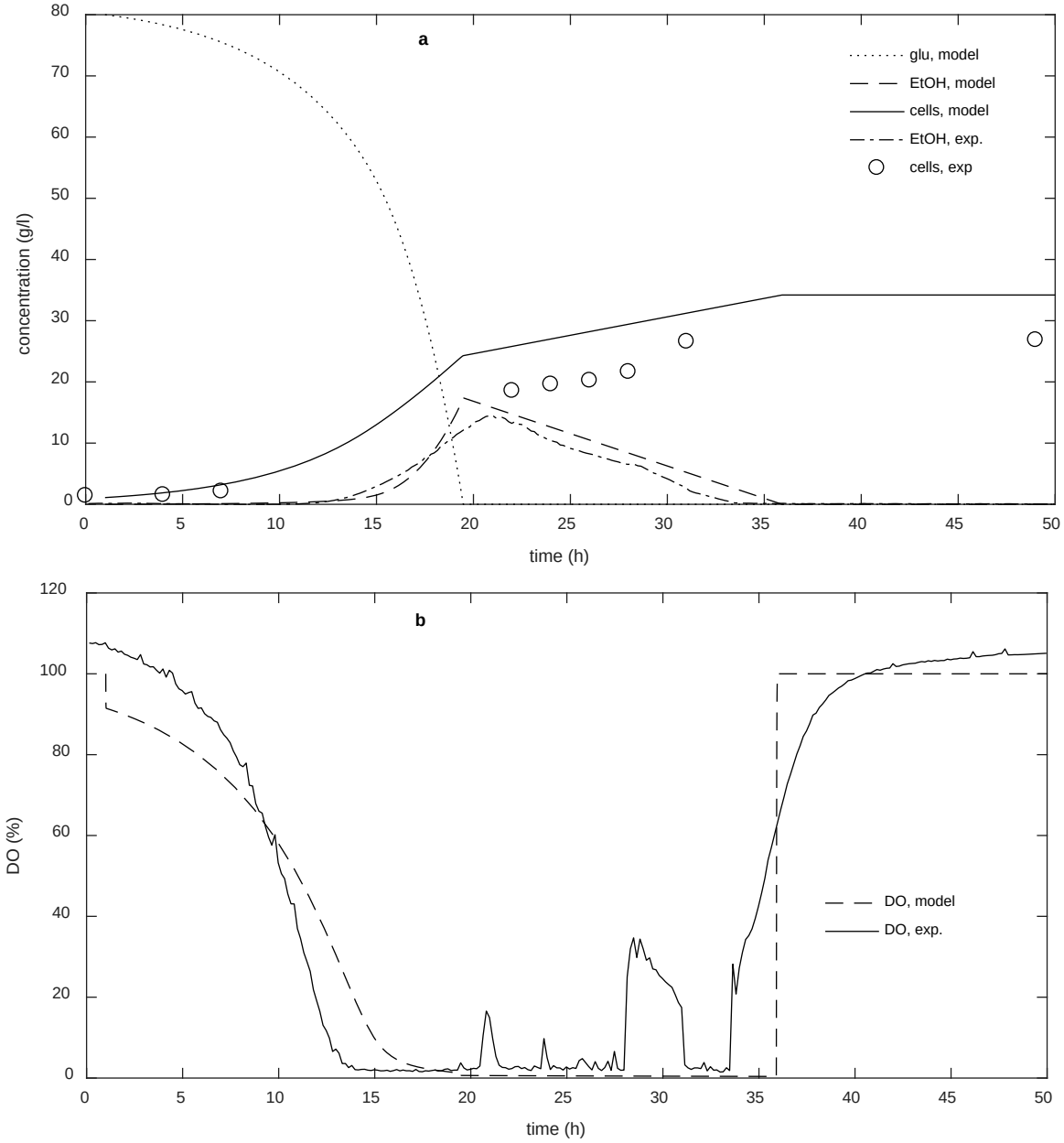

Figure 7. Comparison of model prediction to batch cultivation data in STR, additional lag time of one hour was added to the model prediction. Estimated $k_L a$ for the simulations was 250 h^{-1} a) glucose, ethanol and cell concentration b) dissolved oxygen. Reprinted from [6] with permission from Elsevier.

Three main phases can be distinguished from the batch cultivation. The first phase lasts until about 14 hours, during which glucose is consumed via fully respiratory metabolism. However, due to increase in cell concentration, the dissolved oxygen drops to almost zero, which results in respirofermentative metabolism, during which glucose is utilized to produce both cell mass and ethanol. This phase lasts until 21 hours after which glucose is exhausted, and peak ethanol concentration reaches 14 g/l. After this, until about 34 hours, ethanol is aerobically consumed for cell mass production although with lower growth rate. The model captures well the main phases of the batch cultivation. Only the cell mass is somewhat over

predicted. In addition, the model fails to capture the short peak in dissolved oxygen at 21 when the yeast switches the carbon source from glucose to ethanol. This is expected, as the model does not include detailed metabolism and enzyme kinetics inside the cell. The short increase in DO between 28 and 31 hours is due to temporary increase in the agitation during the experiment, and the model prediction was calculated with constant k_La. Model sensitivity analysis is presented in [6], and a more detailed global parameter analysis and model refinement is being planned for future work.

3.2 Mixing and mass transfer experiments in lab scale

The performance of OKTOP9000® reactor was tested in the laboratory scale and compared to traditional STR with three Rushton turbines. The results for gas distribution with constant agitation rate and varying gas feed rates are presented in Figure 7 for both reactor types. The results were averaged over the whole measurement volume and are presented as two-dimensional plane. One can directly see that the gas hold-up is more uniform in the STR whereas the gas is more concentrated on the bottom part in the OKTOP9000® reactor. However, due to more efficient overall circulation and less compartmentalization, the uneven distribution of gas is not necessarily a downside. Complete dispersion is achieved only with the lowest gas flow rate for both reactors. This was confirmed visually, and can be interpreted from the EIT-measurements as it is the only measurement at which the highest gas hold-ups are detected below the impeller plane and extending near the reactor wall.

With increasing air flow, the bubbles are not fully recirculated in the lower parts of the reactors. Increasing the air flow in the OKTOP9000® reactor shifts the highest gas volume fractions more in the annulus part around the draft tube. For the STR, the effect is more drastic as the lowest impeller is loaded with no significant radial distribution of the gas. For the highest gas flow, the gas is fully distributed only at the highest impeller which can be seen as the gas hold-up is concentrated in the upper part. It should be noted that the spatial resolution of the EIT-measurements is not high enough to catch very high volume fractions at the center of the reactor or around the impeller blades. The measurements of k_La are presented in Figure 8 for the whole measurement range, and the values for P/V = 500 W/m^3 are in the range of 0.04 – 0.07 s^{-1}.

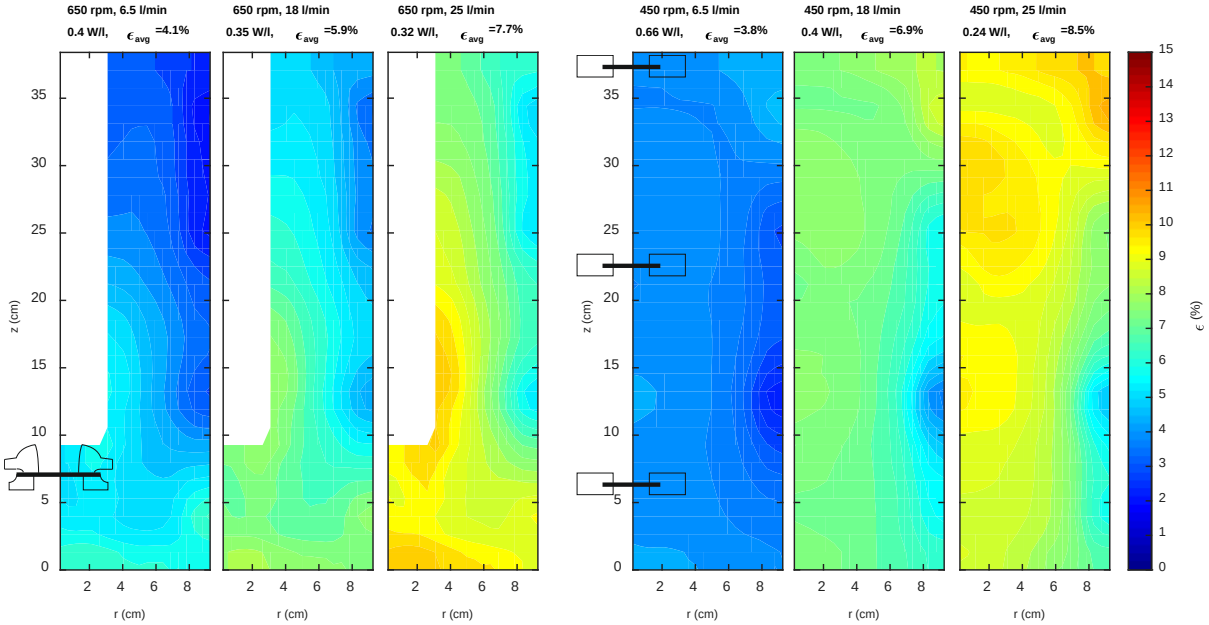

Figure 8. EIT results with constant agitation rate and varying gas flow rate for OKTOP9000® (left) and STR (right). The gas flow rates 6.5, 18 and 25 l/min correspond to v_s of 0.004, 0.011 and 0.015 m/s.

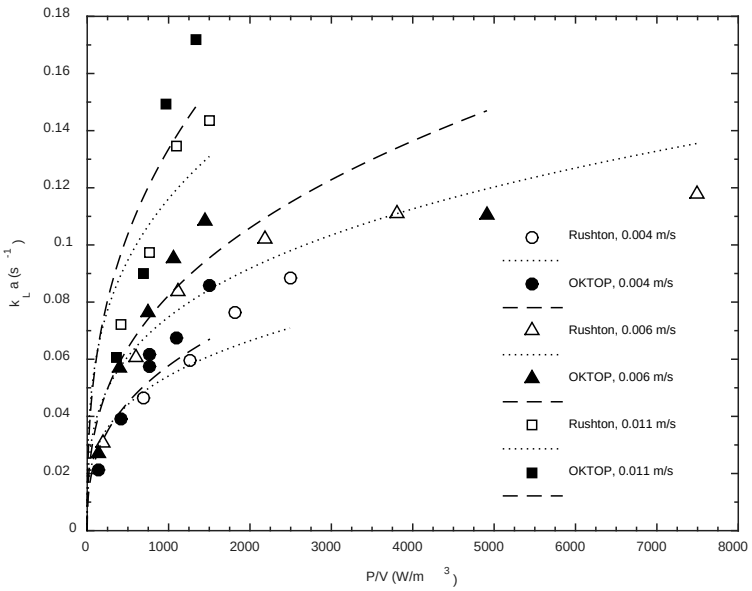

Figure 9. Estimated kLa-values from gas in / gas out experiments. Reprinted from [5] with permission from Elsevier.

3.3 OKTOP CFD model & simulations

The CFD-model was simulated with gas flow rates of 0, 2000, 4000 and 6000 m3/h, corresponding to superficial gas velocities of 0, 0.012, 0.024 and 0.037 m/s. The stirrer speed was 60 rpm, corresponding to volumetric power input of about 500 W/m^3. The corresponding liquid flow velocities are presented in Figure 9. The radial flow from the impeller is pushed upward by the gas flow, and this effect is more significant with increasing gas flow. It can also be seen that the downward flow velocity inside the draft tube decreases

with increasing gas flow. Near the solution surface, the flow velocities are more affected by the gas escaping the liquid.

For the estimation of mass transfer and cultivation conditions, additional values were estimated from the CFD-simulation. Sauter mean diameter (d_{32}) of the bubbles and local k_La are presented in Figure 10. The bubble size is at minimum in the most turbulent regions of the radial flow near the impeller and higher values are found under the impeller and in the central area close to the liquid surface. It can also be noted that the increase in gas flow increases the bubble size below the impeller, which results from the lower liquid velocities (Figure 9). Similar trends can be seen for the specific mass transfer coefficient in Figure 10. Highest values for k_La are near the impeller. The increase in gas flow rate increases the values especially in the upper part of the annulus and in the draft tube of the reactor.

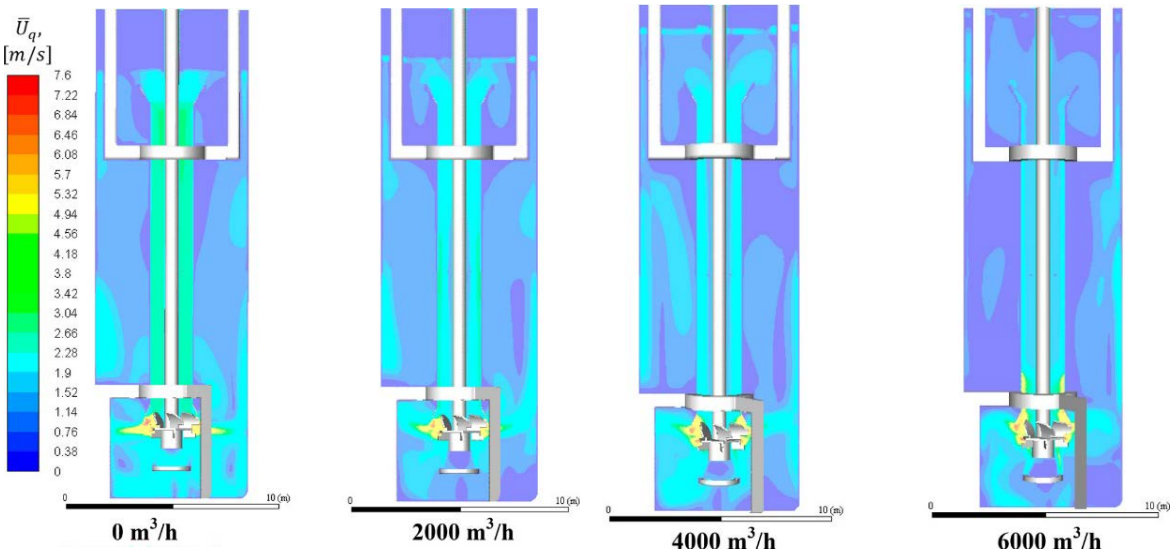

Figure 10. Liquid flow velocity in the converged CFD-simulations with varying gas flow rate. Reprinted from [7] under CC-BY license.

Finally, the growth model of Pichia pastoris and the CFD-models were combined to simulate a batch cultivation in the industrial scale reactor with the approach shown in the Figure 4. The initial conditions were similar as for the laboratory cultivations with initial glucose and cell concentrations of 80 g/l and 2 g/l, respectively. The results are presented in Figure 11 for glucose, ethanol and cell concentrations. The batch simulations were carried out with the gas flow rates reported previously (2000, 4000 and 6000 m_3/h), and the experimental values from laboratory cultivations are included in the figure. The simulations in the CFD-model follow qualitatively the results from the laboratory experiments. Similar phases of batch process can be distinguished. Ethanol is produced in the beginning of the process due to oxygen limitation, and ethanol is consumed in the later phase. Moreover, the maximum ethanol concentration depends on the gas flow rate and less ethanol is produced in the simulations with increasing gas flow, resulting in better oxygen transfer conditions.

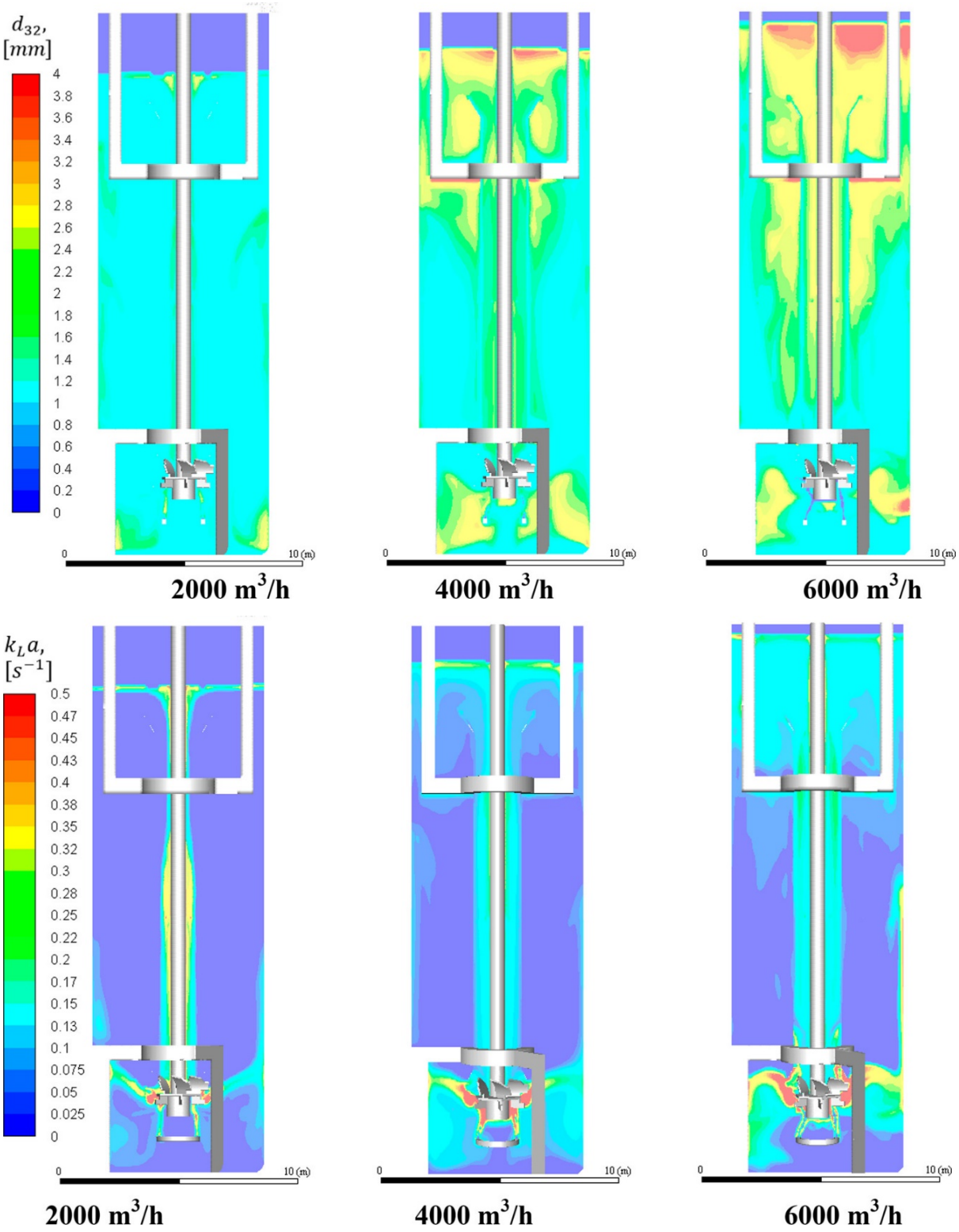

Figure 11. Mean sauter diameter (d_{32}, upper row) and $k_L a$ (lower row) estimated from the CFD-simulations with varying gas flow rate. Reprinted from [7] under CC-BY lisence.

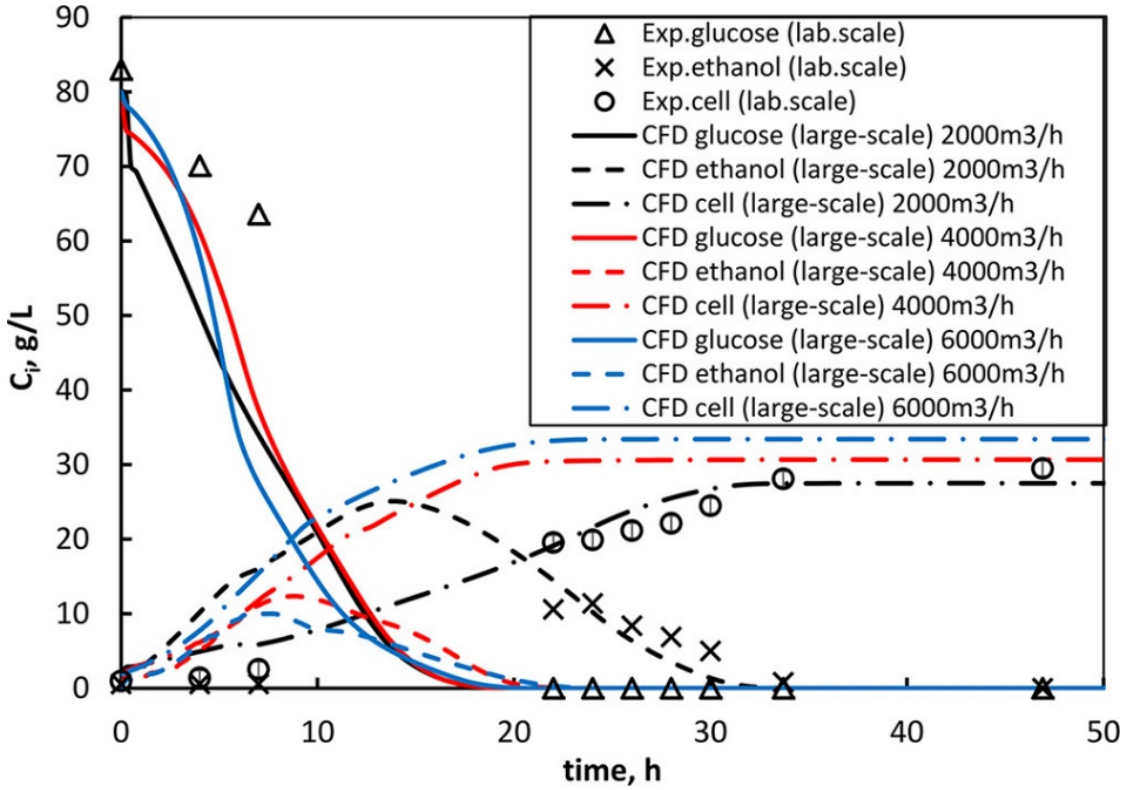

Figure 12. Time-course data from the simulations of batch cultivation with varying gas flow rate. Reprinted from [7] under CC-BY lisence.

Conclusions

In the studies presented above, we have developed and validated a growth model for Pichia pastoris in the laboratory scale. Furthermore, the reactor concept of OKTOP9000® draft tube reactor was adopted for laboratory scale in which it performed well in mixing and mass transfer experiments when compared to regular STR. CFD-model was implemented to simulate flow conditions in the industrial scale OKTOP9000® reactor with estimation of relevant mass transfer parameters. By adopting the growth model into the CFD-model, we simulated time course data of batch yeast cultivation. These results showed qualitative agreement with the laboratory scale cultivation data. The validation of the CFD-model and the refinement of yeast growth model are left for future work.

Acknowledgements

The authors are grateful to the Finnish Funding Agency TEKES and, in particular, to Outotec Finland Oy and Neste Engineering Solutions Oy collaborating under FERMATRA project (908/31/2016 and 958/31/2016), for active supervision and financial support.

References

[1] F. Garcia-Ochoa and E. Gomez, 'Bioreactor scale-up and oxygen transfer rate in microbial processes: An overview', *Biotechnology Advances*, vol. 27, no. 2, pp. 153–176, 2009.

[2] F. Garcia-Ochoa, E. Gomez, V. E. Santos, and J. C. Merchuk, 'Oxygen uptake rate in microbial processes: An overview', *Biochemical engineering journal*, vol. 49, no. 3, pp. 289–307, 15 2010.

[3] E. K. Nauha, O. Visuri, R. Vermasvuori, and V. Alopaeus, 'A new simple approach for the scale-up of aerated stirred tanks', *Chemical Engineering Research and Design*, vol. 95, pp. 150–161, 2015.

[4] E. K. Nauha, Z. Kálal, J. M. Ali, and V. Alopaeus, 'Compartmental modeling of large stirred tank bioreactors with high gas volume fractions', *Chemical Engineering Journal*, vol. 334, pp. 2319–2334, Feb. 2018.

[5] P. Tervasmäki, M. Latva-Kokko, S. Taskila, and J. Tanskanen, 'Mass transfer, gas hold-up and cell cultivation studies in a bottom agitated draft tube reactor and multiple impeller Rushton turbine configuration', *Chemical Engineering Science*, vol. 155, pp. 83–98, Nov. 2016.

[6] P. Tervasmäki, M. Latva-Kokko, S. Taskila, and J. Tanskanen, 'Effect of oxygen transfer on yeast growth — Growth kinetic and reactor model to estimate scale-up effects in bioreactors', *Food and Bioproducts Processing*, vol. 111, pp. 129–140, Sep. 2018.

[7] D. V. Gradov *et al.*, 'Numerical Simulation of Biomass Growth in OKTOP®9000 Reactor at Industrial Scale', *Ind. Eng. Chem. Res.*, vol. 57, no. 40, pp. 13300–13311, Oct. 2018.

[8] M. Carnicer *et al.*, 'Quantitative metabolomics analysis of amino acid metabolism in recombinant Pichia pastoris under different oxygen availability conditions', *Microbial Cell Factories*, vol. 11, p. 83, Jun. 2012.

[9] A. Solà, H. Maaheimo, K. Ylönen, P. Ferrer, and T. Szyperski, 'Amino acid biosynthesis and metabolic flux profiling of Pichia pastoris', *European Journal of Biochemistry*, vol. 271, no. 12, pp. 2462–2470, Jun. 2004.

[10] K. Baumann *et al.*, 'A multi-level study of recombinant Pichia pastoris in different oxygen conditions', *BMC Syst Biol*, vol. 4, p. 141, Oct. 2010.

[11] K. Baumann, M. Maurer, M. Dragosits, O. Cos, P. Ferrer, and D. Mattanovich, 'Hypoxic fed-batch cultivation of Pichia pastoris increases specific and volumetric productivity of recombinant proteins, *Biotechnol. Bioeng.*, vol. 100, no. 1, pp. 177–183, May 2008.

The extracurricular learning environment at :metabolon - an authentic learning site for knowledge transfer and lifetime learning

Yannick Bucklitsch[1], Marc Härtkorn[1]

[1] Extracurricular learning site :metabolon, waste disposal centre Leppe, Lindlar, Germany*

***Correspondence:** :metabolon c/o waste disposal centre Leppe, Am Berkebach 1, 51789 Lindlar, E-Mail: yb@bavmail.de, mhk@bavmail.de, Internet: www.metabolon.de

The project

Fig. 1. Aerial image of the waste disposal centre

The whole site of the waste disposal centre Leppe in Lindlar has been modified by the project :metabolon into an authentic learning site for knowledge transfer. Addressing all age groups, the project offers insights into environmental knowledge and explains contexts of resources and material flows. The site conditions allow practical outlooks on future energy systems. Following the meta theme of "lifetime learning", pupils and students are addressed by different modules, considering their individual learning levels.

That learning landscape has been shaped hand in hand with surrounding education institutions to enhance the project. The formation of networks with partners of industry, craft, research and education facilitates the exchange in respect to specific demands and enables the view beyond individual horizons.

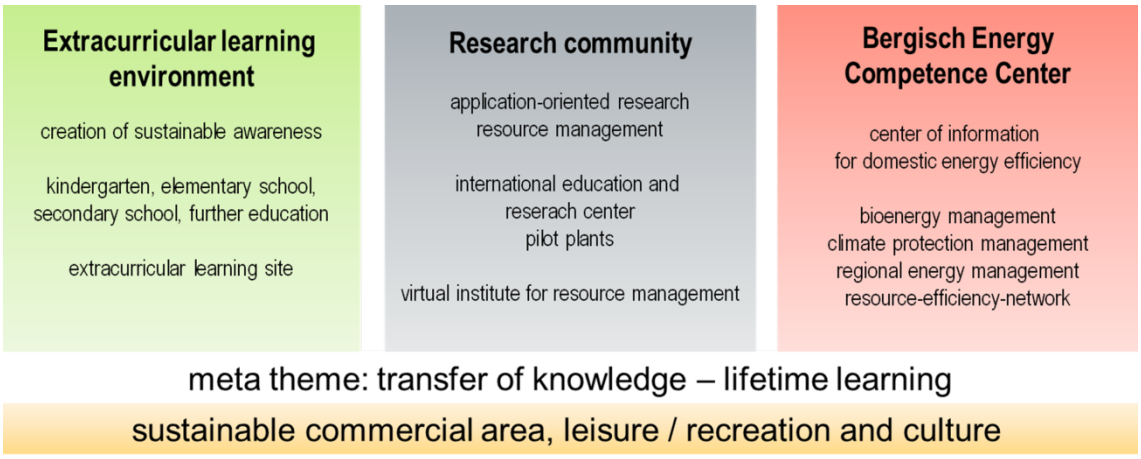

Fig. 2. Project structure of :metabolon

Extracurricular learning environment

By means of different initiatives like “Haus der kleinen Forscher”-network for day care centers and primary schools, supported by the Hans Hermann Voss foundation, all ages of children and students can be reached. For primary and secondary education, extracurricular learning sites and school labs have been installed and interlinked with offers for vocational trainings and academic education. By means of playful learning as well as informative communication systems, visitors can increase their knowledge in site related topics like waste management, re- and upcycling, resources efficiency,- sufficiency or sustainability. Also the utilization of renewable energies can be experienced directly on site.

The different offers of the extracurricular learning site :metabolon are starting with content for pre- and primary school. The provided topics are broken down age-appropriate to enable a first sustainable contact with the themes waste prevention and -recycling, resources and renewable energies. A playful approach and connections to situations of reality allow a better understanding of the topics.

Fig. 3 Impressions of the extracurricular learning site

For secondary school the offered topics are covered more intensely. Pupils are getting motivated to compile different issues in small working groups and to scrutinize topic related processes. The promotion of natural sciences and sensitization for the topics environment, resources and future energy systems are subjects at the students lab “MINT LAB”. This extracurricular learning site is a consistent progression with the aim to delight pupils for natural and technical topics. In addition the pupils learn more about their future opportunities by starting a study or an apprentice-ship within the field of natural or technical sciences.

For qualified teachers the topics of the extracurricular learning site provide a wide range for integration into school education. The attending of the extracurricular learning site is a practical and useful addition to common school life.

Acknowledgements: The project is sponsored by the European Regional Development Fund.

Nitrification monitoring – Determination of bacterial groups in a biocoenosis with selective inhibition and oxygen uptake rate measurements

Christoph Steiner*[1,2], Nitesh Annepogu[1], Lara Schluckebier[1], Astrid Rehorek[1,2]

[1] University of Applied Sciences Cologne, teaching and research center :metabolon,

Am Berkebach 1, 51789 Lindlar, Germany

[2] Institute for Sustainable Technologies and Computational Services for Environmental and Production Processes (STEPs), University of Applied Sciences Cologne, Betzdorfer Str. 2, 50679 Köln, Germany

*Corresponding author: christoph.steiner@th-koeln.de

Keywords: Oxygen uptake rate, Nitrification, selective inhibition, bacterial groups

Abstract

In the degradation of ammonia (NH_4^+) to gaseous nitrogen (N_2), the nitrification is one of the two reaction steps. The nitrification itself is divided in two steps and is performed by two different types of bacteria. Current literature has shown that there are types of bacteria, which have the genetic equipment to perform both steps in one bacteria. Nevertheless, in wastewater and landfill leachate treatment, ammonia-oxidizing organisms (AOO) and nitrite-oxidizing organisms (NOO) occur as a symbiosis. The intermediate of the two consecutive reaction steps (NO_2^-, nitrite) is toxic. For this reason, both steps are necessary for the two bacterial groups. To determine the ratio of AOO, NOO and heterotrophic bacteria (which use organic compounds as carbon and energy source) the oxygen uptake rate (OUR) with selective inhibition with N-allylthiourea (ATU) and azide is used. In the inflow of a pilot plant in one street a step by step increased amount of a process water out of a fermentation plant was added to the landfill leachate. For comparison, the other street was supplied only with landfill leachate with the same amount of nitrogen. As a result, comparable values for the different bacterial groups and reproducible results were measured and lead to a better understanding of the analysed nitrification sludge. Deeper understanding of the behavior of the different groups will result in a reduce risk of malfunctions and a more stable operation in the wastewater or landfill leachate treatment plant.

1. Introduction

The nitrogen pathway is very important. Although nitrogen is essential for all organisms, molecular nitrogen is difficult to assimilate. The assimilation is only possible via bacteria, the ions of ammonia (NH_4^+) and nitrate (NO_3^-) or artificial out of N_2 and H_2 via the Haber-Bosch process. Ammonia is a degradation product of wastewater and landfill leachate and leads untreated and without oxygen to eutrophication. The nitrification, the oxidizing of ammonia, can be subclassified in two different steps.

Recent research revealed an identification of organisms, who got the genetic setup to perform both steps alone [1], [2]. Nevertheless, in wastewater and landfill leachate treatment ammonia-oxidizing organisms (AOO) and nitrite-oxidizing organisms (NOO) occur as a symbiosis (Formula 1).

Ammonia oxidizing organisms (AOO)	$NH_4^+ + 1{,}5\ O_2$	→	$NO_2^- + H_2O + 2\ H^+$
Nitrite oxidizing organisms (NOO)	$NO_2^- + 0{,}5\ O_2$	→	NO_3^-
Total reaction/*Comammox*	$\boldsymbol{NH_4^+ + 2\ O_2}$	→	$\boldsymbol{NO_3^- + H_2O + 2\ H^+}$

Formula 1. Reaction steps of the nitrification with AOO, NOO and Comammox.

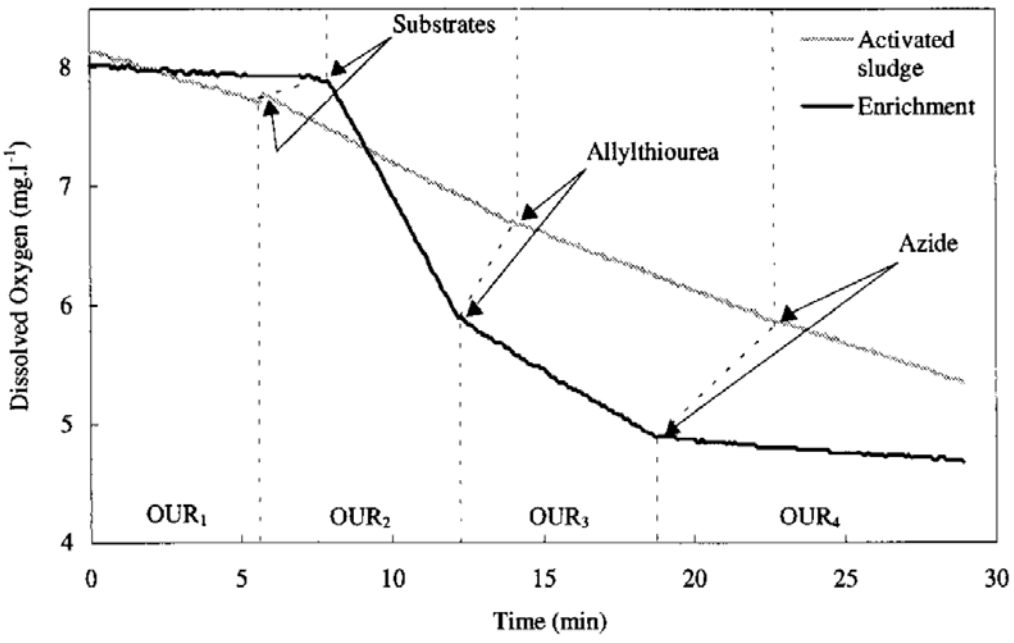

Fig. 1. Different slopes of different OUR with selective inhibition [3]

The treatment of landfill leachate is a continuous operation. The analytics rely on sum parameters such as ion concentration (ammonia, nitrite and nitrate), flow measurement, organic/inorganic dry mass and dissolved oxygen concentration. These parameters are sufficient for a stable operation, but they lack of a deeper understanding of the process. The scope of this research is, to analyse parameters, which are directly connected to the bacterial composition.

For the nitrification, oxygen is crucial. A measurement of the oxygen uptake rate characterizes the process of nitrification. In addition, with selective inhibitors, an estimation of the shares of the different bacterial groups AOO, NOO and heterotrophs is possible. In figure 1, the resulting different slopes of the OURs with inhibition are shown.

The scientific question of the experiment in general was, if the combined treatment of landfill leachate with process water out of a fermentation plant has a short-term and long-term influence on the nitrification. With the pilot landfill leachate treatment plant, a direct comparison between the two streets is possible [4].

2. Materials and Methods

For the experiments with the selective OUR, the Cenotox 2.0 of Dimatec was used. The analytical device does not use model sludge like other devices; the sludge is taken directly out of the process. With the device, an online and atline analysis is possible.

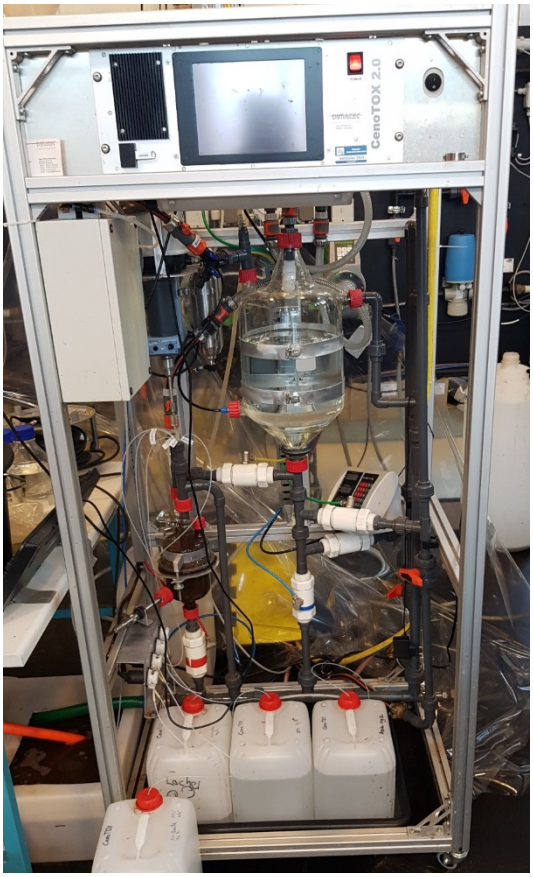

Fig. 2. Picture of the Dimatec Cenotox 2.0

Together with the company Dimatec, the device was improved with the collaboration of TH Cologne. Designed for big scale plants some changes were necessary. In the first method the measurement of all three OURs (simultaneously) lead to loss of a high amount of sludge. Hence, the analytical method was changed from online to atline. In addition, a new software is developed to enable the online measurement.

In figure 2, the Cenotox is shown. The activated sludge is aerated in the big reactor on the top of the picture. Afterwards, the aerated sludge is transferred to the measurement reactor at the bottom. The carbon source, the nitrogen source and the inhibitors are placed on the ground of the device.

According to literature [3] N-Allylthiourea and Azide were used for inhibition. In own experiments we got better results with a concentration of 120 µM ATH and Azide. In contrast, the concentrations of ATH (86 µM, [3]) and Azide (24 µM, [3]) were different in literature. The monitoring was started at day 280 of the experiment. Before and during the whole experiment, the ratio of process water was increased step by step. At day 480 of the experiment, the activated sludge of the control street was disposed and activated sludge from the other lane was transferred in the emptied street.

3. Results & Discussion

The online setup of the Dimatec Cenotox 2.0 is shown in Fig. 3. The red arrows indicate the bioreactor 1-1 (left side) and 2-1 (right side). With blue arrows and lines, the sampling location of the bioreactors and the piping is shown. On comparison with atline measurement, online measurements required 4 times more sludge. Therefore, the measurements were performed in atline mode instead of online mode.

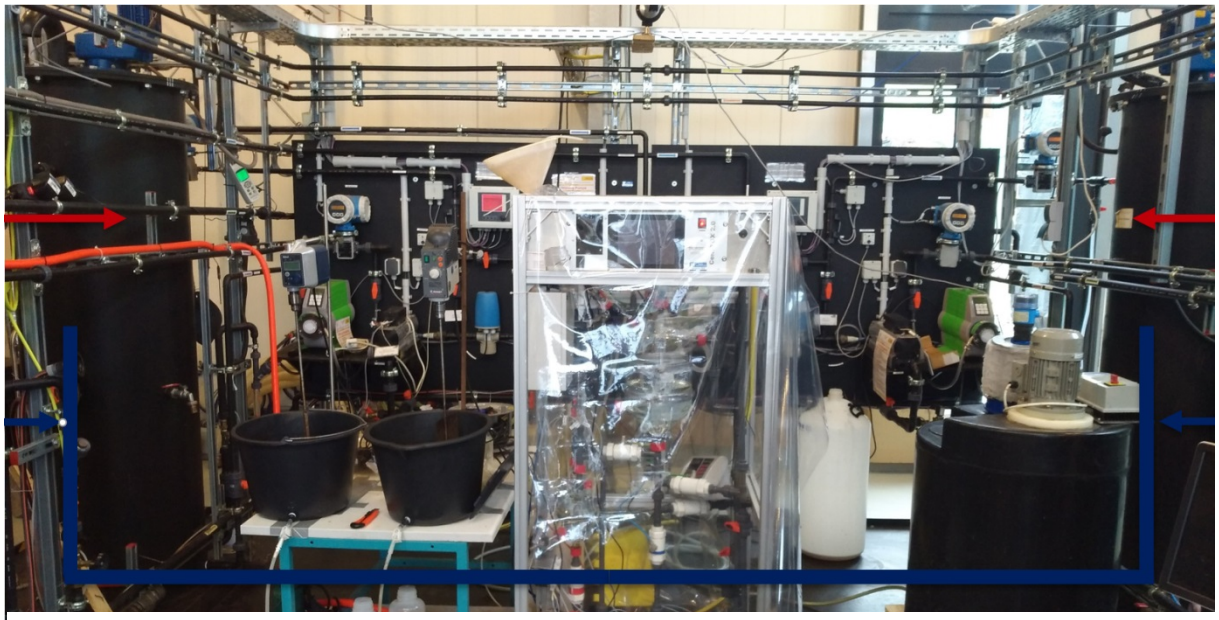

Fig. 3. Dimatec Cenotox 2.0 implemented in the semi-technical scale

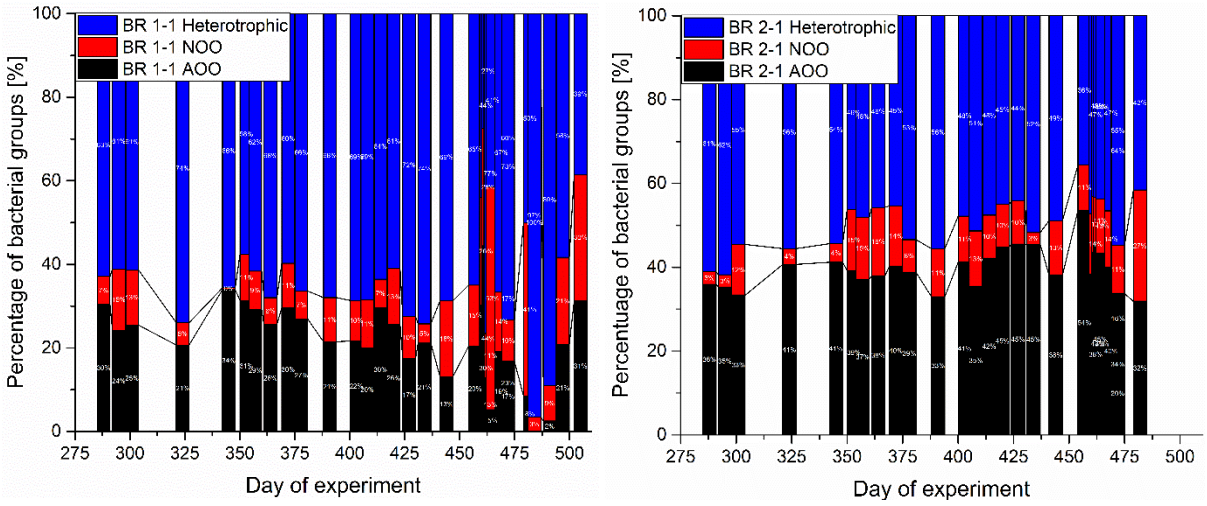

Fig. 4. Results of AOO, NOO and Heterotrophic bacteria in BR 1-1 (left) and BR 2-1 (right)

In Fig. 4 the results of the measured OURs are shown. Over the whole experiment, on average the share of AOO and NOO is reduced in the street with process water. Nevertheless, the measured values are stable within a range of ± 10 %. This result is, due to

the increased ratio of process water during the investigated period, remarkable. As a first result, the used concentrations of process water is not toxic for the nitrification and a stable operation of the nitrification step is possible. In addition, the transfer of the sludge from street one in street two and the stress for the biocoenosis is in comparison with the measured values comprehensible. For this reason, as a second result of the experiments, interruptions and malfunctions of the continuous process are reflected in the measured OURs.

Conclusions

The selective OUR is a suitable tool to determine the activity of the bacterial groups for nitrification. The Cenotox 2.0 was successfully customized for the pilot plant. The nitrification was monitored over 250 days and the control of a stable nitrification. No short-term or long-term toxic effect on the biocoenosis was observed. In addition, mechanical stress for the activated sludge could be comprehended in the measured values of the OUR.

Acknowledgements

The authors would like to thank the “Bergischer Abfallwirtschaftsverband” (BAV) for the excellent cooperation. A share of the funding for this study is made by the European Commission and the European Regional Development Fund (ERDF) under the slogan “Investing in our future”. The authors have declared no conflict of interest.

References

[1] van Kessel, M. A. H. J. *u. a.*, Complete nitrification by a single microorganism, *Nature*, Bd. 528, Nr. 7583, S. 555–559, 2015.

[2] Daims, H. *u. a.*, Complete nitrification by Nitrospira bacteria, *Nature*, Bd. 528, Nr. 7583, S. 504–509, 2015.

[3] Ginestet, P., Audic, J. M., Urbain, V., und Block, J. C., Estimation of nitrifying bacterial activities by measuring oxygen uptake in the presence of the metabolic inhibitors allylthiourea and azide, *Appl. Environ. Microbiol.*, Bd. 64, Nr. 6, S. 2266–2268, 1998.

[4] Steiner, C., Rehorek, A., und Denecke, M., Entwicklung in der Deponienachsorge – Forschungs-Sickerwasseranlage im halbtechnischen Maßstab, in *Recy&Depotech*, 2016, S. 350–356.

Comparative analysis of non-natural acceptor glucosylation with sucrase enzymes of family GH 70

Johannes Nolte[1,2], Ulrich Schörken[1]

[1] TH Köln – Campus Leverkusen, 51368 Leverkusen, Germany

[2] Vetter Pharma-Fertigung GmbH & Co. KG, 88212 Ravensburg, Germany

***Correspondence:** Ulrich Schörken, TH Köln – Campus Leverkusen, Faculty of Applied Natural Sciences, CHEMPARK E39, Kaiser-Wilhelm-Allee, 51368 Leverkusen, Germany;

Email: ulrich.schoerken@th-koeln.de

Abstract

Mutan- and alternansucrase were analyzed for their non-natural glucosylation potential with catecholic compounds caffeic acid and nordihydroguaiaretic acid (NDGA) as well as with non-catecolic p-coumaric acid and umbellic acid. Mutansucrase accepted both catecholic substrates and high glucosylation yields of 92 % with caffeic acid and 81 % with NDGA were obtained. The enzyme showed a clear regio-preference for the catechol 4-OH, which corresponds to findings from our previous work with *Leuconostoc* and *Weissella* derived glucansucrases. The substrate spectrum of the alternansucrase was broader and all substrates were successfully glucosylated with a preference for the catechols. Interestingly alternansucrase possessed a different regio-specificity. With caffeic acid the 3-O-α-D-glucoside was the major product. A similar substrate spectrum and regioselectivity pattern was observed in previous glucansucrase screenings only with glucansucrase from strain *Weissella beninensis* DSM 22752. Therefore it may be concluded that the *W. beninensis* enzyme is an alternansucrase type enzyme as well.

1. Introduction

Glucansucrases of family GH70 are found in lactic acid bacteria. They are divided into different groups according to the type of glucan they synthesize (Fig. 1). Dextransucrases generate polymers with mainly α-1,6-glycosidic bonds, mutansucrases, isolated from *Streptococcus*, produce preferentially α-1,3-glycosidic bonds and reuteransucrases synthesize α-1,4-linked glucans. While the former three groups are classified into enzyme class E.C. 2.4.1.5, alternansucrases belong to enzyme class E.C. 2.4.1.140. They are found in *Leuconostoc* species and produce polymers with alternating α-1,3- and α-1,6-glycosidic bonds. Typical enzymes from the different groups are e.g. dextransucrase DSR-S from *Leuconostoc mesenteroides* B-512 [1], mutansucrase GTF-B from *Streptococcus mutans* S5 [2] and alternansucrase ASR from *Leuconostoc mesenteroides* B-1355 [3]. Compilations of

sequenced glucansucrases and their specificities are found in reviews by *Andre et al.* [4] and *Leemhuis et al.* [5].

The non-natural acceptor side reaction of glucansucrases was originally shown with a *Streptococcus* glucansucrase and (+)-catechin as substrate by *Nakahara et al.* [6]. Besides flavonoids like catechin some other polyphenols were accepted by glucansucrases. The glycosylation of epigallocatechin gallate yielded nine different products with mono-, di- and triglucosylated products [7]. Glucose was either attached to the catechol motifs in 4-O- and 5-O-position or to the 7-O-position of the dihydroxylated non-catecholic aromatic ring structurally comparable to the 7-O-glycosylation of flavonoids [8,9]. From the glycosylation of catecholic polyphenols caffeic acid [10] and L-DOPA [11] it became obvious that the 4-O-glycoside is the preferred product species in all cases. Also the transformation of methylcatechol led to a preference for the 4-methyl- over the 3-methylcatechol [12]. A detailed study on the glycosylation of catechol revealed the tendency to form multiple glycosylations with glucose moieties attached to each other whereas a glycosylation of both adjacent catechol hydroxyl groups could not be observed [13]. Though exhibiting low activity, a few non-catecholic phenols could be glycosylated with glucansucrases. Glucosides of resveratrol [14], hydroquinone [15] and salicyl alcohol [16] were isolated and structurally identified.

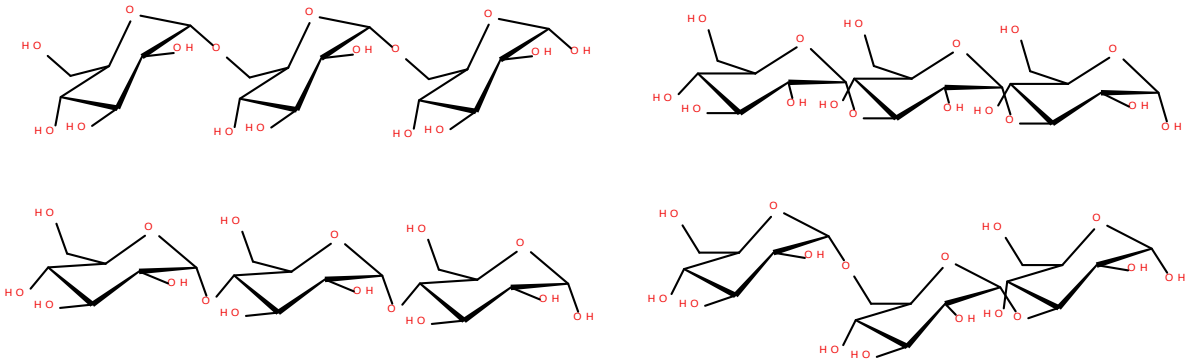

Fig.1. Major glucose repeating units of A) dextran (upper left), B) mutan (upper right), C) reuteran (lower left) and D) alternan (lower right)

In previous studies by our group *Leuconostoc* and *Weissella* glucansucrases were analyzed for their non-natural acceptor glucosylation potential [17,18]. Both genera are good sources of glucansucrases, the majority of them being dextransucrase type enzymes [19]. Caffeic acid and several structurally related catecholic and non-catecholic substrates were successfully glucosylated with the newly isolated glucansucrases. The enzyme from *Leuconostoc citreum* DSM 5577 was the best enzyme for caffeic acid glucosylation [17]. The biologically active nordihydroguaiaretic acid (NDGA) was glucosylated less efficiently by most enzymes. Upon reaction optimization by statistical design the successful glucosylation with > 90 % yield was achieved with glucansucrase from *Leuconostoc pseudomesenteroides* DSM 20193 [18].

The goal of this study was the comparative analysis of the glucosylation potential of mutan- and alternansucrase. Caffeic acid and structurally related non-catecholic p-coumaric acid and

umbellic acid as well as the bicatecholic NDGA were investigated and compared to our previously identified glucansucrases from *Leuconostoc* and *Weissella* species.

2. Materials and Methods

2.1 Enzymes and chemicals

Mutansucrase and alternansucrase were obtained from exoxx Technologies GmbH. Caffeic acid, 4-coumaric acid and umbellic acid were purchased from Sigma Aldrich and NDGA was obtained from Alfa Aesar.

2.2 Glucansucrase activity

Glucansucrase activity was determined spectrophotometrically in microtiter plate format with 3,5-dinitrosalicylic acid (DNS method) using a SpectraMax 190 plate reader at 540 nm as described before [17,18].

2.3 Biocatalytical glucosylation and glycoside purification

Glucosylation mixtures contained 200 mM sucrose, 40 mM polyphenol in 20 mM sodium acetate, pH 5.4 supplemented with 0.45 mM $CaCl_2$ and 15 % (v/v) dimethyl sulfoxide (DMSO). Reactions were started by addition of 0.375 U/ml glucansucrase and incubated statically for up to 24 hours at 30 °C. Samples were taken periodically and the reaction was stopped by addition of 9 vol. of ethanol (-20 °C). Samples were vortexed for 20 s and precipitated glucans were removed by centrifugation at 3,300 x g for 20 min at 4 °C according to the method of Overwin et al. [20]. Ethanol was evaporated from the glycoside containing samples under reduced pressure. The samples were lyophilized and dissolved in 20 % (v/v) acetonitrile in water. Preparative HPLC was carried out with an Interchim puriflash 4250/250 system as described before [17,18].

2.4 Chromatographic and spectroscopic analysis of glucosides

LC-UV was carried out with a Thermo Scientific Accela system equipped with an Accela 80 Hz PDA detector and a Hitachi LaChrom II C18 reversed phase column (4.6 x 250 mm, 5 µm) as described before [17,18]. Mass spectrometric analyses were performed using a Shimadzu LC-30AD with a SPD M20A diode array detector and a LCMS-2020 single quadrupole mass spectrometer with electrospray ionization (ESI-MS) equipped with the same column. 1H- und 13C-NMR spectra including 2D-NMR experiments were recorded with a 400 MHz Bruker Ascend™ 400 as described before [17,18].

3. Results & Discussion

3.1 Glucosylation with mutansucrase

Mutansucrase from *Streptococcus* species was already successfully utilized for the glucosylation of flavonoids like catechin [6,9,20], methylcatechol [12] and other phenolic compounds [14] before. The mutansucrase, which was obtained from recombinant

expression in *E. coli*, showed good glucosylation efficacy with the catecholic compounds caffeic acid and NDGA (Fig. 2). The high turnover of the non-natural acceptor substrates suggests that the parallel formation of mutan polymers is relatively slow and that enough sucrose is available for catechol glucosylation. Mutansucrase exhibits a clear regiopreference for the 4-OH-position with both substrates as was judged from LC retention times with our previously synthesized glucosides [17,18]. The regioselectivity pattern is in accordance with data obtained for methylcatechol by *Meulenbeld et al.* [12]. The caffeic acid-3-*O*-α-D-glucoside is visible in LC-UV analysis only as a minor peak at a retention time of 8 – 8.3 min. With both substrates the formation of some di- and oligoglucosides was observed, whereas the 4-*O*-α-D-monoglucoside was the major product with both substrates. The non-catecholic substrates p-coumaric acid and umbellic acid were not glucosylated by mutansucrase under the chosen glucosylation conditions.

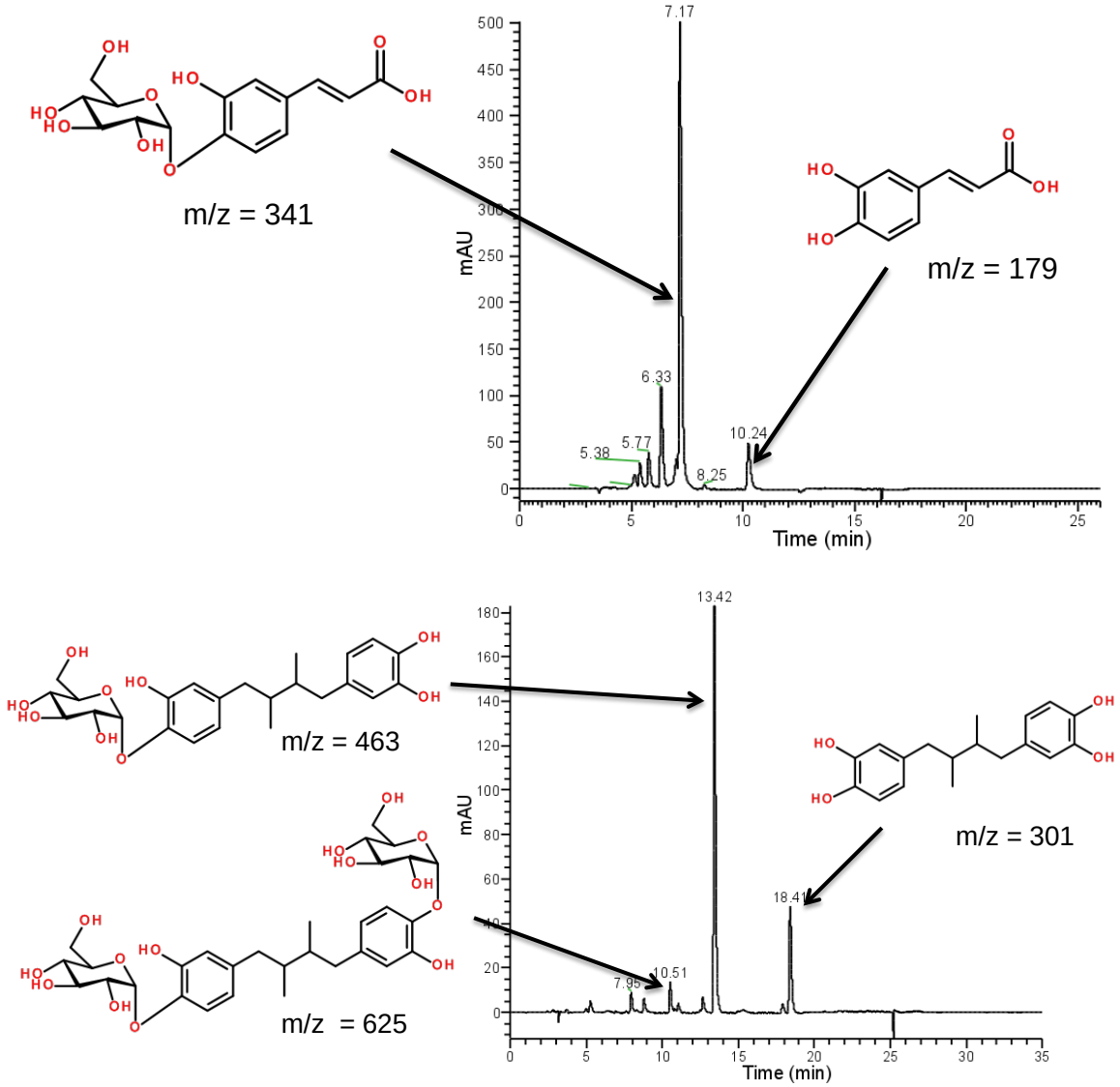

Fig. 2. Mutansucrase catalyzed transformation of caffeic acid (top) and NDGA (bottom), LC-UV analyses with mass and structure assignments, caffeic acid di- and oligoglucosides elute at 5 - 7 min and NDGA di- and oligoglucosides elute in the range of 7 – 13 min.

3.2 Glucosylation with alternansucrase

Alternansucrases have so far been seldom used for non-natural acceptor glucosylations. The successful transformation of flavonoids [8] as well as the glucosylation of stevioside [21] was shown with this class of enzymes. In contrast to mutansucrase the alternansucrase accepted the catecholic as well as the non-catecholic substrates (Fig. 3). With caffeic acid a divergent regioselectivity was detected. The peak at retention time of 8.1 min was the major reaction product, which was purified by preparative HPLC and spectroscopically analyzed by NMR. In agreement to our previously published data [17], the structure was identified as the caffeic acid-3-*O*-α-D-glucoside. Besides that also the 4-*O*-α-D-glucoside was synthesized and some di- and oligoglucosides were observed as well. The transformation of NDGA led to one major product, which was identified with good probability as the 4-*O*-α-D-glucoside by comparison of the LC retention times of the mutansucrase biotransformation and our previous results [18]. As the product was not isolated for NMR structure elucidation it might be possible that the 3-*O*-α-D- and 4-*O*-α-D-glucosides possess identical retention times however. The transformation of the non-catecholic substrates umbellic acid and p-coumaric acid were verified by mass spectrometric assignment of the product peaks. With umbellic acid mono- and oligoglucosides were detected and in the case of p-coumaric acid a weak diglucoside peak was found together with the monoglucoside. The non-catecholic substrates were less efficiently glucosylated than the catechols however.

3.3 Comparison of mutan- and alternansucrase glucosylation to glucansucrases obtained from *Leuconostoc* and *Weissella* screening

Comparison to the best glucosylation catalysts from *Leuconostoc citreum* DSM 5577 and *Leuconostoc pseudomesenteroides* DSM 20193 identified in our lactic acid bacteria screening revealed, that mutansucrase is an efficient glucosylation catalyst (Table 1). The highest initial caffeic acid glucosylation yield was obtained with mutansucrase and also transformation of the more hydrophobic and sterically hindered NDGA was comparable to that of DSM 20913. Alternansucrase displayed a different behavior regarding regioselectivity and acceptor substrate acceptance. In our previous screening only glucansucrase from *Weissella beninensis* DSM 22752 exhibited a similar glucosylation pattern (Table 1), which suggests that the *Weissella* enzyme belongs to the group of alternansucrases.

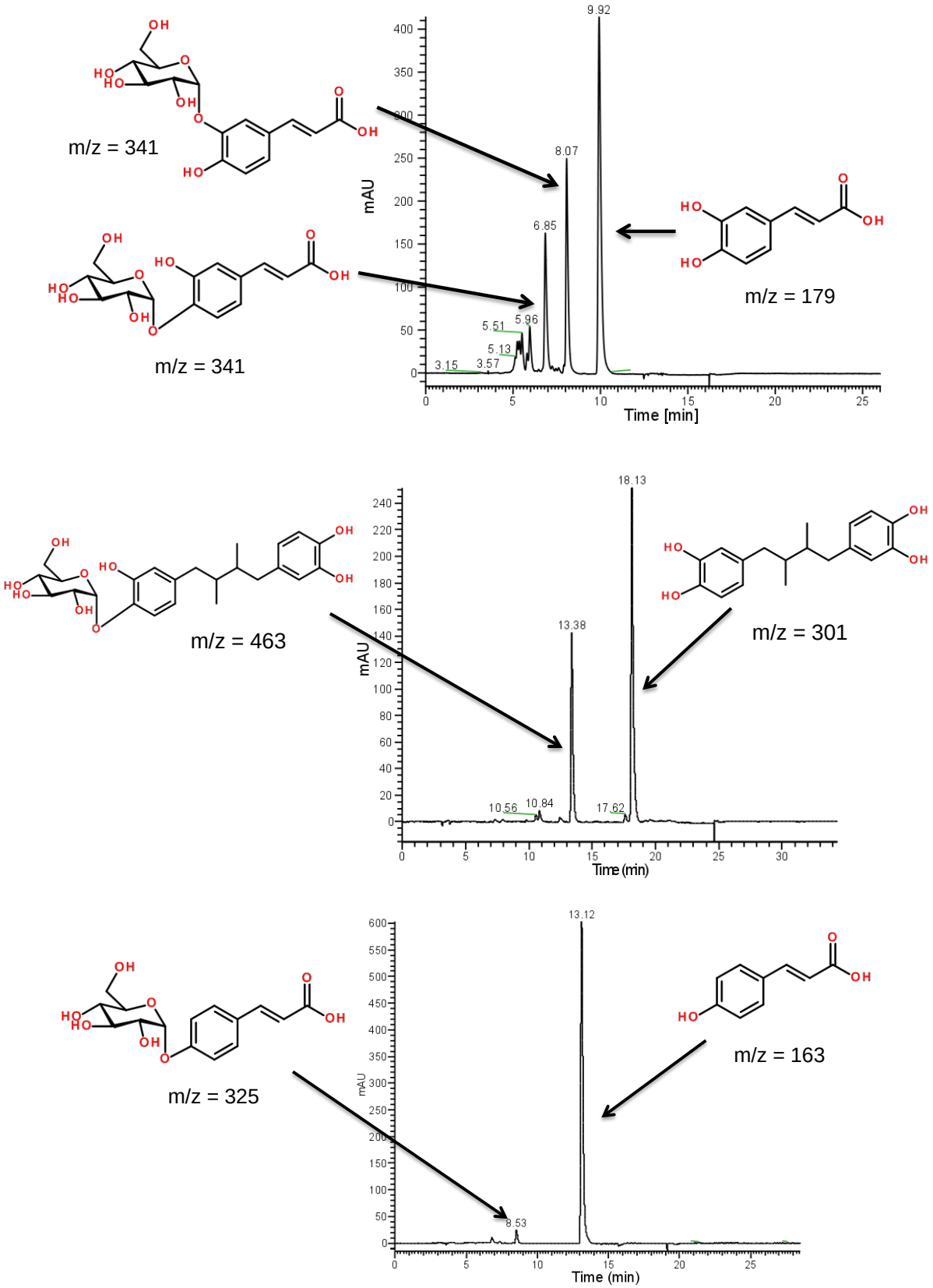

Fig. 3. Alternansucrase catalyzed transformation of caffeic acid (top) NDGA (middle) and p-coumaric acid (bottom), LC-UV analyses with mass and structure assignments, caffeic acid di- and oligoglucosides elute at 5 - 7 min and NDGA di- and oligoglucosides elute in the range of

7 – 13 min, glucoside structures of NDGA and p-coumaric acid were not analyzed by NMR and represent the most probable glucosides.

Table 1: Analysis of alternan- and mutansucrase transformations in comparison to glucansucrases from *Leuconostoc* and *Weissella* strains (data taken from [17,18]), nd = not detected

	Mutansucrase	**DSM 5577**	**DSM 20913**	**Alternansucrase**	**DSM 22752**
Caffeic acid	92	66	28	52	32
(4-O- : 3-O-)	99 : 1	99 : 1	99 : 1	40 : 60	50 : 50
NDGA	81	20	79	36	< 5
Umbellic acid	nd	1	nd	11	5
Coumaric acid	nd	1	nd	4	1

Conclusions

Alternan- and mutansucrase are efficient glucosylation biocatalysts. Mutansucrase is especially suited for the high yield transformation of catecholic substrates, while alternansucrase allows for the glucosylation of a broader spectrum of phenolic compounds. Reaction engineering was not yet done and according to our optimization studies done with *Leuconostoc* glucansucrases [17,18] further increase of glucosylation yields should be possible with both enzymes.

Acknowledgements

This work was supported by the NRW Ministry of Innovation, Science and Research within the program FH Struktur. We thank evoxx Technologies for the donation of enzymes.

The authors have declared no conflict of interest.

References

[1] V. Monchois, M. Remaud-Simeon, R.R. Russell, P. Monsan, R.M. Willemot, Characterization of *Leuconostoc mesenteroides* NRRL B-512F dextransucrase (DSRS) and identification of amino-acid residues playing a key role in enzyme activity, Appl Microbiol Biotechnol 48 (1997) 465-472.

[2] T. Shiroza, S, Ueda, H.K. Kuramitsu, Sequence analysis of the gtfB gene from *Streptococcus mutans*, J Bacteriol 169 (1987) 4263-4270.

[3] M.A. Arguello-Morales, M. Remaud-Simeon, S. Pizzut, P. Sarcabal, R. Willemot, P. Monsan, Sequence analysis of the gene encoding alternansucrase, a sucrose glucosyltransferase from *Leuconostoc mesenteroides* NRRL B-1355, FEMS Microbiol Lett 182 (2000) 81-85.

[4] I. Andre, G. Potocki-Veronese, S. Morel, P. Monsan, M. Remaud-Simeon, Sucrose-utilizing transglucosidases for biocatalysis, Top. Curr. Chem. 294 (2010) 25–48.

[5] H. Leemhuis, T. Pijning, J.M. Dobruchowska, S.S. van Leeuwen, S. Kralj, B.W. Dijkstra, L. Dijkhuizen, Glucansucrases: three-dimensional structures, reactions, mechanism, α-glucan analysis and their implications in biotechnology and food applications, J. Biotechnol. 163 (2013) 250–272.

[6] K. Nakahara, M. Kontani, H. Ono, T. Kodama, T. Tanaka, T. Ooshima, S. Hamada, Glucosyltransferase from *Streptococcus sobrinus* catalyzes glucosylation of catechin, Appl. Environ. Microbiol. 61 (1995) 2768–2770.

[7] J. Kim, T.T.H. Nguyen, N.M. Kim, Y.-H. Moon, J.-M. Ha, N. Park, D.-G. Lee, K.-H. Hwang, J.-S. Park, D. Kim, Functional properties of novel epigallocatechin gallate glucosides synthesized by using dextransucrase from *Leuconostoc mesenteroides* B-1299CB4, J. Agr. Food Chem. 64 (2016) 9203–9213.

[8] A. Bertrand, S. Morel, F. Lefoulon, Y. Rolland, P. Monsan, M. Remaud-Simeon, *Leuconostoc mesenteroides* glucansucrase synthesis of flavonoid glucosides by acceptor reactions in aqueous-organic solvents, Carbohydr. Res. 341 (2006) 855–863.

[9] G.H. Meulenbeld, H. Zuilhof, A. van Veldhuizen, R.H.H. van Den Heuvel, S. Hartmans, Enhanced (+)-catechin transglucosylating activity of *Streptococcus mutans* GS-5 glucosyltransferase-D due to fructose removal, App. Environ. Microbiol. 65 (1999) 4141–4147.

[10] D. Auriol, R. ter Halle, F. Lefevre, Industrial production of caffeic acid-a-D-O-glucoside, in: J. Whittall, P.W. Sutton (Eds.), Practical Methods for Biocatalysis and Biotransformations 2, Wiley, 2012, pp. 240–243.

[11] S.-H. Yoon, D.B. Fulton, J.F. Robyt, Enzymatic synthesis of L-DOPA alpha-glycosides by reaction with sucrose catalyzed by four different glucansucrases from four strains of Leuconostoc mesenteroides, Carbohydr. Res. 345 (2010) 1730–1735.

[12] G.H. Meulenbeld, S. Hartmans, Transglycosylation by *Streptococcus mutans* GS-5 glucosyltransferase-D: acceptor specificity and engineering of reaction conditions, Biotechnol. Bioeng. 70 (2000) 363–369.

[13] E.M. te Poele, P. Grijpstra, S.S. van Leeuwen, L. Dijkhuizen, Glucosylation of catechol with the GTFA glucansucrase enzyme from *Lactobacillus reuteri* and sucrose as donor substrate, Bioconjugate Chem. (2016) 937–946.

[14] H. Shim, W. Hong, Y. Ahn, Enzymatic preparation of phenolic glucosides by *Streptococcus mutans*, B. Kor. Chem. Soc. 24 (2003) 1680–1682.

[15] E.-S. Seo, J. Kang, J.-H. Lee, G.-E. Kim, G.J. Kim, D. Kim, Synthesis and characterization of hydroquinone glucoside using *Leuconostoc mesenteroides* dextransucrase, Enzyme Microb. Tech. 45 (2009) 355–360.

[16] E.-S. Seo, J.-H. Lee, J.-Y. Park, D. Kim, H.-J. Han, J.F. Robyt, Enzymatic synthesis and anti-coagulant effect of salicin analogs by using the *Leuconostoc mesenteroides* glucansucrase acceptor reaction, J. Biotechnol. 117 (2005) 31–38.

[17] J. Nolte, A. Kempa, A. Schlockermann, M. Hochgürtel, U. Schörken, Glucosylation of caffeic acid and structural analogues catalyzed by novel glucansucrases from *Leuconostoc* and *Weissella* species, Biocatal. Agric. Biotechnol. 19 (2019) 101114, DOI: 10.1016/j.bcab.2019.101114

[18] J. Nolte, L.-A. Pöttgen, J. Sperlich, A. Grossert, A. Kempa, N. Teusch, U. Schörken, Glucansucrase catalyzed synthesis and functional characterization of nordihydroguaiaretic acid glucosides, Enz. Microb. Technol. 120 (2019) 69-76.

[19] M.-S. Bounaix, V. Gabriel, S. Morel, H. Robert, P. Rabier, M. Remaud-Siméon, B. Gabriel, C. Fontagné-Faucher, Biodiversity of exopolysaccharides produced from sucrose by sourdough lactic acid bacteria, J. Agr. Food Chem. 57 (2009) 10889–10897.

[20] H. Overwin, V. Wray, B. Hofer, Flavonoid glucosylation by non-Leloir glycosyltransferases: formation of multiple derivatives of 3,5,7,3',4'-pentahydroxyflavane stereoisomers, Appl. Microbiol. Biotechnol. 99 (2015) 9565–9576.

[21] A. Musa, M. Miao, T. Zhang, B. Jiang, Biotransformation of stevioside by *Leuconostoc citreum* SK24.002 alternansucrase acceptor reaction, Food Chem. 146 (2014) 23–29.

Intermittently Fed Anaerobic Digestion: Requirement and Process Control

Robin Eccleston*,[1]

[1] Institut für Automation & Industrial IT (AIT), Informatik und Ingenieurwissenschaften, TH Köln

***Correspondence:** (Robin Eccleston, Technische Hochschule Köln, Gummersbach Campus, Steinmüllerallee 1, 51643 Gummersbach, Germany; Email: robin.eccleston@th-koeln.de)

Abstract

The electricity network is undergoing a change due to reducing costs for renewable energy sources. Subsidy programs for renewable energy sources are changing and the funding available is being reduced. This will have an impact on anaerobic digestion which in some cases may struggle financially. Overfeeding is one of the most common mechanisms of inhibition in the process, and by shifting to intermittent feeding for on-demand production, this change will provide more information about the digestion process and could be used to detect the beginning of inhibition due to overfeeding. This paper discusses the shift towards intermittent production and how this change can be used to monitor the anaerobic digestion process.

1. Introduction

Climate change is an ongoing concern for the world, as the combustion of fossil fuels is causing long term change to the environment [1]. Consequently, there has been an increasing shift towards the use of renewable energy sources [2]. Solar and wind power have seen particular increases, where for example in many countries there are subsidies for electricity generation from renewable energy sources. These subsidy programs have helped growth of the market, and enabled lower prices for new installations due to the cost decreasing as the market has increased in size.

One of the draw backs of increasing the amount of energy from solar and wind power, is that both of these power sources are dependent upon the weather. Solar power will only work during the day time, and during cloudy periods the output will be significantly reduced. Similarly for wind power, the output will vary with the wind which can change significantly over a short period of time. As a larger proportion of energy is created by weather dependant renewable sources, this puts the electrical grid under greater stress. The electricity supplied to the grid must match the demand very closely, otherwise the power provided will no longer meet the specifications, and can result in damage or power cuts to connected equipment [3]. For the traditional electricity networks, balancing is typically performed by varying the output power from gas turbines, with some further assistance provided by pumped storage. However, the amount of energy stored at a pumped storage

facility is relatively small compared to the demands of the electricity network, and gas turbines are still using a fossil fuel. A coal power plant, in addition to using fossil fuels, will take much longer to adjust the production rates, and so cannot quickly change from a low power output to a high power output, as would be necessary to meet the demand as a result of the wind dropping.

Anaerobic digestion is a source of renewable energy that operates by putting organic waste in to a tank and allowing microbes to break down the organic material. One of the outputs from this process is biogas, which contains a significant amount of energy and can be burnt in a CHP (Combined Heat & Power) unit for creating both electricity and heat. The use of anaerobic digestion is of further interest, because unlike solar and wind power sources, it is not dependent upon the weather. A typical anaerobic digestion plant will have the ability to store gas for a short time, and furthermore, biogas production can be controlled by varying the feeding amounts and times. This allows the system to be used as a renewable energy source, over which the plant operator has control over the time at which biogas is produced.

A CHP unit running on biogas could be operated in a similar way as the gas turbines used at the time of writing. This would allow anaerobic digestion to provide a renewable energy source that is capable of contributing to the balancing of the energy grid. Furthermore, generally the weather can be predicted with a high degree of accuracy over a short time, and electricity consumption trends are largely predictable using historical data. It would be possible in the future that a biogas plant operator can anticipate an increase of demand a day in advance for example, and feed the biogas plant an increased amount of biomass before the electrical demand increases. This will produce additional biogas as it is required, and will allow the plant operator to generate more electricity and support other renewable energy sources.

Such a mode of operation is in contrast to the current operating methodology of biogas plants, which is to run the CHP at the maximum power possible for as much time as possible. That is as a result caused by two boundary conditions, firstly the subsidies provided from the government to the plant operators, and secondly as a result of the agreements that are contracted between biogas plant operators and the electricity companies that are buying the electricity. At the time of writing, in Germany the subsidy program for the production of electricity from biogas has been significantly limited [4] with a cap on the total installed production that will be awarded subsidies, meaning that in the future as the existing agreements expire, it may no longer be financially viable to run a biogas plant for the electricity cost alone. The electricity price is generally higher when it is required for balancing the grid, and so by selling electricity when the price is higher, it may be possible for biogas plants to still operate at a profit, when compared to operating continuously and selling the electricity for the lower "base load" price [5].

There is a further complication with the operation of a biogas plant: overfeeding the plant can be extremely expensive. As the anaerobic digestion process features many groups of microbes, what can happen at high feeding rates is that one group of microbes will work

faster, but another group will not be able to keep up. This can result in the first group of microbes poisoning the digester, which ends up in a cycle whereby the anaerobic digester is no longer able to operate. When this happens, the entire digester must be emptied, the contents must be disposed of, and the fermentation process must be started again from the beginning. This process involves a lot of time and cost, and it can take up to 3 months until the anaerobic digester is running at the same level as before the failure. This results in an understandable high level of caution from the plant operators concerning modifications in the operation process. Clearly it is better to run a biogas plant slightly below its optimum level, rather than risking a huge cost and reduction of income for 3 months.

Anaerobic digesters traditionally do not have a large number of instruments to monitor the process. One study performed a survey of over 400 plants and found that the process is mostly analysed using laboratory methods, and that on-line measurements are lacking [6]. Laboratory analysis requires time and a skilled operator, and also requires sample preparation, and so can require several hours or even longer until results are available. When trying to closely monitor and control a biogas plant, this lack of real time information about the performance of the plant is a problem, as it is a further reason that the biogas plant would be operated conservatively. For example in the scenario where inhibition starts to occur, with an online monitor this could be detected in a matter of minutes and compensated for, however for a system where the only testing performed is a laboratory analysis of a sample once a week, then the process may have become inhibited before the sample has even been analysed. Thus by improving the state of instrumentation and monitoring of the biogas plant, the safety margin can be reduced and the output of the biogas plant can be increased. Clearly this can increase the amount of income from exporting electricity from using the same equipment, and so better availability of affordable online sensors would enable more efficient operation of biogas plants.

2. The goals of anaerobic digestion

There are two operating scenarios that describe the majority of anaerobic digesters in operation. The first scenario is that where the primary goal is the handling of waste, such as waste water treatment whereby the waste water must be purified and organic matter in the stream must be reduced. For water with a sufficiently high concentration of organic matter, anaerobic digestion is used and methane is a by-product, which is profitable for the digester operator to capture and burn in a CHP allowing the use or sale of electricity and generation of an extra income stream. There is a similar situation for disposal of municipal food waste and garden waste, where the waste must be disposed of properly as without proper disposal the food waste formerly has been sent to a landfill site where it would slowly be degraded over a longer time scale, and the methane released would contribute to the greenhouse gas effect. Today organic waste often is incinerated, a process of low or zero energetic output caused by the high degree of moisture of the waste.

By processing the food waste at centralised anaerobic digesters, the released methane can be captured and utilised. By a well-planned handling process, extra income can be generated by capturing the released methane and using it for electricity production. There may still be advantages in these scenarios to optimisation, for example if the incoming waste is higher than the loading rate then the extra waste is likely to be incinerated, incurring additional costs.

The second scenario is that of an anaerobic digester which is operated primarily for the generation of financial profits and is not concerned with the handling of organic waste. These digesters represent the majority of the anaerobic digesters that are present in Germany as of 2017. In these cases, crops are grown specifically to feed anaerobic digesters, and an increase in loading capacity will give an increase in the power generation and thus increase in income. This is of importance as subsidies are being reduced and a more flexible operation is necessary today. Improvements in operation can ensure that such systems maintain profitability and can help to contribute to a renewable energy grid.

3. Electricity production from anaerobic digestion

In Germany, in 2015 there were 10551 operating biogas plants that were identified [7]. In 2015, the reported total installed electrical power was 4379MWe [7]. As of 2011, in Germany between 90 and 95% of biogas plants were operating on a mixture of manure and crops [8], which makes them the vast majority of AD plants in Germany and also means that this large amount of plants will be faced with financial challenges once the subsidies are cut.

By comparison, in the United Kingdom, as of March 2017, there are 747MWe of operational landfill gas plants, and 38MWe of operational sewage sludge digestion plants counting only the plants with over 1MWe capacity [9]. A separate source reports details on anaerobic digestion facilities including smaller plants, and as on the 31st March 2016 had records of 78MWe from 150 farm fed plants, and 141MWe from 104 waste fed plants [10]. For both of these groups, around 80% of the total generated biogas is used for CHP. This gives a total of 182MWe of CHP capacity, although only 69MWe of this capacity could be converted to flexible generation, and the remaining capacity has an operational requirement to process the incoming waste. However even in the cases where the feeding is not flexible, the running of the CHP units could still be changed to run on demand, and the available power could be increased by increasing the biogas storage capacity. These figures show that in the United Kingdom, there is a smaller amount of energy crop based anaerobic digestion systems, but still a significant number.

So whilst any optimisation techniques or new monitoring technology that are developed could be applied to both operating scenarios, it is more necessary for the agricultural biogas plants than the systems primarily interested in the handling of waste, as the waste handling installations are able to operate profitably in the absence of funding, whereas agricultural biogas plants will struggle financially and may be faced with closure.

4. Inhibition Mechanisms

There are a range of mechanisms that can cause inhibition. One reason can be "wash out". The HRT (hydraulic retention time) of an AD plant is calculated by dividing the volume of the digester by the volume that is added each day. For example, a 1000m^3 digester with 50m^3 of liquid added per day would have a HRT of 20 days. If this HRT is less than the time that it takes for the bacteria to double, then washout occurs [11]. Under this condition, the bacteria growth rate is not sufficiently high enough to maintain a stable population, and so too much bacteria is washed away from the reactor. Washout primarily occurs when the level of volatile solids in the feedstock is too low, such as in slurries which contain large amounts of water. For feedstocks such as maize, the level of volatile solids can be in the range of 90-95% of the dry matter, and so a smaller amount can be fed when compared to slurry. This results in a longer HRT, giving the bacteria more time to reproduce before being carried out of the digester. By comparison, dairy waste contains approximately 10.5% volatile solids [12], requiring 9 to 10 times higher volumes to be fed in to the reactor in order to achieve the same organic loading rate. This higher loading rate leads to a higher probability of wash out.

A second cause of inhibition is organic overloading. When the volatile solids feeding level for a digester is too high, then the synergistic relationship between the microbes starts to break down. The first stages are able to cope better with the higher loading rate. The methanogenesis stage however at higher loading rates will not be able to convert enough of the volatile fatty acids to keep up with the rate at which they are produced. This results in the VFAs accumulating in the digester, which then results in the pH of the digester dropping causing a loss of alkalinity [13]. As the pH changes, the digester conditions are no longer optimal for the bacteria and their work rate drops. VFA accumulation can reduce the rate of hydrolysis and at very high levels can cause inhibition, even in cases where the process pH is optimal [14]. There are differing accounts of the effects of VFAs, with some publications showing that propionic acid can cause digester failure, and with others showing that propionic acid accumulates as a result of inhibition elsewhere, rather than causing it [15].

The drop in the work rate of the bacteria then results in a faster accumulation of VFAs, resulting in a further rate drop, and so this feedback can generate a quick process stop. This type of inhibition can occur at any stage, however if for example the hydrolysis stage is inhibited, then this will reduce the substrate consumption of the later phases, and the entire process will perform more slowly. However if the final stage (methanogenesis) is inhibited, then there are a build-up of intermediate products which is more difficult to recover from.

In addition to these inhibition mechanisms, there can be inhibition occurring separately as a result of the substrate composition, for example ammonia inhibition can occur when the feeding load contains high concentrations of ammonia such as poultry waste. Similarly, a high level of sulphur in the feedstock can lead to high H_2S (Hydrogen Sulphide) concentrations which will also inhibit the microbes. Sulphide inhibition can occur when there are high levels of sulphates or other sulphur compounds in the feedstock fed to a digester.

This is more of a concern for anaerobic digestion containing waste streams of industrial process which tend to have higher levels of sulphides [16]. Similarly, the presence of heavy metals can also cause inhibition and process failure and are also more of a problem for specific industrial waste sources [16].

If the process is only slightly inhibited, then it is important to quickly correct the digester operating point to a stable state where all of the microbes at the different stages are able to function correctly. This change in operation can be achieved by reducing the OLR (Organic Loading Rate), or by changing the substrate composition. If the entire process has completely stopped then there is little chance of recovering the process, and instead the digester will be drained and refilled. Once refilled, it can take several months for the microorganisms to regrow and for biogas production rates to reach the same level that they were before the digester was drained. Clearly this has a high cost, and results in a reduced income for several months until the digester recovers to a similar performance level that it was previously operating at. This is the reason that feeding regimes tend to be conservative, in order to avoid the expensive problem of inhibition occurring.

Due to the anaerobic digestion process using synergistic relationships between microbial communities, the point at which inhibition begins is difficult to accurately predict. The communities are capable of adapting to new environmental conditions, and will adjust with time. As a result, any fixed values that are given, for example the feeding rate of volatile solids, or the target value for a specific process parameter, are not actually considering the characteristics of the microbes. The thresholds are typically chosen as reasonably safe thresholds that have experimentally been found to have a low failure rate. In order to optimise the process, thresholds are necessary for each individual digester with its associated microbial community.

As there are multiple stages in the process, it often occurs that inhibition of one stage can happen, but the later stages are still functioning. As a result, it may appear that the process is still functioning well until the inhibition finally propagates to the produced biogas, at which point it can be too late to recover [16].

5. Intermittent Production Data Analysis & Control

By shifting the operation of a biogas plant from continuous to intermittent in order to provide power on demand, there is a potential financial benefit, and this can be achieved without significantly impacting the cumulative output of the digester [17]. Other research has shown that by using a continuously fed digester, and adjusting the feeding rate, it is possible for a digester operator to estimate the state of the digester and make decisions on the feeding levels based on the response to the changes in feeding rate [18]. The consequence is that when feeding a digester intermittently, there are large variations in the feeding rate, and by observing the change in gas production rate after changing the feeding rate, it is possible to make an estimate about the condition of the digester and whether the system is stable or approaching the maximum capacity. The measured change in the system

output following a feeding event will consider the entire process, and so the rate limiting step within the process will have an observable effect on the final output, which is the biogas production rate. By analysing the gas production rate, it is possible to estimate the digester condition and use this to control the feeding rate to reach a high feeding level whilst maintaining stable operation. Experimental results have shown that such analysis performs well when feeding materials that result in a fast response such as maize silage or milled grass silage, and by contrast with cattle slurry this was not observed due to washout [19]. This analysis was then able to control an ADM1 simulation [20] and converged on a stable level with daily feeding events.

Conclusions

There is a change in the energy market which has been instigated by the reduction of costs for producing renewable energy sources such as wind and solar. These sources are weather dependant and as such are not a controllable energy source. Anaerobic Digestion has not experienced such a rapid reduction in cost, however is well suited to operate as an intermittent power source, which would enable generation at times when other renewable sources are not able to meet the demand. Such an operation will then provide further information about the anaerobic digestion process and can be used to control the feeding amounts to help maintain a stable operation. By using intermittent feeding, it may be possible to detect conditions leading to inhibition and reduce the feeding levels in advance, however it is not possible to detect other sources of inhibition such as washout by using such an analysis.

Acknowledgements

This work was funded by Metabolon IIb project and from the European Union's Seventh Framework Programme under grant agreement no. 316838.

The author has declared no conflict of interest.

References

[1] T. M. Letcher, Ed., *Climate Change - Observed Impacts on Planet Earth*. Elsevier B.V., 2009.

[2] REN21, *Renewables 2017 Global Status Report*. 2017.

[3] T. Persson *et al.*, "A perspective on the potential role of renewable gas in smart energy grids." IEA Bioenergy, 2014.

[4] German Federal Ministry for Economic Affairs and Energy, *Erneuerbare-Energien-Gesetz: 2017*. 2017.

[5] M. Lauer *et al.*, “Flexible power generation scenarios for biogas plants operated in Germany: impacts on economic viability and GHG emissions,” *Int. J. Energy Res.*, vol. 41, no. 1, pp. 63–80, 2017.

[6] H. Spanjers and J. van Lier, “Instrumentation in anaerobic treatment: research and practice,” *Water Sci. Technol.*, vol. 53, no. 4–5, pp. 63–76, Mar. 2006.

[7] J. Daniel-gromke *et al.*, “DBFZ Report Nr. 30: Anlagenbestand Biogas und Biomethan – Biogaserzeugung und -nutzung in Deutschland,” Leipzig, Germany, 2017.

[8] J. Murphy *et al.*, “Biogas from Crop Digestion,” *Development*, 2011.

[9] Department for Business Energy & Industrial Strategy, “Renewable energy planning database monthly extract.” [Online]. Available: https://www.gov.uk/government/publications/renewable-energy-planning-database-monthly-extract. [Accessed: 21-Apr-2017].

[10] “Operational AD sites | WRAP UK.” .

[11] A. Wellinger, J. Murphy, and D. Baxter, *The Biogas Handbook: Science, Production and Applications*. Cambridge: Woodhead Publishing Limited, 2013.

[12] D. A. Burke, “Dairy Waste Anaerobic Digestion Handbook,” 2001.

[13] M. H. Gerardi, *The Microbiology of Anaerobic Digesters*. 2003.

[14] I. Siegert and C. Banks, “The effect of volatile fatty acid additions on the anaerobic digestion of cellulose and glucose in batch reactors,” *Process Biochem.*, vol. 40, no. 11, pp. 3412–3418, Nov. 2005.

[15] A. J. Ward, P. J. Hobbs, P. J. Holliman, and D. L. Jones, “Optimisation of the anaerobic digestion of agricultural resources.,” *Bioresour. Technol.*, vol. 99, no. 17, pp. 7928–40, Nov. 2008.

[16] S. Aiba, L. T. Fan, and K. Schugerl, *Anaerobic Digestion Processes in Industrial Wastewater Treatment*, vol. 2. 1986.

[17] E. Mauky, S. Weinrich, H. F. Jacobi, H. J. Nägele, J. Liebetrau, and M. Nelles, “Demand-driven biogas production by flexible feeding in full-scale - Process stability and flexibility potentials,” *Anaerobe*, 2016.

[18] J.-P. Steyer, P. Buffière, D. Rolland, and R. Moletta, “Advanced control of anaerobic digestion processes through disturbances monitoring,” *Water Res.*, vol. 33, no. 9, pp. 2059–2068, Jun. 1999.

[19] R. Eccleston and M. Bongards, “Determining Conditions of Intermittently Fed Digesters from Biogas Production Rate Data.” IV. Conference on Monitoring & Process Control of Anaerobic Digestion Plants, Leipzig, Germany, 2019.

[20] D. J. Batstone *et al.*, “The IWA Anaerobic Digestion Model No 1 (ADM1).,” *Water Sci. Technol.*, vol. 45, no. 10, pp. 65–73, Jan. 2002.

Future of anaerobic digestion in Germany

Himanshu Himanshu*[1], Christian Wolf[1]

[1] Institut für Automation & Industrial IT (AIT), Informatik und Ingenieurwissenschaften, TH Köln

***Correspondence:** (Dr. Himanshu, TH Köln, Steinmüller Allee 1, 51643 Gummersbach; **Email:** himanshu.himanshu@th-koeln.de)

Abstract

The introduction of Feed-in tariffs in the German Renewable Energy Act (EEG) fuelled the growth of anaerobic digestion (AD) industry making Germany the country with highest number of operational AD plants. However, the rapid expansion of AD industry resulted in some unwanted side-effects such as food vs fuel debate, increased prices for electricity and the temporal mismatch between supply and demand of electricity grid. Subsequent amendments in EEG has tried to address some of these issues by reduction in Feed-in tariffs, introduction of a cap on cereal based feedstocks and providing premium for energy production in accordance with market demand. Furthermore, the Feed-in tariffs which were introduced for 20 years are soon going to expire. The changes in legal and political discourse is soon going to introduce some new challanges to the AD industry. This paper has discussed some of these challanges and their potential solutions.

1. Introduction

Anaerobic digestion (AD) is playing a major role in providing renewable energy in European Union especially Germany. Several countries, including Germany, provided subsidies either in the form of feed-in tariffs or through supporting investments to promote renewable energy production from AD [1-4]. The German Renewable Energy Act (EEG) of 2000 obliged energy supply companies to feed electricity generated from renewable sources into the grid at guaranteed tariffs over a period of 20 years [1, 5, 6], while the amendments in 2004 and 2009 set strong incentives for the cultivation of energy crops dedicated to AD [7]. This fuelled the growth of biogas plant construction in Germany making it the country with the highest number of operational AD plants. Most of these AD plants are farm based which utilize energy crops as their primary feedstock and generate electricity as base load power supply.

This rapid growth of AD industry due to the EEG has also resulted in some unforeseen side effects including food vs. fuel debate by occupying land for energy crop cultivation [8], biodiversity loss by converting species-rich grasslands into less diverse arable land [9-11], increase of land rental prices [12] and the increase in energy costs due to feed-in tariffs [7]. Furthermore, the growth of electricity share from renewable has increased the mismatch between supply and demand of the electricity grid especially due to the somewhat

unreliable and non-flexible nature of electricity generation from solar and wind and operation of AD plant as base load power supply.

To address some of the side effects the EEG was amended in 2012, 2014 and 2016/2017 resulting in reduction of Feed-in tariffs, introduction of cap on cereal based crops (an upper limit for new AD plants of 60% from 2014, 50% since 2016 and 44% from 2021), limitation on the annual expansion of the installed electrical capacity, introduction of a premium for flexible biogas [1, 5, 6, 8, 13]. The current AD industry in Germany is going to face some challenges in near future due to introduction of change in legal and political framework. This paper has discussed some of these challenges and their potential solutions.

2. New feedstocks

Cereal based crops are currently the primary feedstocks for AD plants in Germany, however, these crops needs substantial resources and carbon input in the form of fertilizer, machinery etc for production. Furthermore, the land which was previously used for food production is now being used to produce fuel, however, the food demand remains same and probably has to be imported from somewhere else giving raise to the food vs. fuel debate. It is necessary to explore alternative feedstocks which require low carbon input for production and doesn't compete with food production or change the current agriculture practices. In Italy, a recently developed strategy, Biogasdoneright^{TM}, has shown that farm scale AD can be adapted so it doesn't compete with traditional food and/or feed production on an agricultural farm. In several regions of Italy, only a single crop per year was norm due to lack of markets for the double crop. However as per the new this strategy a double-cropping was adopted where the first crop (traditional crops) was grown to supply the existing food/feed markets while the second or double-crop e.g. winter rye, triticale, forage wheat, or corn silage was grown, harvested, ensiled for year-round operation of AD plants [14-16]. Also, along with energy crops multiple agro-industrial residues were co-digested for biogas production [17-19].

The residues originating from the entire food supply chain (production, processing, distribution, storage, and sale) and organic fraction of municipal solid wastes (OFMSW) (e.g., organic residues from households, kitchens, restaurants, factory lunch rooms and supermarkets, as well as leaves, grass clippings, or yard trimmings), are also valuable feedstocks for AD [20-25]. Currently, in Germany out of 9.8 Million tons of organic household residues, only 20-30% is utilised for AD [8]. However, these feedstocks are highly heterogeneous with temporal and spatial variations in their digestion characteristics [21-25]. On the basis of digestibility, these can be divided in three different fractions, readily digestible fraction e.g. food waste, medium to slowly digestible fraction e.g. grass clippings and inert fraction e.g. plastic bags. The food waste is of special interest for biogas production due to its high methane yield and short digestion time. Furthermore, in Germany, about 15 million tonnes of food waste is generated, of which, about 60% is generated by households and usually discarded in 'brown bins'[26, 27].

Besides organic residues, biomass from aquatic plants and algae has also been reported as potential feedstocks for biogas production. These feedstocks, generally considered as advanced or third generation feedstock, due to high biomass yield potentials caused by rapid growth and high photosynthetic efficiency, high diversity, no need for fertile agricultural land for cultivation and thus, no direct competition with food production [28-30]. Also, these feedstocks have low lignin concentration which impedes microbial digestion in terrestrial feedstocks. The AD of water based feedstocks is still in infancy and faces many challenges such as economical production and process instability due to high protein, lipid, sulphur, polyphenol, halogen or saline concentrations [28, 31]. Furthermore, the chemical composition and thus the methane potential and optimal harvest time vary with season and location [32].

3. On-demand biogas production

The revision of EEG in 2017 replaced the Feed-in tariff with a tender system and instead of receiving a fixed price for each kilowatt hour fed into electricity grid the supplier can now participate in variable electricity rate determined by the supply and demand of the market [5]. In this scheme, the suppliers have market their electricity themselves and are paid the difference between the feed-in tariff a plant would be entitled to and the average market value of the generated electricity [33]. The premium is designed to motivate the AD plant operators to update their AD facilities from base load supply to flexible energy supply which is determined by the market demand. Furthermore, there are special incentives for acquiring the infrastructure needed for upgrade existing AD plants for flexible energy production. Following approaches can be used for flexible electricity production.

3.1 Biogas storage

3.1.1 On-farm storage

Most of the agriculture AD plants use low or no pressure, single or double layer membrane biogas storage domes which can store biogas for about 4-6 hours [34, 35]. In on-farm storage scenario the AD plant is operated in state of the art manner to constantly produce the biogas, the produced biogas is stored onsite while the electricity from combined heat and power (CHP) is generated only when there is a demand. However, for on-site biogas storage an investment of €10-80 m^{-3} of stored biogas is required [36]. Furthermore, additional cost will be involved to update the AD facility to satisfy the legal requirements posed by the increased amount of biogas storage.

3.1.2 Grid injection

The biogas produced from the AD facility can be further upgraded to biomethane and stored in gas grid which has large storage capacity and this stored biomethane can be used to produce electricity on-demand [37]. This method has gained attention over last few years in Sweden, France, Austria, the Netherlands, Switzerland and Germany [38]. In Germany more than 100 large scale AD facilities are upgrading and injecting the biogas in grid [5]. However,

this approach might not be suitable for smaller AD facilities as the current biogas upgradation technologies are economical for large AD facilities. The cost of gas grid connection has to be covered by both grid operator and AD facility operator which depend on the connection length. The electricity generation from gas grid can result in higher electricity conversion efficiency compared to small decentralized AD facilities as the large gas reservoir from the gas grid can be used to operate natural gas combined cycle gas turbines which electricity conversion efficiencies of more than 60% [39].

3.2 Flexible biogas production

The biogas production from multi-step AD process has been identified as a somewhat robust procedure which can be controlled by varying feeding intervals and changing feed types thus producing biogas on-demand. Following two approaches can be followed to achieve this.

3.2.1 Substrate feeding regime

On-demand biogas production can be achieved by either changing the feeding regime from continuous to pulse or by spiking the slowly digestible feedstock with readily digestible components. Mauky et al. [40] tested different feedstock mixtures in full scale digesters where the feeding interval was altered. Their results show that by flexible substrate feeding, the daily gas production rate can be modulated up to ±50% of the daily average gas production rate. Electricity shutdown up to 3 days was possible with ~ 60% reduction in biogas production. Furthermore, no process instability was observed. Similarly, Mulat et al. [41] tested three feeding frequencies i.e. 2, 24 and 48 h with ‘distiller’s dried grains and reported 14% higher methane yield with 48 h feeding frequency and no adverse effects on the process stability. Feng et al. [42] spiked the AD reactors running on cattle slurry with maize silage and reported peaks of +130% of methane yield and no process instability in short term. This is an attractive option as to achieve flexible biogas production comparatively less additional infrastructure is required and currently in Germany there are grants available to obtain these infrastructure. However, with this approach the microbiome of the AD facility should be resilient enough to cope with rapid changes in feedstock concentrations and the limits of flexible feedings should be well known. Furthermore, a reliable and fast monitoring and control system is also required to control the accumulation of inhibitory substances such as volatile fatty acids (VFA) and ammonia.

3.2.2 Multi stage plant configuration

Another option for flexible gas production is physical the separation of the hydrolysis/acidogenesis steps from the acetogenesis/methanogenesis steps in a two-stage processes. The effluent produced during hydrolysis/acidogenesis stage which is rich in organic acids can be stored and fed in a secondary reactor which will carry out acetogenesis/methanogenesis steps to rapidly produce methane on-demand. Different configurations (Figure 1) of two-stage reactor systems have been suggested for demand-driven biogas production, combining a continuous stirred tank reactor or leach-bed reactor as the first stage with an high-performance reactor such as an upflow anaerobic sludge

blanket or fixed-bed reactor as the second stage [43-45]. However, a two-stage system requires significant investment due to additional infrastructure.

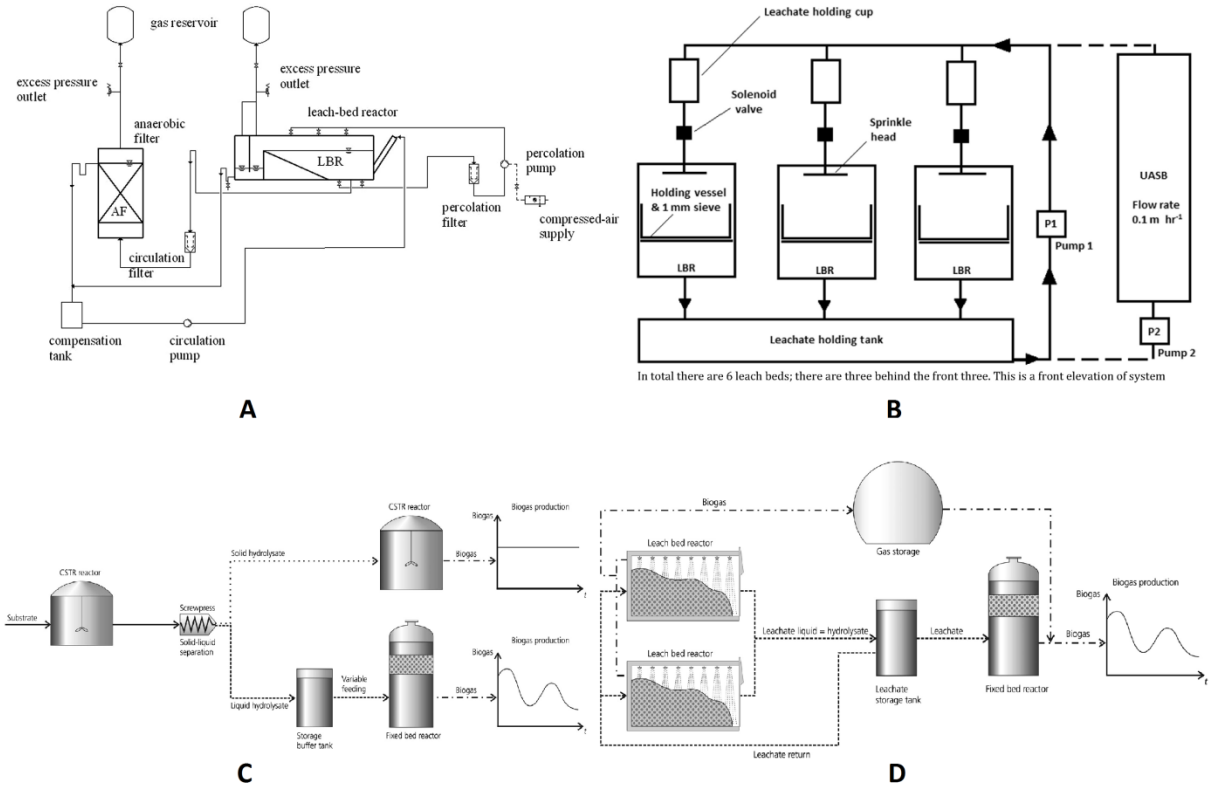

Figure 13. Different configuration of two stage AD reactors used for flexible biogas production. A – Hahn et al.[33]; B – Wall et al.[45]; C and D – Hahn et al.[33]. AF: anaerobic filter, LBR: leach bed reactor.

Conclusion

The goal of this study was to identify some of the challenges posed to German AD industry due to recent changes in legal and political situation and potential solutions for these challenges. Based on the review following conclusions can be drawn.

- Due to food vs. fuel debate, expiration of Feed-in tariffs and a cap on cereal based feedstocks, new feedstock options have to be explored. Agro-industrial waste, macro and micro algae, food waste from entire supply chain and OFMSW are promising candidates.
- There is a temporal mismatch between the supply from renewable sources and demand from electricity grid. AD can play a significant role to fill these gaps. Multiple approaches including on-site biogas storage, biomethane storage to gas grid and flexible operation of AD facility can be followed to produce on-demand electricity.

Acknowledgements

This work was funded by Metabolon IIb project.

Conflict of interest

The authors have declared no conflict of interest.

References

[1] Kemausuor F, Adaramola M, Morken J. A review of commercial biogas systems and lessons for Africa. Energies. 2018;11:2984.

[2] Adams P, Mezzullo W, McManus M. Biomass sustainability criteria: Greenhouse gas accounting issues for biogas and biomethane facilities. Energy Policy. 2015;87:95-109.

[3] Agostini A, Battini F, Padella M, Giuntoli J, Baxter D, Marelli L, et al. Economics of GHG emissions mitigation via biogas production from Sorghum, maize and dairy farm manure digestion in the Po valley. Biomass and Bioenergy. 2016;89:58-66.

[4] Chen Y, Yang G, Sweeney S, Feng Y. Household biogas use in rural China: a study of opportunities and constraints. Renewable and Sustainable Energy Reviews. 2010;14:545-9.

[5] Daniel Gromke J, Rensberg N, Denysenko V, Stinner W, Schmalfuß T, Scheftelowitz M, et al. Current developments in production and utilization of biogas and biomethane in Germany. Chemie Ingenieur Technik. 2018;90:17-35.

[6] Purkus A, Gawel E, Szarka N, Lauer M, Lenz V, Ortwein A, et al. Contributions of flexible power generation from biomass to a secure and cost-effective electricity supply—A review of potentials, incentives and obstacles in Germany. Energy, Sustainability and Society. 2018;8:18.

[7] Britz W, Delzeit R. The impact of German biogas production on European and global agricultural markets, land use and the environment. Energy Policy. 2013;62:1268-75.

[8] Herbes C, Jirka E, Braun JP, Pukall K. The social discourse on the" maize cap" before and after the 2012 amendment of the German Renewable Energies Act (EEG)/Der gesellschaftliche Diskurs um den" Maisdeckel" vor und nach der Novelle des Erneuerbare-Energien-Gesetzes (EEG) 2012. GAIA-Ecological Perspectives for Science and Society. 2014;23:100-9.

[9] Gevers J, Høye TT, Topping CJ, Glemnitz M, Schroeder B. Biodiversity and the mitigation of climate change through bioenergy: impacts of increased maize cultivation on farmland wildlife. GCB Bioenergy. 2011;3:472-82.

[10] Lüker-Jans N, Simmering D, Otte A. The impact of biogas plants on regional dynamics of permanent grassland and maize area—The example of Hesse, Germany (2005–2010). Agriculture, Ecosystems & Environment. 2017;241:24-38.

[11] Stein S, Krug A. The boom in biomass production–a challenge for grassland biodiversity. Biodiversity and animal feed–future challenges for grassland production Uppsala. 2008:730-2.

[12] Appel F, Ostermeyer-Wiethaup A, Balmann A. Effects of the German Renewable Energy Act on structural change in agriculture–The case of biogas. Utilities Policy. 2016;41:172-82.

[13] Balussou D, McKenna R, Möst D, Fichtner W. A model-based analysis of the future capacity expansion for German biogas plants under different legal frameworks. Renewable and Sustainable Energy Reviews. 2018;96:119-31.

[14] Dale BE, Sibilla F, Fabbri C, Pezzaglia M, Pecorino B, Veggia E, et al. Biogasdoneright™: An innovative new system is commercialized in Italy. Biofuels, Bioproducts and Biorefining. 2016;10:341-5.

[15] Valli L, Rossi L, Fabbri C, Sibilla F, Gattoni P, Dale BE, et al. Greenhouse gas emissions of electricity and biomethane produced using the Biogasdoneright™ system: four case studies from Italy. Biofuels, Bioproducts and Biorefining. 2017;11:847-60.

[16] Selvaggi R, Valenti F, Pappalardo G, Rossi L, Bozzetto S, Pecorino B, et al. Sequential crops for food, energy, and economic development in rural areas: the case of Sicily. Biofuels, Bioproducts and Biorefining. 2018;12:22-8.

[17] Valenti F, Zhong Y, Sun M, Porto SMC, Toscano A, Dale BE, et al. Anaerobic co-digestion of multiple agricultural residues to enhance biogas production in southern Italy. Waste Management. 2018;78:151-7.

[18] Giuliano A, Bolzonella D, Pavan P, Cavinato C, Cecchi F. Co-digestion of livestock effluents, energy crops and agro-waste: Feeding and process optimization in mesophilic and thermophilic conditions. Bioresource technology. 2013;128:612-8.

[19] Muradin M, Foltynowicz Z. Potential for Producing Biogas from Agricultural Waste in Rural Plants in Poland. Sustainability. 2014;6:5065.

[20] Dahiya S, Kumar AN, Shanthi Sravan J, Chatterjee S, Sarkar O, Mohan SV. Food waste biorefinery: Sustainable strategy for circular bioeconomy. Bioresource technology. 2018;248:2-12.

[21] Tyagi VK, Fdez-Güelfo LA, Zhou Y, Álvarez-Gallego CJ, Garcia LIR, Ng WJ. Anaerobic co-digestion of organic fraction of municipal solid waste (OFMSW): Progress and challenges. Renewable and Sustainable Energy Reviews. 2018;93:380-99.

[22] Campuzano R, González-Martínez S. Characteristics of the organic fraction of municipal solid waste and methane production: A review. Waste Management. 2016;54:3-12.

[23] Jain S, Jain S, Wolf IT, Lee J, Tong YW. A comprehensive review on operating parameters and different pretreatment methodologies for anaerobic digestion of municipal solid waste. Renewable and Sustainable Energy Reviews. 2015;52:142-54.

[24] Sen B, Aravind J, Kanmani P, Lay C-H. State of the art and future concept of food waste fermentation to bioenergy. Renewable and Sustainable Energy Reviews. 2016;53:547-57.

[25] Xu F, Li Y, Ge X, Yang L, Li Y. Anaerobic digestion of food waste–Challenges and opportunities. Bioresource technology. 2018;247:1047-58.

[26] Barabosz J. Consumer behavior and production of food waste in sample households (German: Konsumverhalten und Entstehung von Lebensmittelabfällen in Musterhaushalten). Stuttgart Online unter: https://www respect-food eu/fileadmin/user_upload/pdf/2011_09_26_Endversion_Diplomarbeit pdf Stand. 2011;22:14.

[27] Göbel C, Teitscheid P, Ritter G, Blumenthal A, Friedrich S, Frick T, et al. Determination of discarded food and proposals for a minimization of food wastage in Germany. Studie für den Runden Tisch „Neue Wertschätzung von Lebensmitteln “des Ministeriums für Klimaschutz, Umwelt, Landwirtschaft, Natur und Verbraucherschutz des Landes Nordrhein-Westfalen. 2012.

[28] Bahadar A, Khan MB. Progress in energy from microalgae: a review. Renewable and Sustainable Energy Reviews. 2013;27:128-48.

[29] Dębowski M, Zieliński M, Grala A, Dudek M. Algae biomass as an alternative substrate in biogas production technologies. Renewable and Sustainable Energy Reviews. 2013;27:596-604.

[30] Allen E, Browne J, Hynes S, Murphy J. The potential of algae blooms to produce renewable gaseous fuel. Waste Management. 2013;33:2425-33.

[31] Saratale RG, Kumar G, Banu R, Xia A, Periyasamy S, Saratale GD. A critical review on anaerobic digestion of microalgae and macroalgae and co-digestion of biomass for enhanced methane generation. Bioresource technology. 2018;262:319-32.

[32] Herrmann C, FitzGerald J, O’Shea R, Xia A, O’Kiely P, Murphy JD. Ensiling of seaweed for a seaweed biofuel industry. Bioresource technology. 2015;196:301-13.

[33] Hahn H, Krautkremer B, Hartmann K, Wachendorf M. Review of concepts for a demand-driven biogas supply for flexible power generation. Renewable and Sustainable Energy Reviews. 2014;29:383-93.

[34] Böhnke B, Seyfried C, Bischofsberger W. Handbuch der anaeroben Behandlung von Abwasser und Schlamm: Springer; 1993.

[35] Eder B. Biogas in practice. Fundamentals, projecting, plant construction, exemplary plants, economic efficiency, environment. ; Biogas-Praxis. Grundlagen, Planung, Anlagenbau, Beispiele, Wirtschaftlichkeit, Umwelt. 2012.

[36] Klinski S. Einspeisung von Biogas in das Erdgasnetz. Studie. 2006.

[37] Schaaf T, Grünig J, Schuster MR, Rothenfluh T, Orth A. Methanation of CO 2-storage of renewable energy in a gas distribution system. Energy, Sustainability and Society. 2014;4:2.

[38] Petersson A, Wellinger A. Biogas upgrading technologies–developments and innovations. IEA bioenergy. 2009;20:1-19.

[39] Persson T, Murphy J, Jannasch A-K, Ahern E, Liebetrau J, Trommler M, et al. Perspective on the Potential Role of Biogas in Smart Energy Grids. In IEA Bioenergy 2014, Technical Brochure. Available online: https://www.dbfz.de/fileadmin/user_upload/Referenzen/Studien/Smart_Grids_Final_web.pdf (accessed on 10 April 2019). 2014.

[40] Mauky E, Weinrich S, Jacobi H-F, Nägele H-J, Liebetrau J, Nelles M. Demand-driven biogas production by flexible feeding in full-scale – Process stability and flexibility potentials. Anaerobe. 2017;46:86-95.

[41] Mulat DG, Jacobi HF, Feilberg A, Adamsen APS, Richnow H-H, Nikolausz M. Changing Feeding Regimes To Demonstrate Flexible Biogas Production: Effects on Process Performance, Microbial Community Structure, and Methanogenesis Pathways. Applied and Environmental Microbiology. 2016;82:438.

[42] Feng L, Ward AJ, Guixé PG, Moset V, Møller HB. Flexible biogas production by pulse feeding maize silage or briquetted meadow grass into continuous stirred tank reactors. Biosystems Engineering. 2018;174:239-48.

[43] Linke B, Rodríguez-Abalde Á, Jost C, Krieg A. Performance of a novel two-phase continuously fed leach bed reactor for demand-based biogas production from maize silage. Bioresource technology. 2015;177:34-40.

[44] Hahn H, Ganagin W, Hartmann K, Wachendorf M. Cost analysis of concepts for a demand oriented biogas supply for flexible power generation. Bioresource technology. 2014;170:211-20.

[45] Wall D, Allen E, O'Shea R, O'Kiely P, Murphy J. Investigating two-phase digestion of grass silage for demand-driven biogas applications: Effect of particle size and rumen fluid addition. Renewable Energy. 2016;86:1215-23.

Oxidation of Methane in Boggy Sediment, Industrial Biogas Plant and a Landfill Leachate Treatment Plant

Sebastian Schröder, Astrid Rehorek

TH Cologne, Computer Science and Engineering, :metabolon Institute

Abstract

For use in a landfill, a laboratory reactor for safe and environmentally friendly biological utilization of low-concentration methane gas will be further developed. The current principle of denitrification-coupled aerobic methane oxidation will be replaced by methane oxidation under anaerobic conditions. Anaerobic methane oxidation offers the advantage that, in addition to methane, nitrate also undergoes biodegradation. Another advantage is that the oxygen content can be significantly lower. This reduces the risk of the formation of an explosive atmosphere in the reactor. Currently, the principle of anaerobic methane oxidation is known. However, organisms capable of doing so are not yet available as a pure culture. Therefore, several biomasses were probed for the ability of anaerobic methane oxidation. It was found that moor-heavy sediment, activated sludge from the leachate treatment plant and biomass from the local biogas plant oxidize methane after the natural carbon source (C source) was been removed.

1. Introduction

When operating a landfill leachate accumulates. Leachate contains the nitrogen compounds ammonium (NH_4^+) and nitrate (NO_3^-), which are converted into elemental nitrogen (N_2) by nitrification and denitrification [1]. Denitrification requires an external C source, mostly acetic acid [2]. So cost-effective solutions to overcome carbon limitation for denitrification are needed. When operating a landfill, in addition to leachate, the greenhouse gas methane (CH_4) is also produced. In low concentrations, the energy content of methane is insufficient to utilize it energetically. At the same time, CH_4 forms an explosive atmosphere in concentrations of 4-17% (v / v) together with oxygen (O_2) [3]. CH_4 in low concentrations (<25% (v / v)) is therefore eliminated via methane oxidation [4]. As a cost-effective solution, the acetic acid is to be replaced by CH_4 by trying to couple the methane oxidation with the denitrification. A coupling of the methane oxidation with the denitrification can be achieved via the methanotrophic bacterium *Methylocystis rosea*. *M. rosea* can metabolize CH_4 to methanol with the help of atmospheric O_2 (Figure 1) [5], which can be used by the denitrifiers. Since denitrification, in contrast to classical methane oxidation, takes place under anaerobic conditions, it is difficult to run both processes unimpeded in one reactor. Recently, the phenomenon of anaerobic methane oxidation has been discovered [6], [7].

Bacteria, such as *Canidatus methylomirabilis oxyfera*, can metabolize CH_4 under anaerobic conditions by recovering O_2 for oxidation from NO_2^- (*Equation 1*).

Equation 4: $3\,CH_4 + 8\,NO_2^- + 8\,H^+ \rightarrow 3\,CO_2 + 4\,N_2 + 10\,H_2O\,, \Delta G = -928\,kJ\,mol^{-1}$

The AOM is explained by the example of the bacteria of the NC10 phylum and NO_2^-, as it is well described. Also, an AOM is possible with NO_3^- [8]. Bacteria of this species can be found in wetlands [6], [7]. Other sources of suitable micro biocoenoses with an anaerobic environment, a high methane and nitrogen content are landfill sites and biogas plants. Anaerobic methanotrophic bacteria could enter the leachate treatment plant (LLTP) with the leachate emanating from the landfill site. Since bacteria with denitrifying and methane oxidizing properties are not yet available, natural micro biocoenoses for the development of a laboratory reactor for the biological utilization of low-concentration methane gas should be investigated for these properties. The following should be investigated: moor-heavy sediment (BS), activated sludge from the leachate treatment plant (LLTP) and biomass from the fermentation and composting plant (BGP) at the site: metabolon.

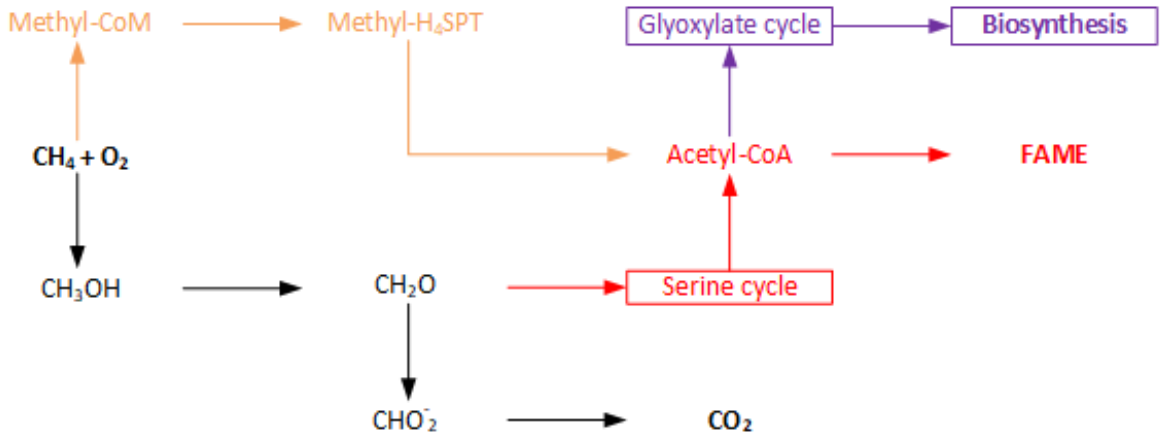

Figure 14: Classic methane oxidation using the example of Methylocystis rosea: reverse methanogenesis using methyl coenzyme M (orange), serine cycle and formation of fatty acid methyl esters (FAME) (red) and glyoxylate cycle and biosynthesis (violet) [5].

2. Material and Methods

For investigation, sediment samples and samples of LLTP and BGP with a high solids content were taken. Samples BS 1 to BS 3 were all taken at different locations (of different nature) at the same location. Sample BS IV was taken for comparison in another boggy area. Subsequently, the samples were diluted with a 0.9% NaCl solution. For trial A (with natural C source), 1 mL of diluted biomass was transferred to 9 mL of medium (0.9% NaCl solution with a NO_3^- content of 500 mg L^{-1}) in a methane atmosphere. For trial B (without natural C source), the bacteria were isolated from the diluted biomass with a sterile filter (pore size 0.45 µm) and dissolved in 10 mL of medium (0.9% NaCl solution with a NO_3^- content of 500 mg L^{-1}) resuspended. The culture tubes also contained a CH4 atmosphere. At the

beginning, the gas composition in the samples was measured and it was ensured that the methane content in the batches was at least 90% (v/v). After 2 months, the atmospheres in the culture tubes were again measured by gas chromatography. To measure the gases, a modified version of the type 1310 gas chromatograph from ThermoFisher Scientific was used. The modified version is designed in terms of detection limits of relevant gaseous molecules specifically for the analysis of biogas and landfill gas. The gas chromatograph uses the columns HayeSep Q and Rtx®-1 from RESTEK (size exclusion), so that in a series connection of both columns and the carrier gas helium, the compounds CH_4, CO_2, O_2, N_2, N_2O, H_2S, and H_2O can be separated and analysed.

3. Results

The results of the gas phase measurements of incubation trials with natural C source are shown in Table 1, the results of the gas phase measurements of the incubation trials without natural C source inTable 2.

Table 2: Changes in the atmospheres in the incubation approaches with native C source. It is shown an average of 5 replicas. BS = bottom sediment, LLTP = biomass from a landfill leachate treatment plant, BGP = biomass from a biogas plant. "Samples SP 1 - 3 belong to the same location, SP IV was taken elsewhere.

sample	CO_2 mmol	O_2 mmol	N_2 mmol	CH_4 mmol	N_2O mmol
BS 1	0,95	-1,82	3,17	-12,43	1,79
BS 2	0,05	-2,59	-5,99	-4,55	0,69
BS 3	1,58	-6,20	-7,33	-2,35	2,50
BS IV	1,27	-5,89	-7,41	-1,08	2,14
LLTP	1,04	-4,02	-4,85	1,08	1,84
BGP	-0,37	-4,47	-7,20	-0,59	0,22

Table 3: Changes in the atmospheres in the incubation approaches without natural C source. It is shown an average of 5 replicas. BS = bottom sediment, LLTP = biomass from a landfill leachate treatment plant, BGP = biomass from a biogas plant. "Samples SP 1 - 3 belong to the same location, SP IV was taken elsewhere.

Sample	CO_2 mmol	O_2 mmol	N_2 mmol	CH_4 mmol	N_2O mmol
BS 1	-0,15	5,02	21,16	-25,81	0,46
BS 2	1,85	0,82	21,48	-26,62	2,74
BS 3	0,73	0,83	11,83	-15,78	1,47
BS IV	0,52	-0,12	8,12	-13,99	1,24
LLTP	4,59	-7,99	6,33	-3,68	5,93
BGP	5,31	-5,37	18,94	-26,36	6,74

4. Discussion

Figure 2 shows the changes in the atmospheres in the natural C source incubation approaches. BS 1 shows a CO2 formation of 0.5 mmol, which can occur independently of aerobic (Figure 1) [5] and anaerobic (Equation 1) [9] metabolic pathways. An explanation for the CO_2 formation can be the metabolism of the natural C source in the incubation approach. In addition to the formation of CO_2, the consumption of -1.82 mmol O_2 is also observed. An O_2 consumption was not expected because the air in the approach should be completely replaced by methane. Because the control of the atmosphere in the 20 mL batches was difficult due to the small size of the batches, it is possible that some residual O_2 was present in the batches. BS 1 also shows formation of N_2, which may have been caused by denitrification [1] as well as by AOM [6], [7], [9]. N_2O, as an intermediate of denitrification, in the samples also indicates denitrification [1], [10]. Consumption of -12.43 mmol CH_4, was not expected. The approach included natural C source, so it should be metabolized first. It is possible that CH_4 after the natural C source was also metabolized. Assuming an AOM, the formation of N_2O is not only an indicator for denitrification [1], but also of methanotrophic organisms [11]. The incubation approach BS 3 behaves in a similar way to BS 2. However, the large error on the measured values of N_2 and CH_4 is noticeable. This error can be explained by a possible inhomogeneity of the number of bacteria and carbon amount in the 5 trials. Also noteworthy is the consumption of 5.99 mmol N_2. This can only be explained by a measurement error or by nitrogen-fixing organisms or plants. BS 3 and BS IV show the same tendency as BS 2. The trial LLTP leads to similar results as the trials BS 2 to BS IV with the difference that a smaller amount of CH_4 was formed. The formation can be explained by a possible measurement error. Another explanation would be the

formation by methanogenic bacteria from the landfill body. Because especially in the non-ventilated dead spaces of the plant, in which organic material is deposited, fermentation due to O_2-deficiency can take place. Figure 2 shows that BGP is also similar to trials BS 2 to BS IV. The BGP is the only sample of the trials with natural C source and a CO_2-consumption. This was not to be expected, since CO_2 should be formed as a metabolite product. One explanation would be algae in the landfill leachate [12], which metabolize CO_2 to O_2. Even if the results of the incubation approaches with natural C source are not very clear and the changes in atmosphere are not pronounced, they can be explained quite well. In addition, Figure 2 shows a small CH4 degradation, as was due to the natural C source.

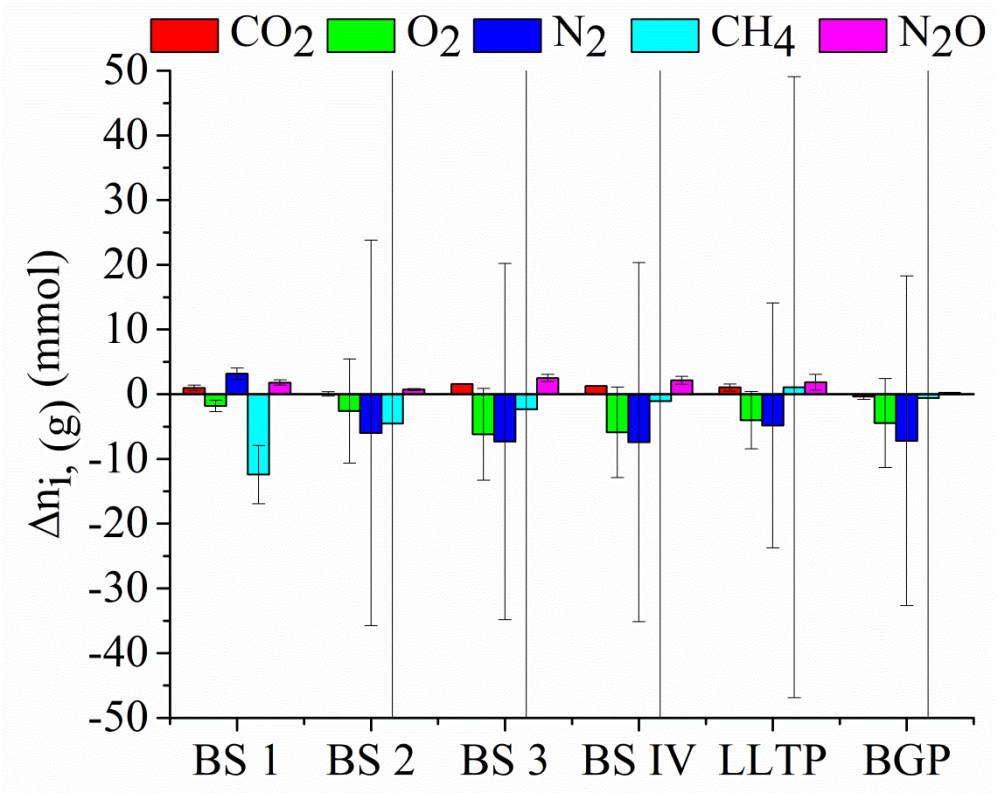

Figure 15: Changes in the atmospheres in the incubation approaches with native C source. The average and standard deviation of 5 replicates are shown. BS = bottom sediment, LLTP = biomass from a landfill leachate treatment plant, BGP = biomass from a biogas plant. "Samples SP 1 - 3 belong to the same location, SP IV was taken elsewhere.

This becomes particularly clear in comparison with Figure 3. Figure 3 shows changes in the atmospheres in the incubation trials without natural C source. Compared to Figure 2, significantly more N_2 is produced and CH_4 is significantly more eliminated. Furthermore, in comparison to Figure 2, a significantly lower error is observed on the mean values in the approaches. This can be explained, on the one hand, by the larger changes in the trials. On the other hand, a sterile filter was used to isolate the bacteria. The filtration ensured that the bacteria and the C source were much more homogeneous in the samples. As a result, the CH_4 consumption began at the same time and much earlier, whereby the error was

significantly reduced. In Sample BS 1 a low CO_2 consumption was detected. The consumed CO_2 is probably the small amount, which is in the ambient air. The consumption can be caused by algae. The formation of about 5 mmol O_2 is also an indication for algae. Algae in the samples make the balancing difficult because they change the O_2 and CO_2 content unchecked. Another explanation for the low amount of CO_2 may be the solubility, since CO_2 can be dissolved in aqueous solution as carbonic acid.

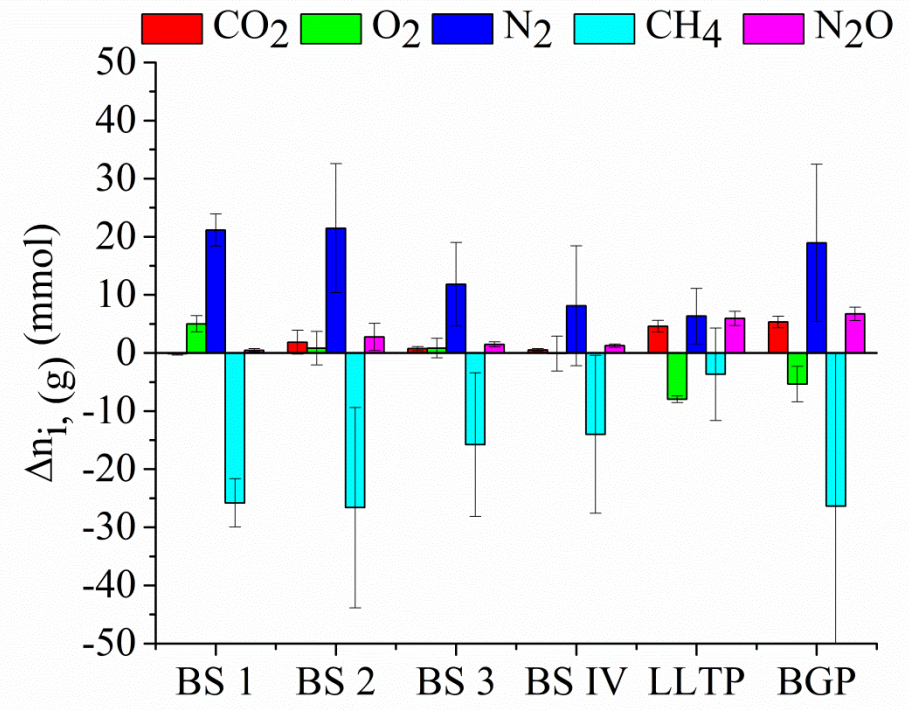

Figure 3: Changes in the atmospheres in the incubation batches without native C source). The average and standard deviation of 5 replicates are shown. BS = bottom sediment, LLTP = biomass from a landfill leachate treatment plant, BGP = biomass from a biogas plant. "Samples SP 1 - 3 belong to the same location, SP IV was taken elsewhere.

Another explanation for missing carbon in the gas phase can also be the metabolism to fatty acid methyl esters (FAME) or the formation of biomass, as shown in Figure 1. The formation of about 21 mmol N_2 can be attributed to denitrification or to the AOM. Since CH_4 was also used, in addition to the denitrification an AOM is assumed. A reason for the increased consumption of CH_4 is the removal of the natural C source. As already observed in the test series with natural C source, N_2O was also formed in BS 1 after the removal of the natural C source, presumably as an intermediate product of denitrification [11]. BS 2 and BS 3 behave like BS 1. The changes in the gas phase of BS 3 are less pronounced than in BS 1. Of the BS samples, the changes in the gas phase are lowest in BS IV. This can be explained by the age of the sample, since BS IV was already taken 2 weeks before the other samples. In contrast to BS 1 to BS IV LLTP and BGP show a significantly higher CO_2 formation and a higher O_2 consumption. The formation of N_2O is also increased in the LLTP and BGP. The increased O_2 consumption is due to an increased amount of O_2 at the beginning of the incubation. This shows that the method and the practical implementation can still be optimized. In addition,

an uneven gas composition initially makes balancing difficult. However, it makes the distinction between aerobic and anaerobic methane oxidation particularly difficult. As long as O_2 is present, aerobic metabolic pathways including aerobic methane oxidation can occur. After consumption of O_2, anaerobic methane oxidation and denitrification can additionally take place. An increased O_2 consumption is also an explanation for the increased amount of CO_2. Particularly noteworthy is the small amount of N_2 in LLTP. The mixed culture in LLTP specialized in denitrification should form the most N_2. At this point one might assume that the specialized mixed culture is particularly sensitive to the presence of O_2 or the lack of usable C source. Although the biomass in BGP is anaerobically adjusted, unlike LLTP it does not react sensitively. This suggests that biomass of BGP is much more robust to changes in the environment.

Summary and Outlook

In this work boggy sediment, biomass from the Landfill Leachate Treatment Plant and a biogas plant have been investigated. It was found that significantly more methane was metabolized after removal of the natural C source. Samples with naturally C source, except for BS 1, metabolised no CH_4. The changes in the gases CO_2, O_2, N_2 and N_2O were also minimal (Figure 2). An explanation was the untreated biomass, which allowed an original metabolism. In contrast, in all samples without a natural C source a CH_4 degradation and N_2 formation were observed Figure 3. No O_2 was measured in BS 1 to BS IV, so that an anaerobic methane oxidation is possible. Since a N_2 formation and a CH_4 degradation are approximately reciprocal, a stoichiometric correlation is supposed. A stoichiometric relationship between CH_4 degradation and N_2 formation is required for anaerobic methane oxidation. However, it is not excluded that the formation of N_2 was due (inter alia) to denitrification. LLTP and BGP also showed CH_4 degradation and N_2 formation. However, as O_2 was metabolized in these two samples, it is uncertain whether aerobic or anaerobic methane oxidation occurred. It is quite possible that as long as O_2 was present, CH_4 was oxidized aerobically and subsequently anaerobically. Since CH_4 degradation was found in all of the investigated biomass, the assumptions made at the beginning are considered to be true. According to the literature [6], [7] anaerobic methane oxidizers were found in sediments of a wet area. Anaerobic conditions and natural methane formation are the reasons for the methane-oxidizing property of the sediment. The activated sludge of the LLTP also showed a methane-oxidizing property. As previously suggested, landfilling is also a good environment for the development of methanotrophic organisms due to its anaerobic character and increased methane content. Such a finding can be confirmed by the literature [13]. Bacteria from the landfill can then be rinsed out and carried in leachate treatment plant. But the methanotrophic bacteria do not have to come exclusively from the landfill. These could also settle in the leachate treatment plant, as is the case in sewage treatment plants. As previously assumed, the methanotrophic property was also found in the biomass of the biogas plant [14]. It is not clear if this is an aerobic or anaerobic methane oxidation. But independent studies have also detected methanotrophic bacteria in biogas plants [15].

For identification, a quantitative polymerase chain reaction (qPCR) was made. A qPCR would be an evidence. Since a qPCR is not yet possible at this time, it should be scheduled for later. For the following series of experiments, it is advisable to isolate the methanotrophic bacteria directly from the biogas plant. Furthermore, a repetition in the 1 L scale with an improved experimental procedure is recommended. Care should be taken to ensure complete replacement of the air with methane. This step can also be skipped, as a 10 L scale-up is planned. Performing in a 10 L scale-up reactor also provides better process monitoring with ion and gas chromatography. At the same time, the pH value and the redox potential can be monitored. While running in a 10 L scale-up reactor, not only an absolute difference in methane change, but also a gas kinetics of degradation can be measured.

References:

[1] N. Savaglio and R. Puopolo, Eds., *Denitrification: processes, regulation and ecological significance*. New York: Nova Science Publishers, 2012.

[2] C. Steiner *et al.*, 'Influence of different carbon sources including liquid additives out of fermentation or composting on the purification of leachate water', in *Waste-to-Resources 2017: VII International Symposium MBT and MRF: resources and energy from municipal waste: proceedings, 16th-18th May 2017*, 1. Auflage., Göttingen: Cuvillier Verlag Göttingen, internationaler wissenschaftlicher Fachverlag, 2017, pp. 688–698.

[3] 'GESTIS-Stoffdatenbank: Methan'. [Online]. Available: http://gestis.itrust.de. [Accessed: 16-Apr-2018].

[4] R. A. Simonet, 'Energiegewinnung aus Abfalldeponien', *Gas-Wasser-Abwasser*, 1985.

[5] J. M. Clomburg, A. M. Crumbley, and R. Gonzalez, 'Industrial biomanufacturing: The future of chemical production', *Science*, vol. 355, no. 6320, p. aag0804, Jan. 2017 https://doi.org/10.1126/science.aag0804.

[6] M. L. Wu *et al.*, 'Ultrastructure of the Denitrifying Methanotroph "Candidatus Methylomirabilis oxyfera," a Novel Polygon-Shaped Bacterium', *J. Bacteriol.*, vol. 194, no. 2, pp. 284–291, Jan. 2012 https://doi.org/10.1128/JB.05816-11.

[7] L. Shen, H. Wu, Z. Gao, X. Liu, and J. Li, 'Comparison of community structures of Candidatus Methylomirabilis oxyfera-like bacteria of NC10 phylum in different freshwater habitats', *Sci. Rep.*, vol. 6, no. 1, Sep. 2016 https://doi.org/10.1038/srep25647.

[8] M. F. Haroon *et al.*, 'Anaerobic oxidation of methane coupled to nitrate reduction in a novel archaeal lineage', *Nature*, vol. 500, no. 7464, pp. 567–570, Aug. 2013 https://doi.org/10.1038/nature12375.

[9] M. Cui, A. Ma, H. Qi, X. Zhuang, and G. Zhuang, 'Anaerobic oxidation of methane: an "active" microbial process', *MicrobiologyOpen*, vol. 4, no. 1, pp. 1–11, Feb. 2015 https://doi.org/10.1002/mbo3.232.

[10] J. Oh and J. Silverstein, 'Oxygen inhibition of activated sludge denitrification', *Water Res.*, vol. 33, no. 8, pp. 1925–1937, Jun. 1999 https://doi.org/10.1016/S0043-1354(98)00365-0.

[11] J. Myung *et al.*, 'Production of Nitrous Oxide from Nitrite in Stable Type II Methanotrophic Enrichments', *Environ. Sci. Technol.*, vol. 49, no. 18, pp. 10969–10975, Sep. 2015 https://doi.org/10.1021/acs.est.5b03385.

[12] X. Zhao *et al.*, 'Characterization of microalgae-bacteria consortium cultured in landfill leachate for carbon fixation and lipid production', *Bioresour. Technol.*, vol. 156, pp. 322–328, Mar. 2014 https://doi.org/10.1016/j.biortech.2013.12.112.

[13] J. P. Sheets, X. Ge, Y.-F. Li, Z. Yu, and Y. Li, 'Biological conversion of biogas to methanol using methanotrophs isolated from solid-state anaerobic digestate', *Bioresour. Technol.*, vol. 201, pp. 50–57, Feb. 2016 https://doi.org/10.1016/j.biortech.2015.11.035.

[14] L. A. B. Siniscalchi, I. C. Vale, J. Dell'Isola, C. A. Chernicharo, and J. Calabria Araujo, 'Enrichment and activity of methanotrophic microorganisms from municipal wastewater sludge', *Environ. Technol.*, vol. 36, no. 12, pp. 1563–1575, Jun. 2015 https://doi.org/10.1080/09593330.2014.997298.

[15] T. May, D. Polag, F. Keppler, M. Greule, L. Müller, and H. König, 'Methane oxidation in industrial biogas plants—Insights in a novel methanotrophic environment evidenced by pmoA gene analyses and stable isotope labelling studies', *J. Biotechnol.*, vol. 270, pp. 77–84, Mar. 2018 https://doi.org/10.1016/j.jbiotec.2018.01.022.

Synthesis of Polyurethanes based on 17-Hydroxy-Oleic Acid obtained from Sophorolipids

Maresa Sonnabend[1,2], Christian Zerhusen[1], Ulrich Schörken[1], Marc C. Leimenstoll*[1]

[1] TH Köln, Faculty of Applied Natural Sciences, Kaiser-Wilhelm-Allee E39, 51368 Leverkusen

[2] University of Cologne, Physical Chemistry, Luxemburger Str. 116, Cologne, Germany

*Correspondence: marc.leimenstoll@th-koeln.de

Abstract

Due to the worldwide shortage of petrochemical based resources, the usage of renewable bio-based raw materials for established and novel products becomes increasingly important.[1] Such bio-based resources are already used for the fabrication of a variety of products, e. g. paper, lubricants, detergents or cosmetics. In the future they are expected to emerge in many more applications in industry and household.[1]

A very promising approach relies on the use of glycolipids as a source of hydroxy-oleic acid.[2] Microbial glycolipids are produced for instance via fermentation from natural resources such as plant oils and sugar.[3] After fermentation complex product mixtures are obtained with the composition depending on the microorganism, substrate and fermentation time.[3] The successful use of microbial glycolipids and hydroxy-oleic acid (HOA) derived therefrom as bio-based intermediates requires reliable analytical methods as well as robust manufacturing processes for the synthesis and cleavage of bio-based molecules. In order to obtain hydroxy-oleic acids as bio-based intermediates, the acidic cleavage of microbial derived sophorolipid was investigated. In addition the implementation of HOA in polyurethane (PU) systems was explored.

1 Introduction

Bio-based raw materials for polyurethane and polymer synthesis are of great interest. Conventional raw materials are based on petrochemical intermediates.[4] The carbon chains of the polyols used are produced from mineral oil by cracking. Due to their poor biodegradability and their tendency to damage the environment, they have many disadvantages and the interest in sustainable alternatives for polymer synthesis is growing.[5] Bio-based raw materials have various advantages. They are virtually unlimited, inexpensive and environmentally friendly. Their physical properties are very similar to those of petrochemical-based polymers.[4],[6] The three most important plant-based raw materials are proteins, oils and carbohydrates.[7] The polymers most commonly found in nature are polysaccharides like starch and cellulose. However, low-molecular components can also be obtained by fermentation and converted into polymers by chemical

polymerization.[5],[8] For example, polylactic acid, polycaprolactone and other partially sustainable bio-based polyesters such as polybutylene succinates can be synthesized by chemical polymerization[9],[10] Vegetable oils, sugar or algae can be used as raw materials. Some bio-based polymers can already compete with petrochemical-based polymers in terms of price and properties.[6] However, most bio-based polymers are not yet competitive due to the high costs involved in the production of the raw materials and the process technology.

Sophorolipids are promising bio-based starting materials whose production has already been well researched[11],[12] They are microbially produced from bio-based raw materials such as sugar and vegetable oils. Sophorolipids are one of the most promising types of glycolipid biosurfactants, as the production organisms are not pathogenic and characterized by high productivity and substrate conversion.[11] The components of sophorolipids are sophorose, a diglucose and hydroxy-oleic acid. They are linked by a glycosidic bond. The sophorose unit may contain acetyl groups at 6' and/or 6'' positions. Lactonic sophorolipids (L-SL) can be formed by binding the carboxyl group of the hydroxy-oleic acid and the 4'' hydroxyl group of the sophorose moiety.[13]–[16] Derivatives of sophorolipids are promising candidates for novel bio-based polymers such as polyesters or polyurethanes.[17] Through chemical cleavage, such as saponification, sophorolipids can provide further basic building blocks for polymerization (Fig. 1).[2],[18]

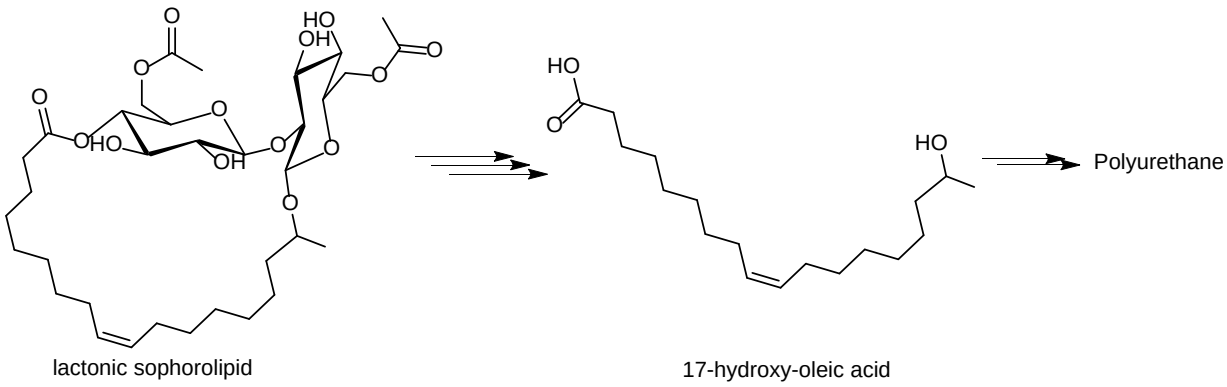

Fig. 1. Schematic illustration of the cleavage of lactonic sophorolipid to obtain 17-hydroxy-oleic acid.

The development of a synthesis route for hydroxy-oleic acids makes these available for further use in polymer synthesis. The special features of hydroxy-oleic acids accessible in this way are that they have terminal carbonyl function and hydroxyl functionality at (ω-1)-position (17-hydroxy-oleic acid). The use of ricinoleic acid, an isomer of the hydroxy-fatty acids (HFAs) synthesized here, is already known in literature.[17],[19]–[21] Ricinoleic acid carries the hydroxyl functionality at the twelfth carbon atom of the chain. This position of the OH group results in polymer chains with six carbon atoms in the side chains, which influence the properties of the polymer in such a way that they act as "plasticizers" by lowering the glass transition temperature. This prevents crystallization, even at very low temperatures[22] It is expected that the absence of side chains in linear HFA polyesters will

provide properties such as higher strength and higher T_G than poly(ricinoleic acid) esters[23] This opens up the possibility of producing polyesters with long hydrophobic carbon chains which can then be incorporated into polyurethane systems.

2 Materials and Methods

2.1 Chemicals

The lactonic sophorolipids used in this work were prepared as described in [24]. The lactonic sophorolipid and the deacetylated acidic sophorolipid were obtained with a purity of 97 %.

Tetrahydrofuran (THF, HPLC grade) and chloroform ($CHCl_3$, purity > 99 %) were obtained from Fisher Chemicals. Acetone (> 99%), acetonitrile (HPLC grade), hydrochloric acid (1M, HCl, grade: for analysis), dibutyltin dilaurate (DBTDL, > 95%), dibutylamine (> 98%), 1,6-hexanediole (1,6-HDO, synthesis grade) and hexamethylene diisocyanate (HDI, purity > 98 %) were purchased from VWR and Sodium hydroxide (purest) was obtained from Bernd Kraft. 4-tert-butylcatechol (99 % purity) was purchased from Acros Organics. Distilled water was taken from the in-house pipeline network.

2.2 Synthesis of 17-Hydroxy-oleic Acid (HOA)

For the synthesis of (ω-1)HFA, lactonic sophorolipid (L-SL) was used as starting material, which was produced *via* fermentation by the yeast strain *Starmerella bombicola*. L-SL with a purity of approx. 97 % dissolved in a 5 molar sodium hydroxide solution at 80 °C. 5 M NaOH was added until a constant pH value was achieved. The pH value was adjusted to 3.5 using HCl. Crystallization of the product was performed at 7 °C. The product was separated and dried by lyophilization. A white powdery product (deacetylated acidic sophorolipid, A-SL) was obtained. Identification was performed by HPLC MS, IR and GPC measurements. 8 mmol of the resulting A-SL were weighed in a 100 mL round bottom flask and dissolved in 50 mL 1 M HCl. The reaction was carried out at 80 °C. The reaction progress was monitored by HPLC measurements. The pH value was then adjusted to 3.5 using NaOH and a liquid liquid extraction (dist. $H_2O/CHCl_3$) was performed. The excess solvent was removed under reduced pressure. The product obtained is yellowish oily (yield: 83.5 %). For the subsequent ester cleavage, a 5 M NaOH solution was used at 80 °C and stirred for approx. 16 hours. This was followed by another liquid-liquid extraction (dist. $H_2O/CHCl_3$). The excess solvent was removed under reduced pressure. A brownish oily liquid was obtained.

2.3 Oligomerization of HOA

The synthesis of OH-terminated hydroxy-oleic acid polyester was carried out on the basis of Nefzger et. al.[25] 0.03 mol 17-hydroxy-oleic acid and 0.006 mol 1,6 hexanediol were placed in a 100 mL multi-necked flask, equipped with a Vigreux column, thermometer and distillation bridge as well as a collecting flask. In addition, 0.042 mmol 4-tert-butylcatechol was added as radical scavenger. A heating-agitating unit with a temperature sensor was used for heating. The reaction mixture was heated to 200 °C over a period of approx. 60 min and

the resulting water was distilled off. After 8 h reaction time tin chloride dihydrate was added. After a reaction time of 24 h, the reaction was stopped.

2.4 Synthesis of HOA-PES polyurethane

For the synthesis of HOA-PES polyurethane, 3.5 g of the product prepared according to section 2.3 was dissolved in 25 mL tetrahydrofuran and heated to 60 °C. 0.58 g HDI and 500 ppm DBTDL were added. After 16 h, the NCO content was titrimetrically and the reaction mixture was cooled to room temperature. The solvent was removed under reduced pressure. The product obtained was a dark brown rubber-like lump. Excess HDI was reacted with an excess of a 0.1 M dibutylamine in acetone solution.

2.5 Analytical methods

HPLC (High Performance Liquid Chromatography) measurements were performed with a Shimadzu Nexera XR equipped with a BM-20 A communications bus module, 2 x LC-20 AD XR, a SIL D0ACXR auto sampler, a column oven and a VWR-ELSD 80 light scattering detector (N_2, 3.5 bar, 40 °C). A C18 RP La Chrom II (Hitachi Ltd., Japan), 4.6 x 250 mm, 5 µm column was used. The measurements were performed at 30 °C with an acetonitrile-water gradient with a flow rate of 1.0 mL min^{-1}, starting with 25 min. 50 % acetonitrile, followed by 60 min. with a linear gradient to 99 % acetonitrile. Samples contain approximately 2.5 mg mL^{-1} substance in tetrahydrofuran. The samples are measured without further preparation.

The NCO-content was determined titrimetrically according to DIN EN ISO-11909-2007.[26] A sample of the reaction mixture was mixed with 10 mL of a 0.2 M dibutylamine solution in acetone. The mixture was diluted with 40 mL acetone and titrated against 0.1 M hydrochloric acid. The automatic titration was performed on a TitroLine 7000 titration unit from SI Analytics. The result is given in weight percent of the NCO groups in relation to the sample weight. The NCO value is calculated according to the following formula.

$$\%NCO = \frac{(V_{Blank} - V_{EP}) \cdot f \cdot c(HCl) \cdot M_A}{10 \cdot m_s} \qquad (6\text{-}1)$$

with:

	V_{Blank}	Blank in mL
	V_{EP}	Consumption Titrant at equivalence point in mL
	$c(HCl)$	Concentration Titrant in mol L^{-1}
	f	Titer
	M_A	Molecular weight NCO; 42.02 g·mol^{-1}
	m_s	Sample mass in g

3 Results and Discussion

3.1 Synthesis of 17-Hydroxy-oleic Acid

The comparatively high purity of L-SL (approx. 97 %) provides an excellent starting point for optimizing the synthesis route for the production of 17-hydroxy-oleic acid. The synthesis sequence is based on the opening of the lactone ring[2],[18] and successive separation of the hydroxy-oleic acid fragment from the sugar units by acidic hydrolysis (Fig. 2).

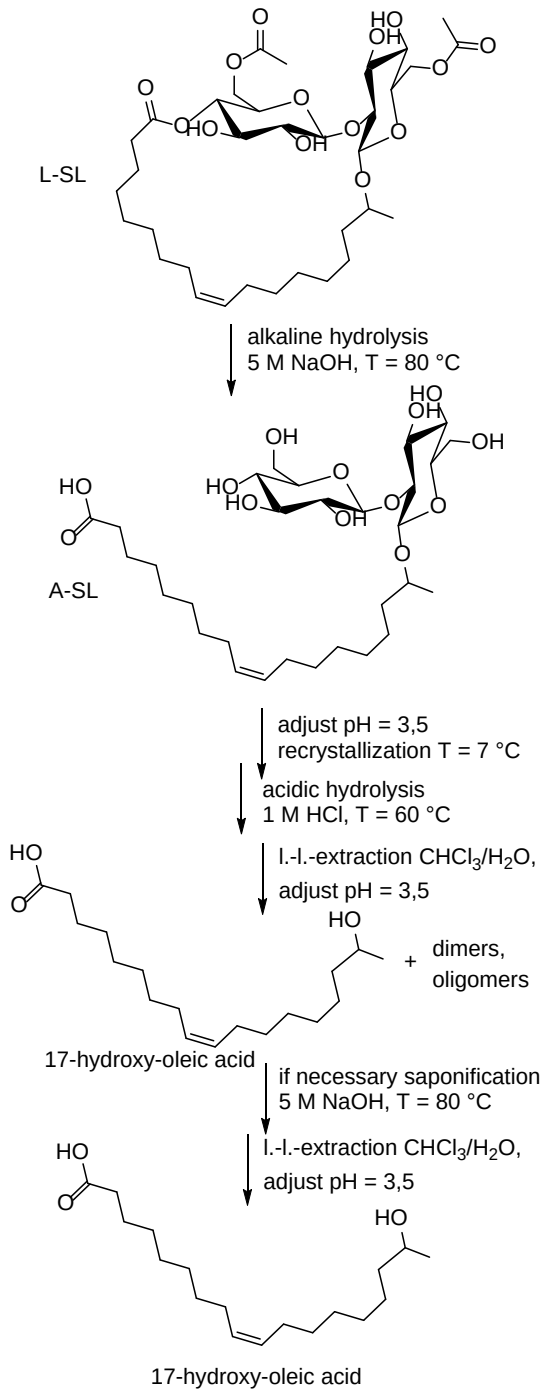

Fig. 2. Synthesis route developed for the production of 17-hydroxy-oleic acid from L-SL.

During the alkaline ring opening, the acetate groups were also removed and free primary hydroxyl groups were formed.[27] The reaction progress was monitored by HPLC-ELSD measurements (Fig. 3). The peaks were identified and assigned by HPLC-MS measurements (Table 1).

S. bombicola not only produced 17-hydroxy-oleic acid but also a small proportion of 18-hydroxy-oleic acid chains, which could be identified by HPLC-MS. Due to their slightly higher hydrophobicity, they are eluted somewhat later. Unidentified peaks are most likely reaction products of 17-hydroxy-oleic acid with monofunctional fatty acids from the initial starting

material mixture. Since this measurement was a reaction tracking measurement and the peaks no longer appeared in the end product after purification, further identification is not necessary.

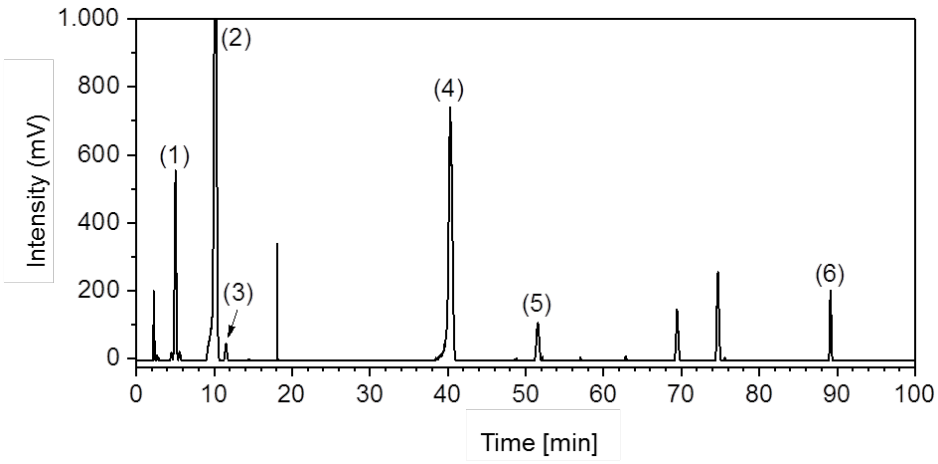

Fig. 3. HPLC-ELSD Chromatogram of the acidic A-SL cleavage with identified peaks after 4 h of reaction time.

Table 4. Assignment of HPLC signals (Fig. 3) to identified substances.

Nr.	molecular weight [g·mol^{-1}]	substance
1	622	A-SL
2	460	Glucose-(ω-1)HFA
3	460	Glucose-ωHFA
4	298	17-hydroxy-oleic acid
5	300	18-hydroxy-oleic acid
6	578	17-hydroxy-oleic acid-dimer

The total reaction time of the acid hydrolysis was between 24 and 72 hours. Since the sophorolipids obtained from fermentation are always product mixtures and the purity of the lactonic sophorolipid was approx. 97 %, substances may be present that inhibit or interfere with acid hydrolysis.[2],[11],[13],[16],[18]

Sugar residues and other impurities were removed from the final product mixture by a liquid-liquid extraction with water/chloroform. Monomers (50.7 % according to HPLC) and dimers (17-hydroxy-oleic acid (49.3 % according to HPLC)) were isolated from the chloroform phase and identified by HPLC. To obtain 17-hydroxy-oleic acid monomers, ester cleavage was performed with 5 M NaOH. The pH value was then adjusted to 3.5 and another liquid-liquid extraction with water/chloroform was carried out. No more dimers were detected in the final product. A small proportion (approx. 4 % according to HPLC) of HFAs bound to glucose residues could not be removed from the end product. By acid hydrolysis of A-SL,

good yields (81.2 - 89.4 %) of 17-hydroxy-oleic acid and 17-hydroxy-oleic acid oligomers mixtures can be obtained. After saponification, the yield was reduced to approx. 54.3 %. The purity obtained was approx. 95 % (according to HPLC).

Due to the poor solubility of 17-hydroxy-oleic acid in NaOH solution, agglomerates formed in the reaction mixture which could not be removed from the reaction vessel. For this reason, ester cleavage results in high yield losses. It should be noted that high purities of the starting materials are necessary for chemical polymerization reactions. The L-SL used was produced by microorganisms and, depending on the batch, may contain different impurities which can influence and interfere with the subsequent reactions.

The purity of the substance mixture is also an important factor in the extraction of 17-hydroxy-oleic acid from sophorolipids. Repeated execution of the synthesis route developed showed that the composition of the educt must have an influence on the reaction time and its products. Already in the recrystallization of the L-SL it became clear that this process was not always reproducible, as disturbing substances were potentially present in the reaction mixture. Possibly these are also inorganic impurities, which could not be detected in further detail. These substances probably also have an influence on the duration of acid hydrolysis. In addition, it was observed that the cleavage process was incomplete and the reaction time was extended when the preparations were scaled up. This increased the formation of di- and oligomers and made it increasingly difficult to process the products. Solubility in chloroform was reduced and a third phase was formed during liquid-liquid extraction.

Ester dissociation is necessary to obtain hydroxy-oleic acids in highest quality. Since ester cleavage is associated with high yield losses and the quantities of starting material present were very small, ester cleavage was only carried out for the final characterization of the hydroxy-oleic acid. 17-hydroxy-oleic acid mixtures of monomers, di- and oligomers were used for polymerization. The yields of 17-hydroxy-oleic acid without ester cleavage are 81.2 to 89.4 % based on A-SL as educt. After ester cleavage, the yield decreased significantly.

The developed route shown in Fig. 2 is quite complex and needs approximately one week of preparation time considering all purification steps. Nevertheless, the synthesis route results in a bio-based building block whose carbon consists of 100% renewable raw materials and that can be used for the synthesis of novel polymers.

3.2 Oligomerisation of 17-Hydroxy-oleic acid

In order to use 17-hydroxy-oleic acid (HOA) as linear polyester building blocks, it must be converted into hydroxyl-terminated polyesters. Hydroxyl-terminated polyester polyols with functionalities of 2 can be obtained by application of a "one-pot" synthesis published by Nefzger et. al. [25] (Fig. 4). Note that the amounts given in section 2.3 lead to molecular weights of ca. 2250 g mol^{-1} and therefore represent the typical molecular weight range of commercially available polyester polyols.

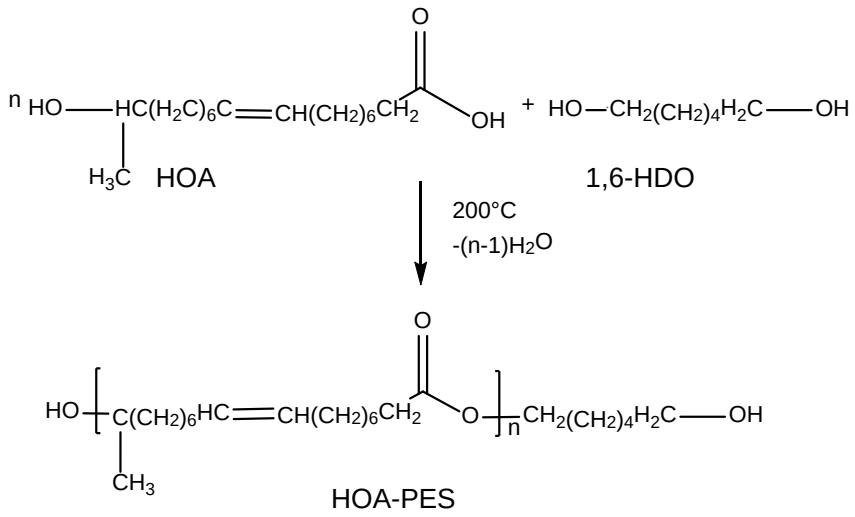

Fig. 2. Schematic reaction equation of the polycondensation of 17-hydroxy-oleic acid and 1,6-hexanediol using the „one-pot“ method.

4-tert-butylcatechol was used as radical scavenger to avoid crosslinking via the double bonds.[28]–[30] Note that the radical scavenger also carries hydroxyl groups and may react with the carboxylic acid functionalities of HOA as well. However, the amount of 4 tert butyl catechol added is insignificant small (1/50 mol%) and can therefore be neglected. The product obtained was of high viscosity and not completely soluble in THF. The soluble part was analyzed by GPC revealing a monomodal distribution for all samples with no 1,6-hexanediol signal observable. Also IR confirmed the formation of the ester groups (results not shown). The acid number was 2.8 mg KOH/g in comparison to ≈ 86 mg KOH/g for the monomeric HOA. All these findings strongly suggest that the majority of the acid groups were esterified and thus the synthesis of the HOA-PES was successful.

3.3 Synthesis of HOA-PES Polyurethanes

For the synthesis of HOA-PES polyurethanes (Fig. 5), the HOA-PES from section 3.2 was used as educt. The molecular weight of the polyester was determined by GPC and used to calculate the required HDI quantity for a NCO/OH ratio of 1.5. After completion of the reaction, the excess isocyanate groups were reacted with a dibutylamine solution. The resulting PU was dark brown and rubbery and no longer entirely soluble in THF. The soluble fraction was further examined by GPC measurement. The GPC chromatograms showed a signal in the molecular range for the product form the conversion of HDI with DBA. The number average molecular weight for the main peak of HOA-PES-PU is 3532 $g \cdot mol^{-1}$. Additionally, molecular weights > 10^6 $g \cdot mol^{-1}$ could also be detected. It seems that during the reaction of HOA-PES with HDI networks were formed leading to a rubber-like product.

The formation of unintended networks may be caused either by crosslinking of the molecules via the double bonds or by increased functionality of the HOA-PES. Latter may be caused by glucose residues.

A comparison of the FT-IR spectra of the polyurethane and monomeric HOA (Fig. 6) show that the signal for the double bond remains visible for HOA-PES-PU. This indicates that no

formation of a network via the double bond had occurred. In addition new bands become visible. The band at about 3330 cm^{-1} is the N-H oscillation of the excess di-butyl amine. The deformation oscillation of the secondary amine at approx. 1621 cm^{-1} can be seen. A band at approx. 1533 cm^{-1} can be assigned to the NH band of the urethane group.

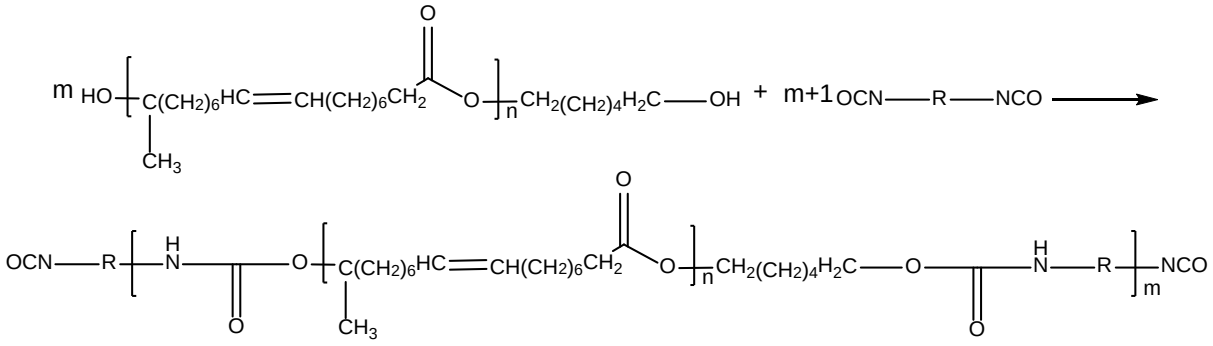

Fig. 3. Equation for the reaction of HOA-PES with HDI to HOA-PES-PU with R = C_6H_{12}.

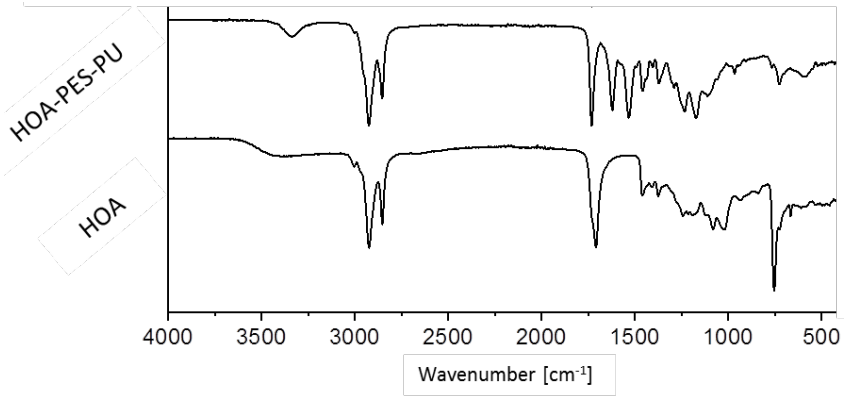

Fig. 4. FT-IR spectra of the HOA-PES polyurethane as well as 17-hydroxy-oleic acid.

DSC measurements showed that HOA-PES-PU has a glass transition temperature (T_G) at -42.85 °C, in contrast to HOA-PES which has no T_G in the temperature range from -60 to 150 °C. The reaction of polyester polyol with HDI and the accompanying formation of hard segments therefore lead to a change (increase) in the glass temperature compared to polyester HOA-PES.

As a conclusion, HOA-PES-PU could successfully be produced. Thus, the synthesis route is generally feasible for the production of polyurethane prepolymers from hydroxy-fatty acids. However, crosslinking occurs to a significant extent most likely due to free glucose impurities in 17-hydroxy-oleic acid raw material. Thus, the quality of 17-hydroxy-oleic acid seems not yet appropriate for the synthesis of polyurethanes and further optimization is required.

Conclusions

Within the scope of this work, a synthesis route for the production of bio-based 17-hydroxy-oleic acids from sophorolipids was successfully developed. The synthesis included an alkaline ring opening of the lactonic sophorolipid to obtain a deacetylated acidic sophorolipid. Subsequent acid hydrolysis cleaved the sophorose unit or the individual glucose units off the molecule and the 17-hydroxy-oleic acid was obtained. In addition to the desired monomers, the product mixture also contained dimers and higher oligomers. In order to obtain pure 17-hydroxy-oleic acid, saponification was necessary; however, the yield was significantly reduced by the ester cleavage step. It was shown that it is possible to obtain 100% bio-based 17-hydroxy-oleic acids from sophorolipids with the developed "one-pot" synthesis based on Nefzger et al.[25] and it was possible to synthesize hydroxyl-terminated polyesters. The resulting bio-based polyester was used to synthesize polyurethanes by conversion with HDI. The products showed a significant crosslinking most likely due to glucose impurities. As a conclusion, polyurethanes containing 17-hydroxy-oleic acids derived from sophorolipids could principally be synthesized. Upon further optimizing the purification strategy these bio-based building blocks could be used in future in high-performance applications, such as low-energy adhesives.

Acknowledgements

This work has been funded by the Federal Ministry of Food and Agriculture in the project “PURe Glue” with project number 22013514. The authors have declared no conflict of interest.

References

[1] Bundesministerium für Ernährung und Landwirtschaft. *Neue Produkte: Aus Natur gemacht*; Berlin, 2014.

[2] P. A. J. Gorin *et al. Can. J. Chem.* 1961, 39 , 846–854.

[3] P. Delbeke *et al. Green Chem.* 2016, 18 (1), 76–104.

[4] A. Noreen *et al. Prog. Org. Coat.* 2016, 91 , 25–32.

[5] H. Cramail *et al.* Preparation of Polyurethanes and Polyesters from Glycolipid Type Compounds. US20140235814A1. 2014.

[6] *Green Gene Technology: Prospects for bio-polymer production in plants;* van Beilen, J.; Poirier, Y., Eds.; Springer Verlag: Berlin, 2007.

[7] H. S. Wool; R. P. Sun. *Bio-Based Polymers and Composites*; Academic Press: London, 2005.

[8] A. J. Ragauskas *et al. Science* 2006, 311 (5760), 484–489.

[9] T. Debuissy *et al. Eur. Polym. J.* 2017, 87 , 84–98.

[10] J. Guan *et al. J. Biomed. Mater. Res. B.* 2002, 61 (3), 493–503.

[11] D. W. G. Develter; L. M. L. Lauryssen. *Eur. J. Lipid Sci. Technol.* 2010, 112 (6), 628–638.

[12] B. M. Dolman *et al. Process Biochem.* 2017, 54 , 162–171.

[13] I. N. A. van Bogaert *et al. Appl. Micorbiol. Bitotechnol.* 2007, 76 (1), 23–34.

[14] N. P. J. Price *et al. Carbohydr. Res.* 2012, 348 , 33–41.

[15] A. Daverey; K. Pakshirajan. *Colloids Surf., B* 2010, 79 (1), 246–253.

[16] P. Jiménez-Peñalver *et al. J. Clean. Prod.* 2018, 172 , 2735–2747.

[17] D. V. Palaskar *et al. Biomacromolecules* 2010, 11 (5), 1202–1211.

[18] U. Rau *et al.* 2001, 13 (2), 85–92.

[19] H. Mutlu; M. A. R. Meier. *Eur. J. Lipid Sci. Technol.* 2010, 112 (1), 10–30.

[20] D. S. Ogunniyi. *Biores. Technol.* 2006, 97 (9), 1086–1091.

[21] M. Ionescu *et al. Eur. Polym. J.* 2016, 84 , 736–749.

[22] Z. S. Petrović *et al. J. Appl. Polym. Sci.* 2008, 108 (2), 1184–1190.

[23] B. Radi *et al. Soft Matter* 2013, 9 (12), 3262–3271.

[24] T. Bollmann; et al. *Tenside Surf Det.* 2019, 56 (5), (approved manuscript, TS110640).

[25] G. Nefzger *et al.* Method for Producing Flexible Polyurethane Foams. WO 2012/069386 AI. 2010.

[26] Deutsches Institut für Normung e. V. *Bindemittel für Beschichtungsstoffe - Isocyanatharze*; Beuth: Berlin, 2007 (DIN EN ISO 1109:2007-05).

[27] P. G. M. Wuts; T. W. Greene. *Greene's Protective Groups in Organic Synthesis*, 4th ed.; Wiley-Interscience, 2007.

[28] J. Clayden *et al. Organische Chemie*, 2. Aufl.; Lehrbuch; Springer Spektrum: Berlin, Heidelberg, 2013.

[29] I. Ernest. *Bindung, Struktur und Reaktionsmechanismen in der organischen Chemie*; Springer-Verlag, 1972.

[30] K. P. C. Vollhardt; N. E. Schore. *Organische Chemie*, 5. Aufl.; Wiley-VCH: Weinheim, 2001.

Lipase catalyzed synthesis of oligomeric diol building blocks utilizing sophorolipid-derived hydroxy fatty acids

Christian Zerhusen[1], Pilar Chavez Linares[1,2], Maresa Sonnabend[1,3], Marc C. Leimenstoll[1], Ulrich Schörken[1]*

[1] Faculty of Applied Natural Sciences; TH Köln; Kaiser-Wilhelm-Allee E39; 51368 Leverkusen; Germany

[2] University of Montpellier, Place Eugène Bataillon, 34095 Montpellier Cedex 5, France

[3] University of Cologne, Physical Chemistry, Luxemburger Str. 116, Cologne, Germany

* Corresponding author: ulrich.schoerken@th-koeln.de

Abstract

The synthesis of 17-hydroxy-oleic acid based oligomeric esters was investigated with immobilized *Pseudozyma antarctica* Lipase B and hexanediol as co-substrate. The effects of different reaction parameters on velocity and product composition at equilibrium conditions were analyzed. The synthesis of oleic acid esters was used as a reference system for initial evaluation of reaction parameters. The reaction with oleic acid and hexanediol was fastest at an enzyme concentration of 5% at 60 °C and high conversions of > 90 % were achieved in non-polar solvents in the presence of molecular sieves. In heptane an oleic acid conversion of 96 % was reached with a final diester to monoester ratio of > 4:1. In syntheses trials with 17-hydroxy-oleic acid the formation of oligomers was verified with GPC, however; conversion was generally lower than with oleic acid. Removal of hydroxyl fatty acid monomers and dimers and the formation ester functionalities could be verified by GC analysis. An increase of the degree of oligomerization was observed simultaneously by GPC analysis. The number-average molecular weight was around 1400 in the best trials corresponding to a degree of oligomerization of around 4 units of hydroxyl-fatty acid attached to a hexanediol core. Though transformations were not complete, the final oligomer size was in the lower range of polyester diols used for polyurethane manufacturing.

1. Introduction

Linear polyurethanes are obtained from the reaction of di-isocyanates with diol building blocks. The diols can be tailored regarding structure, polarity or molecular weight and determine the polyurethane properties. Typical building blocks are polyether, polycarbonate or polyester derived oligomers of petrochemical origin [1]. Biobased diols were already produced from vegetable oils [2], sugar derived hydroxymethylfurfural [3] or ricinoleic acid (12-hydroxy-oleic acid), which was esterified with a polyethylene glycol core to yield a diol building block for PU synthesis [4].

The aim of this work was the lipase-catalyzed synthesis of oligomeric diols starting from hexanediol and 17-hydroxy-oleic acid according to Fig. 1. The unusual 17-hydroxy-oleic acid can be obtained from yeast derived sophorolipid biosurfactants. Depending on yeast strain subterminally or terminally hydroxylated fatty acids are incorporated into the biosurfactants [5-8]. The best sophorolipid producer is *Starmerella bombicola* with yields exceeding 100 g/l [9-11]. The main structure of its sophorolipid is a lactone with subterminally hydroxylated oleic acid [5,6].

Lipases are versatile biocatalysts for the synthesis of bio-based esters e.g. for food, cosmetics, lubricants and fuel applications [12-15]. Their process stability makes them ideal biocatalysts for solvent based ester synthesis [16,17]. Lipase B from *Pseudozyma antarctica* is the most studied enzyme with an exceptional temperature and solvent stability. Numerous examples of esterification and transesterification reactions were shown with this enzyme, which is commercially available in different formulations including the polyacrylate-immobilized Novozym 435 [18-21]. Polyester synthesis with *Pseudozyma antarctica* lipase can either be done by polycondensation under removal of water [22] or by ring-opening polymerization starting from lactones [23,24]. The immobilized enzyme can easily be removed from the polymerization mixture and used repeatedly [25]. Several polymers were synthesized with immobilized lipase B from *Pseudozyma antarctica* and the manifold approaches are summarized in recent review articles [21,26-29].

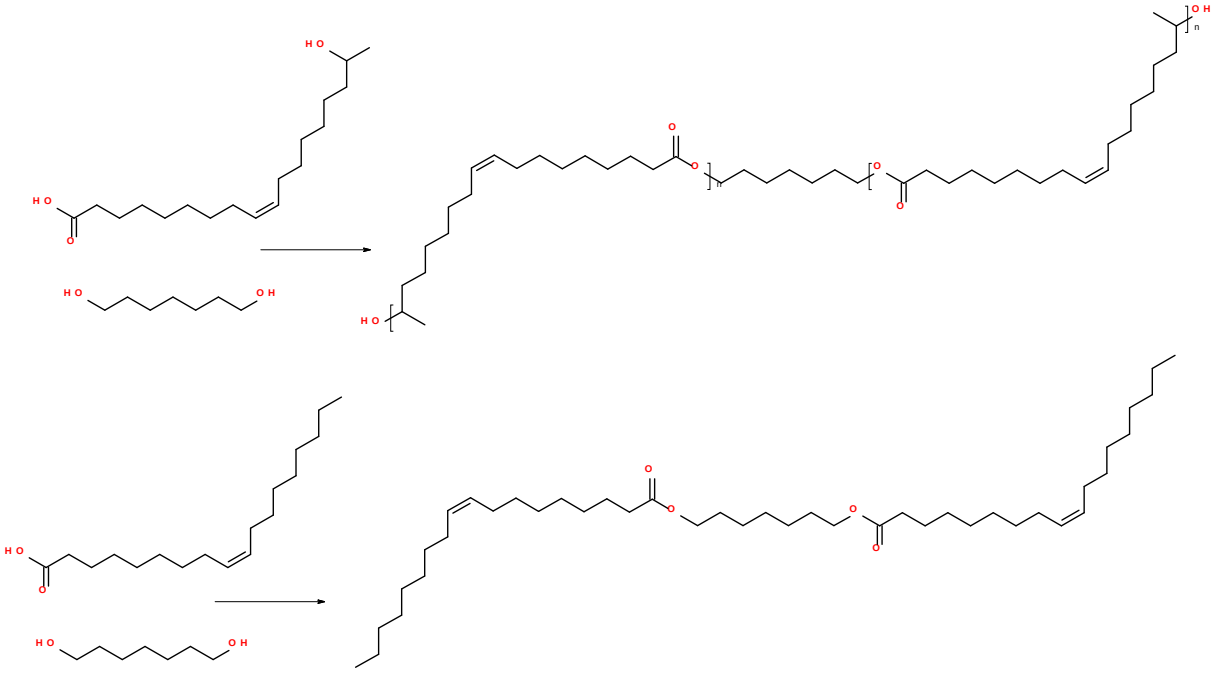

Fig. 1: Lipase catalyzed esterification of hexanediol with 17-hydroxy-oleic acid (top) and oleic acid (bottom)

2. Materials and methods

2.1 Materials

All chemicals were of synthesis grade. BSTFA + 1% TMCS and reference standards for GC calibration were from Carl Roth. Liquid and immobilized lipase B preparations from *Pseudozyma antarctica* (Lipozyme CALBL and Novozym 435) are products from Novozymes and Accurel MP 1000 is a macroporous polypropylene from Membrana. Oleic acid was obtained from DAKO and hexanediol was from Merck. Molecular sieves were obtained from Alfa Aesar. All other chemicals and solvents were from Carl Roth or VWR International. Solvents used in the study were heptane, 2-butanone (MEK) and 2-methyl-2-butanol (2M2B).

2.2 Preparation of immobilized lipase and hydroxylated fatty acids

Lipozyme CALBL was immobilized onto Accurel MP 1000 by adsorption as described in [30]. 2 g of Accurel MP 1000 were soaked for 30 min in 20 mL ethanol. Ethanol was removed and 20 mL of water and 5 mL of Lipozyme CALBL were added and incubated on a rotary shaker overnight at room temperature. The immobilized enzyme was filtered, dried on a sheet of paper and stored at 8 C.

Hydroxylated fatty acids were prepared according to the methods described by Sonnabend et al. [31]. In brief sophorolipids were produced by fermentation of *Starmerella bombicola*, extracted with ethyl acetate and washed with water. The crude sophorolipids were then washed with hexane for fatty acid removal and treated with acid to cleave the glycosidic bonds. The released hydroxylated fatty acids were separated, washed and dried.

2.3 Biocatalytic esterification reactions

The syntheses of oleic acid based diesters and 17-hydroxy-oleic based esters were performed in sealed flasks on a rotary shaker at 250 rpm. Exemplarily 2 eq. oleic acid (8.8 mmol) and 1 eq. hexanediol (4.7 mmol) were dissolved in 15 mL of solvent and the reaction was started by addition of 1 % Novozym-435. After 24h at T = 60 °C the reaction was stopped by filtering off the Novozym-435. Aliquots were taken at different time intervals to monitor the reaction and for final product analysis. The effect of solvents, temperature, enzyme concentration, enzyme support and addition of molecular sieves were analyzed under comparative synthesis conditions. In synthesis trials with 17-hydroxy-oleic acid higher amounts of Novozym 435 of up to 12 % (w/w) were used and the substrates molar ratio was varied from 2:1 to 8:1.

2.4 Analytical methods and calculations

In routine analysis 10 µL of the lipid phase were dissolved in 940 µl of heptane in a GC-vial and 50 µl silylation agent (BSTFA + 1% TMCS) were added. The samples were sealed and incubated in an oven at 80°C for one hour. Analysis was done with a Shimadzu GC 2010 Plus using a MTX Biodiesel TG column (RESTEK, length 14m, ∅ 0.53 mm, film thickness 0.16 µm)

connected to a FID detector with helium as carrier gas and a temperature gradient from 75°C to 410 °C. A split ratio of 5 with an injection volume of 1.5 µl was applied.

Analysis of lipids was done according to the DGF standard method C-V 2 "Acid value and free fatty acid content (Acidity)" with 0.2 – 2 g of lipid sample dissolved in ethanol. Acid values of samples containing organic solvents were normalized to the lipid content in the organic phase. The acid value was determined by titration with 0.1 M KOH solution against phenolphthalein using a Metrohm Dosimat E535 and calculated with the following equation:

$$AV = \frac{\text{ml KOH consumed} \cdot [KOH] \cdot M_{KOH}}{\text{g sample}}$$

Oligomers were analyzed by gel permeation chromatography (GPC), using a PSS polymer safety system with Agilent 1260 hardware modules. The system is equipped with an isocratic pump, a vacuum degasser, a styrene-divinylbenzene copolymer column (5 µm particle size and 1000 Å porosity), a column oven and a standard autosampler. For detection, a refractive index (RI) and UV-visible detectors (250 nm) are used. The column was calibrated with narrow molecular weight distribution polystyrene (ReadyCal Kit standards from PSS polymer). The samples were measured at 30°C and a flow rate of 1 mL min^{-1} with tetrahydrofuran (HPLC grade) as eluent. The sample concentration and injection volumes were 10 mg mL^{-1} and 50 µL respectively.

3. Results and discussion

3.1 Esterification of oleic acid with hexanediol

The esterification of hexanediol with oleic acid was used as a reference system for initial evaluation of suitable reaction conditions. Besides enzyme concentration and temperature the influence of molecular sieves and the solvent system were analyzed. Generally hydrophobic solvents are better suited for esterification reactions; however, the solubility of hexanediol and the 17-hydroxy oleic acid was low in heptane. Therefore different solvent mixtures were analyzed. Addition of 20 % MEK or 2M2B were sufficient to generate a single-phase system.

Reactions were monitored with acid value titration, which allowed the calculation of oleic acid conversion (Fig. 2) and high temperature GC was used for analysis of monoesters and high boiling diesters (Fig. 3+4). In a solvent system containing 80 % heptane and 20 % MEK the reaction velocity at an enzyme concentration of 5 % (w/w substrates) and 60 °C was fastest. Accordingly lipase B from *Pseudozyma antarctica* is known for its exceptional temperature stability. Without addition of molecular sieves the reactions proceeded to a final conversion of approximately 75 %, which is the equilibrium in the heptane / MEK solvent system. Upon addition of molecular sieve (Fig. 2, right) the reaction velocities increased and the equilibrium was shifted towards ester synthesis. In the heptane / MEK solvent system conversions of 91 – 92 % were achieved. The pure heptane system in combination with molecular sieve performed slightly better with a final conversion of 96 %

after 24 h. Greater water retention of the more hydrophilic MEK based solvent system most probably accounts for the differences in equilibrium ester concentration most probably.

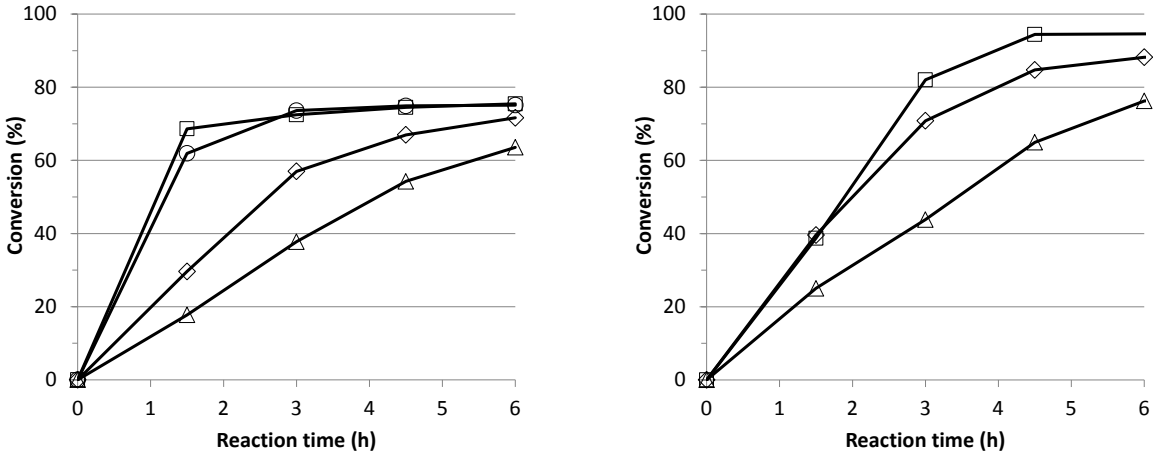

Fig. 2. Conversion of oleic acid esterification analyzed via acid value titration, **left:** analysis of temperature and enzyme concentration with △ = 1 % Novozym 435, 45 °C; ◇ = 5 % Novozym 435, 45 °C; ○ = 1 % Novozym 435, 60 °C and □ = 5 % Novozym 435, 60 °C; **right:** analysis of solvent and molecular sieve effect (5 % each) with 1 % Novozym 435 and △ = 45 °C, heptane/MEK 8:2; ◇ = 60 °C; heptane/MEK 8:2 and □ = 60 °C, 100 % heptane

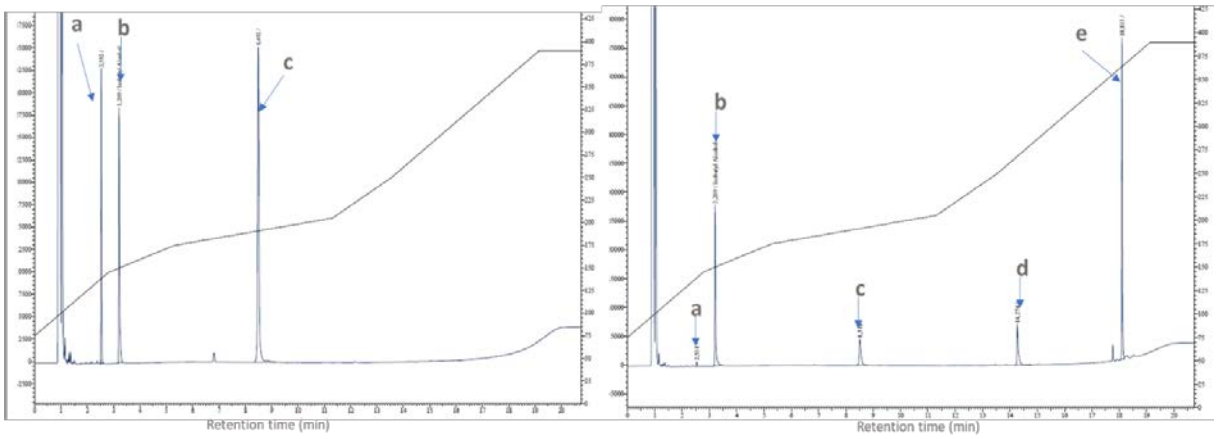

Fig. 3. GC-chromatogram of substrate oleic acid / hexanediol mixture (left) and product mixture after 24 h (right) with a) hexanediol, b) internal standard pentadecane, c) oleic acid, d) hexanediol monoester and e) hexanediol diester.

In GC analysis the course of the reaction was monitored over a period of 24 h and the conversion rates were in good agreement with data obtained from acid value analysis. The reactions at 45 °C without molecular sieve and at 60 °C in the presence of molecular sieves are exemplarily shown in Fig. 4 for the heptane / MEK (8:2) solvent system. In both reactions a fast disappearance of hexanediol was visible, which coincided with an accumulation of the monoester. Diester formation started time-delayed and a monoester maximum of 25 – 35 % after 3 – 4 hours of reaction time was formed in the consecutive reaction. The reaction at 60 °C proceeded significantly faster and a higher final concentration of diesters was achieved

after 24 h in the presence of molecular sieves. The diester to monoester ratio without molecular sieve was 80 : 20, while that with molecular sieve reached 91 : 9. In the pure heptane system a diester to monoester ration of 93 : 7 was reached.

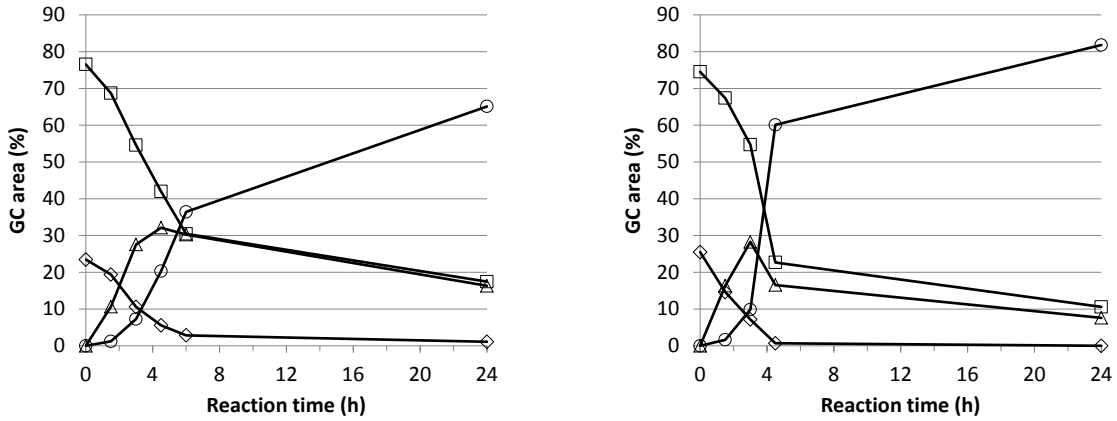

Fig. 4. GC analysis of ester formation in the heptane / MEK 8:2 solvent system with □ = oleic acid, ◇ = hexanediol, △ = monoester and ○ = diester; **left:** reaction with 1 % Novozym 435 at 45 °C without molecular sieve, **right:** reaction with 1 % Novozym 435 at 60 °C in the presence of molecular sieve

3.2 Esterification of 17-hydroxy oleic acid with hexanediol

Analysis of 17-hydroxyoleic acid obtained from acid splitting of *Starmerella bombicola* sophorolipids revealed that the hydroxyl fatty acid was not pure (Fig. 5). Some oligomerization occurred leading e.g. to dimer formation (peak D). From the acid value of 94 it was concluded that intramolecular lactonization as well as formation of higher boiling estolides led to a variety of side products with an average size of a dimer. Upon esterification hexanediol and the monomer peak decreased and new product peaks E and F were formed. Retention time of peaks E correspond to hexanediol monoesters. Peaks in the region of F may either be the monoester of a hydroxyoleic acid dimer or the diester with two hydroxyoleic acid monomers. Higher oligomers could not be detected due to their high boiling points

17-Hydroxyoleic acid was esterified with hexanediol by Novozym 435 as well as by *Pseudozyma antarctica* lipase B immobilized in the hydrophobic polypropylene support Accurel MP 1000 (Fig. 6). In general the reaction was faster with Novozym 435. A clear difference in overall conversion was observed in dependence of the molar ratio of hexanediol to hydroxy fatty acid. In a molar ratio of 1:2 (calculated as monomers) an esterification yield of > 90 % was achieved, while only around 50 % of the acid groups were esterified after 48 h in the trials with 1:8 molar substrate ratios.

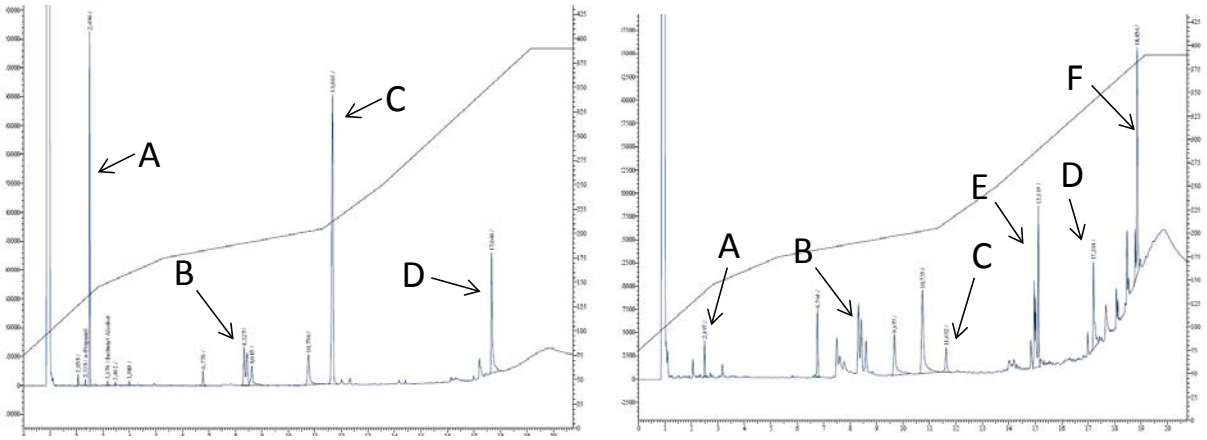

Fig. 5. GC chromatograms of substrate mixture of 17-hydroxyoleic acid and hexanediol (left) and product mixture after transformation with Novo 435 (right), A = hexanediol, B = unknown compounds, C = 17-hydroxyoleic acid, D = dimer of 17-hydroxyoleic acid, E) monoester F) higher esters

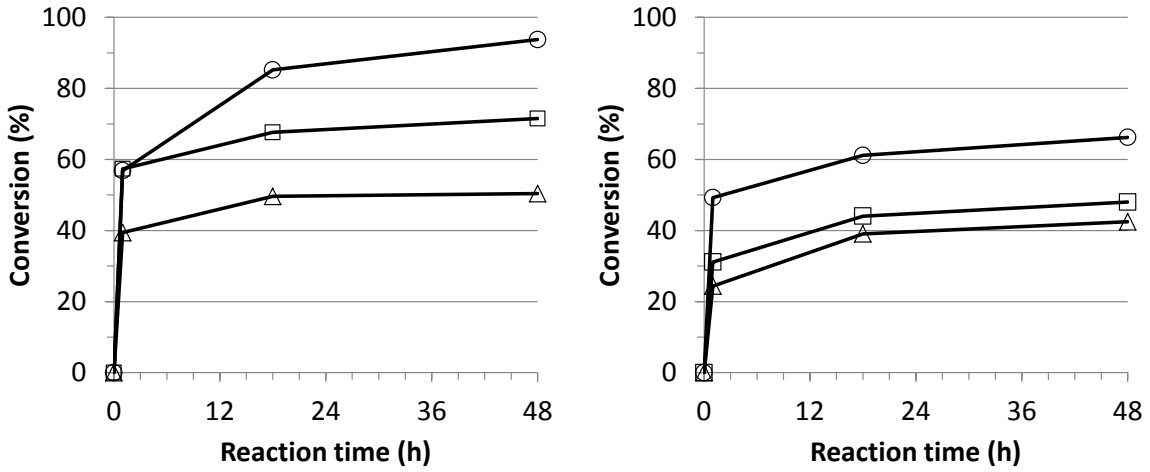

Fig. 6. Top: conversions with Novozym 435 (left) and lipase B immobilized on Accurel MP 1000 with hexanediol to hydroxyl fatty acid substrate ratios of 1:2 (○), 1:4 (□) and 1:8 (△); **right:** GPC overlay of reaction products from conversions with Novozym 435 with black line = 1:2, blue line = 1:4 and red line = 1:8 substrate ratios

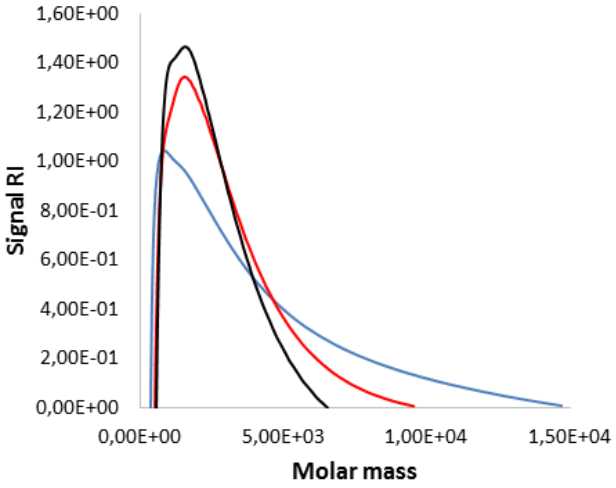

The reactions were conducted with higher enzyme concentrations compared to the oleic acid based reference system and thus the initial esterification was very fast. After 1 h the slope of the conversion curves changed and only a slow increase was observed. An explanation for this behavior is the regioselectivity of the lipase. We believe that the terminal hydroxyl groups of 1,6-hexanediol are esterified rapidly, whereas the secondary hydroxyl groups of the 17-hydroxyoleic acid are hardly recognized by the enzyme. A full transformation in a molar 1:2 ratio is possible, because enough primary hydroxyl groups are available. In contrast, in a 1:8 molar ratio a conversion of 50 % can be achieved, when an average substrate size of a dimer is assumed. Accordingly the GPC chromatograms of the reaction products were comparable with a molar mass of around 1.200 – 1.400 g/mol independent of the molar ratios used. The average degree of polymerization was 4 – 5. Upon longer incubation of the reaction mixtures the esterification yield increased to around 60 %; however, oligomers of significantly higher mass were not obtained. To increase molecular weight, further optimization of reaction conditions or utilization of lipase combinations is needed. Alternatively a chemical pre-oligomerization of the hydroxyl fatty acid prior to enzymatic esterification may be applied.

Conclusions

With the reference system hexanediol / oleic acid the synthesis of diesters was achieved in good yield with more than 90 % of diester content. A solvent system with 80 % heptane and 20 % polar solvent was chosen for the esterification of hydroxyl fatty acids. Molar masses of up to 1.400 were reached corresponding to a degree of polymerization of 4 – 5. Oligomer masses were limited because lipase B of *Pseudozyma antarctica* has a strong preference for the esterification of the primary hydroxyl groups of hexanediol in comparison to the secondary hydroxyl groups of 17-hydroxyoleic acid. Optimizing process conditions, selecting lipases with selectivity for the 17-hydroxy group or combining chemical and enzymatic esterification may be approaches to further increase the degree of polymerization of the polyester diols.

Acknowledgements

This work has been funded by the Federal Ministry of Food and Agriculture in the project “PURe Glue” with project number 22013514. We thank DAKO AG for donation of HOSO fatty acids, Membrana AG for donation of Accurel and Novozymes A/S for donation of lipases.

The authors have declared no conflict of interest.

References

[1] J.O. Akindoyo, M. Beg, S. Ghazali, M. Islam, N. Jeyaratnam, A. Yuvaraj, A. Polyurethane types, synthesis and applications—a review. RSC Adv. 6 (2016) 114453- 114482.

[2] L. Maisonneuve, G. Chollet, E. Grau, H. Cramail, Vegetable oils: a source of polyols for polyurethane materials, OCL 23 (2016) D508.

[3] Z. Mou, E.Y.X. Chen, Polyesters and Poly(ester-urethane)s from Biobased Difuranic Polyols, ACS Sust. Chem. Eng. 4 (2016) 7118-7129.

[4] Y. Xu, Z. Petrovic, S. Das, G.L. Wilkes, Morphology and Properties of Thermoplastic Polyurethanes with Dangling Chains in Ricinoleate-Based Soft segments.Polymer49 (2008) 4248–4258.

[5] A.P. Tulloch, J.F.T. Spencer, Structure and reactions of lactonic and acidic sophorosides of 17-hydroxyoctadecanoic acid, Can. J. Chem. 46 (1968) 1523-1528.

[6] H.J. Asmer, S. Lang, F. Wagner, V. Wray, Microbial production, structure elucidation and bioconversion of sophorose lipids, J. Am. Oil Chem. Soc. 65 (1988) 1460-1466.

[7] M. Konishi, T. Fukuoka, T. Morita, T. Imura, D. Kitamoto, Production of New Types of Sophorolipids by Candida batistae, J Oleo Sci 57 (2008) 359–369.

[8] N.P.J. Price, K.J. Ray, K.E. Vermillion, C.A. Dunlap, C.P. Kurtzman, Structural characterization of novel sophorolipid biosurfactants from a newly identified species of Candida yeast, Carbohydr. Res. 348 (2012) 33–41.

[9] A.M. Davila, R. Marchal, J.P. Vandecasteele, Sophorose lipid fermentation with differentiated substrate supply for growth and production phases. Appl. Microbiol. Biotechnol. 47 (1997) 496-501.

[10] R.T. Otto, H.J. Daniel, G. Pekin, K. Müller-Decker, G. Fürstenberger, M. Reuss, C. Syldatk, Production of sophorolipids from whey, Appl. Microbiol. Biotechnol. 52 (1999) 495–501.

[11] D.W.G. Develter, L.M.L. Lauryssen, Properties and industrial applications of sophorolipids, Eur. J. Lipid Sci. Technol. 112 (2010) 628–638.

[12] K.E. Jaeger, T. Eggert, Lipases for biotechnology, Curr. Opin. Biotechnol. 13 (2002) 390–397.

[13] U. Schörken, P. Kempers, Lipid biotechnology: Industrially relevant production processes, Eur. J. Lipid Sci. Technol. 111 (2009) 627-645.

[14] T. Tan, J. Lu, K. Nie, L. Deng, F. Wang, Biodiesel production with immobilized lipase: a review, Biotechnol. Adv. 28 (2010) 628–34.

[15] M.B. Ansorge-Schumacher, O. Thum, Immobilised lipases in the cosmetics industry. Chem. Soc. Rev. 42 (2013) 6475-6490.

[16] U.T. Bornscheuer, R.J. Kazlauskas, Hydrolases in Organic Synthesis: Regio- and Stereoselective Biotransformations, 2nd edition, Wiley-Blackwell, 2006.

[17] P. Villeneuve, Lipases in lipophilization reactions, Biotechnol. Adv. 25 (2007) 515-536.

[18] P. Adlercreutz, Immobilisation and application of lipases in organic media Chem. Soc. Rev. 42 (2013) 6406-6436.

[19] E. M. Anderson, K. M. Larsson, O. Kirk, One biocatalyst - many applications: The use of *Candida antarctica* B-lipase in organic synthesis, Biocatal. Biotransform. 16 (1998) 181–204.

[20] O. Kirk and M. W. Christensen, Lipases from *Candida antarctica*: Unique Biocatalysts from a Unique Origin, Org. Process Res. Dev., 6 (2002) 446–451.

[21] C. Ortiz, M.L. Ferreira, O. Barbosa, J.C.S. dos Santos, R.C. Rodrigues, Á. Berenguer-Murcia, L.E. Briand, R. Fernandez-Lafuente, Novozym 435: the "perfect" lipase immobilized biocatalyst?, Catal. Sci. Technol., 9 (2019) 2380–2420.

[22] Y. Yang, W. Lu, X. Zhang, W. Xie, M. Cai, R.A. Gross, Two-Step Biocatalytic Route to Biobased Functional Polyesters from ω-Carboxy Fatty Acids and Diols, Biomacromolecules 11 (2010) 259–268.

[23] A. Kumar, B. Kalra, A. Dekhterman, R.A. Gross, Efficient Ring-Opening Polymerization and Copolymerization of ϵ-Caprolactone and ω-Pentadecalactone Catalyzed by *Candida antartica* Lipase B, Macromolecules 33 (2000) 6303-6309.

[24] A. Idris, A. Bukhari, Immobilized *Candida antarctica* lipase B: Hydration, stripping off and application in ring opening polyester synthesis, Biotechnol. Adv. 30 (2012) 550-563.

[25] B. Chen, J. Hu, E.M. Miller, W. Xie, M. Cai, R.A. Gross, *Candida antarctica* Lipase B Chemically Immobilized on Epoxy-Activated Micro- and Nanobeads: Catalysts for Polyester Synthesis, Biomacromolecules 9 (2008) 463–471.

[26] R.A. Gross, A. Kumar, B. Kalra, Polymer Synthesis by In Vitro Enzyme Catalysis, Chem. Rev. 101 (2001) 2097-2124.

[27] S. Kobayashi, H. Uyama, S. Kimura, Enzymatic Polymerization, Chem. Rev. 101 (2001) 3793-3818.

[28] S. Kobayashi, Lipase-catalyzed polyester synthesis - A green polymer chemistry, Proc. Jpn. Acad., Ser. B 86 (2010) 338-365.

[29] A. Douka, S. Vouyiouka, L.M. Papaspyridi, C.D. Papaspyrides, A review on enzymatic polymerization to produce polycondensation polymers: The case of aliphatic polyesters, polyamides and polyesteramides, Progress Polymer Sci. 79 (2018) 1–25

[30] M. Persson, I. Mladenoska, E. Wehtje, P. Adlercreutz, Preparation of lipases for use in organic solvents, Enz. Microb. Technol. 31 (2002) 833-841.

[31] M. Sonnabend, C. Zerhusen, U. Schörken, M.C. Leimenstoll, Synthesis of Polyurethanes based on 17-Hydroxy-Oleic Acid obtained from Sophorolipids, Book of Proceedings of STEPsCON 2018 (2019) 99-109.